Doctorate of National Interest

on

Space Science and Technology

Neural Mechanisms of Motor Imagery and Training-Induced Plasticity: Hypnotizability Relevance to Microgravity Adaptation

Eleonora Malloggi

Supervisor

Prof. Enrica Laura Santarcangelo[1]

Co-Supervisor

Prof. Laura Sebastiani[1]

[1]**Department of Translational Research and New Technologies in Medicine and Surgery, University of Pisa**

Academic year 2024/2025

INDEX

INDEX OF FIGURES

INDEX OF TABLES

INDEX OF SUPPLEMENTARY TABLES

Summary

Long exposure to extreme environments, such as microgravity during spaceflights, induces weightlessness-related physiological alteration regarding sensory information, sensorimotor integration, and interoceptive and vestibular feedback disruption. Such alterations impair postural control, spatial orientation, and fine motor skills. Motor imagery (MI), defined as the mental simulation of movement without overt execution, can counteract sensorimotor alterations by activating the sensorimotor system independently from actual movement execution. On Earth, both physical and MI training (MIT) are reported to improve motor performance. However, the effects of MI training are extremely variable among the general population, which prevents the prediction of its outcome.

Among the factors modulating the physiological correlates of MI, this thesis examines the role of hypnotizability, which is a psychophysiological trait measured by standardized scales, in the efficacy of MI and MIT. The individuals with high hypnotizability scores (highs) display peculiar structural and functional brain characteristics compared to low hypnotizables (lows) - i.e., reduced grey matter volume of the insula and of the cerebellar left lobules IV-VI -, and behavioral/physiological differences, i.e., greater functional equivalence (FE) between actual and imagined perception/action, greater excitability of the motor cortex, lower interoceptive accuracy and more adaptive interoceptive sensibility.

Since highs exhibit greater FE compared to lows, and mediums have not been studied yet, although they represent 70% of general population, this research work aimed a) to support the EEG findings regarding stronger FE and different mode of information processing in highs and lows by employing functional Near Infrared Spectroscopy (fNIRS) (Study 1); b) to investigate whether MIT induces neural plasticity and improvement in the MI cortical correlates after a 15-day MIT in mediums and lows (Study 2); c) to study the role of different cognitive conditions in the duration of an extreme interoceptive condition like voluntary apnea (Study 3). Other hypnotizability-related traits were also considered to possibly interact with hypnotizability, i.e., interoceptive sensibility, absorption, and the ability to imagine movement through visual and kinesthetic imagery (measured by questionnaires).

fNIRS confirmed a stronger FE in highs than in lows and a different mode of information processing in the two groups (Study 1); Study 2 revealed better effects of MIT in highs, although MIT induced neural plasticity also in mediums and lows; Study 3 disclosed a different relevance of hypnotizability to apnea duration associated with attention focused on apnea sensation or with imagery of normal breathing.

In conclusion, hypnotic assessment may predict the adaptation to space environment, mental training may improve the performance of medium-to-low hypnotizables, and motor imagery may buffer the experience of the unpleasant condition of apnea. The reported findings also indicate that, on Earth, hypnotizability may also be relevant to neurorehabilitation treatments.

Keywords: motor imagery, interoception, EEG, fNIRS, microgravity

1. General Introduction

1.1 Microgravity, sensory alterations and countermeasures

In normal gravity, the brain continuously integrates visual, vestibular, and somatosensory inputs to maintain orientation and balance and allow for motor control. In space, microgravity poses unique challenges to human sensorimotor and interoceptive systems; indeed, microgravity disrupts this multisensory integration by altering signals from the vestibular organs and from body proprioceptors due to the absence of gravitational load. These changes impair spatial orientation and motor control; indeed, astronauts often experience spatial disorientation, motion sickness, and degraded motor performance. As a consequence of muscle unloading, microgravity-related reduced sensory feedback from muscles and joints can also produce subtle changes in the muscles structure (Roberts et al., 2010; Koppelmans et al., 2017). Also, astronauts show impaired attention during and after flights (Cebolla et al., 2016; Kuldavletova et al., 2023), and prolonged exposure to weightlessness may increase the risk of neurodegeneration (Clément & Ngo-Anh, 2013; Stahn et al., 2023).

Several electrophysiological studies have revealed specific alterations in cortical frequency bands and connectivity measures during spaceflight. For example, a reduction in alpha power and a decrease in alpha functional connectivity in the Default Mode Network have been observed during flight compared to the pre-flight period, and these changes can persist for several days after return to Earth (Pusil et al., 2023). Recent work has reported modifications in beta-band power, particularly in sensorimotor and frontotemporal regions, and variations in functional connectivity during flights compared to pre- and post-flight recordings, suggesting cortical adaptations to altered vestibular and proprioceptive inputs (Quivira-Lopesino et al., 2025). These EEG alterations are consistent with findings from microgravity analogs, such as head-down bed rest studies, and may reflect both adaptive responses and potential signs of cognitive-sensorimotor impairment if persistent (Pusil et al., 2023; Quivira-Lopesino et al., 2025; Roberts et al., 2010).

In sum, diminished gravity cues challenge the brain structural and functional asset in the sensorimotor domain, prompting the urge to promote an adaptive neural plasticity aimed to reorganize the nervous system functions (Mateos-Aparicio & Rodriguez-Moreno, 2019).

Countermeasures such as physical proprioceptive and vestibular training have been proposed to mitigate these deficits, such as pre- and post-flight balance training (Clément & Ngo-Anh, 2013; Stahn et al., 2023). Mental strategies like motor imagery (MI) might also be advocated to compensate for reduced sensory input and to maintain motor skills in space and after returning to Earth. Motor

imagery (MI) is the cognitive process of imagining a movement without overt action. Neuroimaging studies (Guillot et al., 2009; Ridderinkhof & Bras, 2015) show that MI recruits almost the same sensorimotor network as real movement (premotor cortex, supplementary motor area, parietal cortex, basal ganglia and cerebellum). Behaviorally, MI can be assessed by chronometric index, that indicates the temporal difference between real and imagined movements (Decety, 1996), and self-reported vividness and easiness. However, only few studies employed the chronometric index, which does not correlate with the other measures of MI (Guillot et al., 2008). Physiologically, MI produces signature brain signals, as EEG recordings during MI show desynchronization of sensorimotor rhythms (mu and beta band power decreases), similarly to the actual movement (McFarland et al., 2000). MI also modulates autonomic measures such as heart rate and skin conductance, reflecting mental effort, and can be tracked with haemodynamic imaging (functional magnetic resonance imaging, fMRI, and functional Near-Infrared Spectroscopy, fNIRS), which indicates the concentration of oxygenated and deoxygenated haemoglobin, an indirect measure of the intensity of synaptic activity (Obrig & Villringer, 2003).

1.2 Motor imagery and interoception

MI is widely used in sports and neurorehabilitation to improve motor performance and learning (Schuster et al., 2011). It is known to strengthen motor timing, sequencing, and neural excitability, often producing plastic changes, including both modifications in functional connectivity and changes in EEG activity during resting-state and physical activity (Ruffino et al., 2017). Notably, recent evidence suggests that MI can facilitate the adaptation to novel gravitational contexts: for example, imagining arm-swinging movements in microgravity updates astronauts' internal models so that the imagined movement duration adjusts to weightlessness, whereas mere exposure to microgravity without imagery does not (Rannaud-Monany et al., 2022).

MI is most effective when it engages a correct body perception, that is an integrated representation of one's body, i.e., the sense of the body, which is named interoception (Craig, 2002). Interoception comprises multiple dimensions: accuracy, i.e., the objective ability to detect signals like heartbeat, sensibility, that is the tendency to trust their bodily signals and behave accordingly, and awareness of interoceptive ability (Garfinkel & Critchley, 2015). The insular cortex is central to interoception, as it integrates visceral, auditory, and somatosensory input, and interfaces with the motor system (Zhang et al., 2024).

Individuals with disrupted interoception have impaired MI and body representation (Naraindas et al., 2023). Indeed, effective MI depends on accurate interoceptive feedback and on the ability to mentally simulate bodily states. Interoception, however, is altered in microgravity due to fluids redistribution (Zambetta et al., 2024; Norsk, 2020), dysregulation of aldosterone, cortisol, sex and antidiuretic hormone release (Olde Engberink et al., 2023), altered chest wall mechanics, (Prisk, 2014) as well as gastrointestinal secretions and motility (Akinsuyi et al., 2024; Yang et al., 2020).

1.3 Hypnotizability

Hypnotizability is a stable psychophysiological trait indicating the tendency to modify cognition, behavior and perception according to specific suggestions. It is measured by standardized scales, such as the Stanford Hypnotic Susceptibility Scale, and classifies individuals into highly (highs), medium (mediums), and low (lows) hypnotizable. In the general population, approximately 15% of individuals are highs, 70% are mediums, and 15% are lows (Elkins et al., 2015; Santarcangelo & Scattina, 2016). In the ordinary state of consciousness, different levels of hypnotizability are associated with different behavioral, morphological, and physiological correlates. Highs exhibit reduced grey matter volume of the insula (Huber et al., 2015; Picerni et al., 2019) and of the cerebellar left lobules IV-VI (Picerni et al., 2019); the latter might be responsible for functional cerebellar impairments, as indicated by deficits in postural control (Santarcangelo et al., 2008) and visuomotor adaptation displayed by highs (Menzocchi et al., 2015). Highs also exhibit physiological and behavioral differences compared to lows, i.e., greater similarity between actual and imagined perception and action (i.e., stronger functional equivalence, FE) , which is the neural readout of MI ability (Ibanez-Marcelo et al., 2019), greater excitability of the motor cortex (Spina et al., 2020; Cesari et al., 2020), better cerebrovascular reactivity during cognitive effort (Rashid et al., 2022), less impaired post-occlusion endothelial function, assessed with flow-mediated dilation, during mental stress (Jambrik et al., 2004) and nociceptive stimulation (Jambrik et al., 2005), as well as lower interoceptive accuracy (Giusti et al., 2024), but more “adaptive” interoceptive sensibility (Diolaiuti et al., 2019).

As previously mentioned, EEG topological analysis indicated that highs exhibit stronger FE between actual and imagined movements than lows. Indeed, highs show nearly overlapping cortical activity for an executed and the same imagined movement (Ibanez-Marcelo et al., 2019), which suggests that hypnotizability could serve as a marker for MI skill. Furthermore, the highs’ greater tendency to enter flow states (absorption) (Tellegen & Atkinson, 1974) suggests that they can more fully engage with

mental simulations of both sensorimotor and interoceptive sensations and imagination, enhancing the functional coupling of mind and body.

1.4 Rationale and Objective

Based on the foregoing evidence, hypnotizability might be relevant to the adaptation to microgravity. The diminished sensory feedback in space could be partially compensated by effective MI and flexible processing of body signals, consistently with the somatic marker hypothesis (Damasio, 1994). Highs, exhibiting stronger FE, might naturally buffer the sensorimotor disruptions of weightlessness by relying on imagined body states, like an "as-if body loop" of somatic simulation. When gravitational cues are lacking, highs might better generate internal somatic markers and virtual motor plans that preserve performance. In contrast, lows and, maybe, mediums might experience worse microgravity conditions, unless provided with mental training aimed at improving their imagery ability.

To explore the possible role of mental imagery as a function of hypnotizability in the astronauts' adaptation to microgravity, the current work undertook three experimental studies. After confirming the earlier EEG findings of stronger FE in highs than in lows (Ibanez-Marcelo et al., 2019) by employing fNIRS (Study 1), the research aimed to assess whether MI training can improve MI mediums and lows (Study 2). Finally, given the interaction between MI and interoception, the duration of an extreme interoceptive condition such as apnea was studied as a function of hypnotizability during MI of normal breathing and during attention focused on the interoceptive sensations of absence of breathing (Study 3). In details:

- Study 1: aimed at corroborating the EEG topological findings showing stronger FE in highs than in lows, distributed cortical activity in highs and networked activity in lows during MI (Ibanez-Marcelo et al., 2019) using functional Near Infrared Spectroscopy (fNIRS) as an indirect measure of synaptic activity. Highs are expected to perform MI with less cognitive effort reflected by lower haemodynamic activity than lows, and to exhibit scarce changes in their brain activity compared to baseline.

- Study 2: aimed to verify whether MI training monitored by EEG can improve the effectiveness of MI in the general population represented by mediums (De Pascalis et al., 2000), and to investigate the contribution of absorption and interoceptive sensibility to the training effects, as earlier observed in a single MI session (Malloggi et al., 2024). The EEG changes observed after training could indicate neural plasticity.

- Study 3: aimed to investigate hypnotizability-related differences in apnea duration in cognitively congruent conditions (attention focused on apnea-related sensations) and incongruent conditions (imagery of normal breathing during apnea), which had been explored in the general population (Kanthak et al., 2018). Highs are expected to perform longer-lasting apnea compared to lows both in the cognitively congruent condition, owing to their lower interoceptive accuracy and better interoceptive sensibility that helps them to better manage discomfort sensations, and during the cognitively incongruent condition, owing to their stronger FE between actual and imagined conditions.

All studies were approved by the Pisa University Bioethics Committee (n.29/2022).

2. Experimental Studies

2.1 Study 1. Hypnotizability-related cerebral oxygenation during actual and imagined movements

Abstract

Background

Hypnotizability is an individual trait measured by standard scales and associated with several physiological differences, including the neural functional equivalence of actual and imagined action. EEG studies also revealed different information processing in these conditions in participants with high (highs) and low (lows) hypnotizability scores, in that it is scarcely localized in highs and specifically network-related in lows.

Methods

The study aimed to confirm the EEG findings using functional Near-Infrared Spectroscopy (fNIRS), which indirectly measures the intensity of synaptic activity based on the levels of oxygenated [OHb] and deoxygenated [HHb] haemoglobin. fNIRS was applied to 10 highs and 9 lows, classified according to the Stanford Hypnotic Susceptibility Scale: Form A during actual (M) and imagined (MI) sequential movements of the left arm and hand. The ability to be deeply absorbed in tasks and sensory imagery through the visual and kinesthetic modalities was preliminarily assessed by the Tellegen Absorption Scale (TAS) and the Betts' questionnaire, respectively.

Results

The results showed task-related [OHb] increases in prefrontal areas only in the lows group, whereas the premotor area exhibited greater [OHb] during tasks in both groups. TAS and Betts scores sustained some of the changes. Hypnotizability-related differences were not observed in sensorimotor areas. Correlational analysis between the areas' [OHb] showed that hypnotizability plays a greater role during motor imagery than during actual movement.

Conclusion

The findings support the earlier EEG findings regarding the different information processing of highs and lows by showing lower brain activity in highs during actual and imagined movement.

2.1.1 Background

Hypnotizability is a psychophysiological trait measured by standardized scales that classify individuals as high (highs), medium (mediums), or low (lows) hypnotizables. Highs can experience personal and environmental conditions different from the actual ones and report involuntariness in action better than lows through mental imagery (Elkins et al., 2015; Santarcangelo & Scattina, 2016). Hypnotizability levels are also associated with brain morphofunctional variations and physiological correlates in the cardiovascular, interoceptive and sensorimotor domains (Santarcangelo, 2024).

Behavioral observations regarding the imagination of arm lowering (Santarcangelo et al., 2005), backward falling (Carli et al., 2006), fixating a point/touching a wall in upright stance (Papalia et al., 2014), and having the head rotated toward one side (Santarcangelo et al., 2010) suggested a greater similarity in neural activations (Functional Equivalence, FE) associated with actual and imagined actions in highs than in lows. EEG topological analysis confirmed the hypothesis of stronger FE between actual and imagined conditions (Ibanez-Marcelo et al., 2019a), i.e., greater similarity between the brain activations occurring in the two conditions (Finke et al., 1979; Jeannerod et al., 1995). In addition, they revealed different information processing in highs and lows, as the former exhibit slight, widespread modulations of cortical activity and the latter display task-related networked changes (Ibanez-Marcelo et al., 2019a,b).

Functional near-infrared spectroscopy (fNIRS) can provide further insight into the observed hypnotizability-related EEG differences in sensorimotor imagery, as brain oxygenation reflects the brain synaptic activity. The increases in oxygenated haemoglobin concentration [OHb] with minor reductions in deoxygenated haemoglobin [HHb] indicate cortical activation, while the decreases in [OHb] with increases in [HHb] indicate cortical deactivation (Kaiser et al., 2015). Earlier fNIRS studies have shown that the visual detection of objects embedded in simple scenes does not induce differences in the cerebrovascular reactivity of participants with medium-to-high and low-to-medium hypnotizability scores (Rashid et al., 2022a). Nonetheless, in the former group, cerebrovascular reactivity was negatively correlated with hypnotizability, suggesting lower cognitive effort in the participants with the highest hypnotizability scores. In contrast, during highly demanding cognitive tasks, such as complex mental arithmetic, only medium-to-high levels increase their cerebrovascular reactivity (Rashid et al., 2022b), suggesting that they are more prone than low-to-mediums to adjust their brain blood supply to metabolic demands. This can be attributed to larger availability of endothelial nitric oxide, as suggested by the brachial artery post-occlusion flow-mediated dilation during mental stress and experimental pain (Jambrik et al., 2004a,b).

Based on the hypnotizability-related differences in the cortical representation of actual and imagined action (Ibanez-Marcelo et al., 2019a,b) and on the cerebrovascular reactivity during cognitive tasks (Rashid et al., 2022b), the present study aimed to compare the highs' and lows' tissue oxygenation during actual movement and motor imagery in prefrontal and sensorimotor regions (Yu et al., 2024; Chen et al., 2025; Panikratova et al., 2020) to assess whether the two groups exhibit different haemodynamic responses.

2.1.2 Methods

Participants

One hundred twenty students at the University of Pisa volunteered for the study. After signing an informed consent, they underwent an interview aimed at excluding cardiovascular, neurological, psychiatric, sleep, and attention disorders, and any current drug intake. Hypnotic assessment was conducted with the Italian version of the Stanford Hypnotic Susceptibility Scale: Form A (SHSS: Form A, score 0 - 12) (Weitzenhoffer & Hilgard, 1959) which categorizes the general population into highs, mediums and lows. Ten right-handed (Edinburgh Handedness Inventory, Oldfield, 1971, score $\geq$ 16) highs (SHSS score, 9.44 $\pm$ 1.23, 4 females, age 21 $\pm$ 1.8) and 10 lows (SHSS score, 1.40 $\pm$ 1.71, 4 females; age 22 $\pm$ .7) were recruited consecutively. G*power (Faul et al., 2007) indicated a minimum number of 18 subjects to obtain significant main effects and interactions ($f = .30$, $p = .05$, and $1\text{-}\beta = .80$) for [OHb] and [HHb] studied in prefrontal and sensorimotor areas.

Experimental procedure

Before the experimental session, participants filled in trait questionnaires investigating their proneness to be deeply involved in tasks ("absorption"), through the Tellegen Absorption Scale (TAS, Tellegen & Atkinson, 1974; min 0 - max 34), and their visual and imagery abilities through the visual and kinesthetic scales of the Betts' Questionnaire Upon Mental Imagery (Betts' V, Betts' K, Sheehan, 1967, min 7 - max 1). The experimental session was conducted at the Azienda Ospedaliero-Universitaria Pisana (AOUP), Pisa, at least one week after the hypnotic assessment. Participants were asked to refrain from caffeine and alcohol for the three hours preceding the session. They were invited to sit in a comfortable armchair in a light- and sound-attenuated room and were prepared with a fNIRS cap (Artinis Medical Systems, www.artinis.com). Since the experimental procedure included actual and imagined movements, an experimenter demonstrated the movements the participants had to

perform and then imagine during the procedure. Each movement consisted of a series of five repetitions of flexion–extension of the left arm and hand, along with finger-to-thumb tapping. Afterwards, participants were asked to close their eyes and instructed to perform ten 30-second movement series interspersed by 30-second rest intervals. Thus, each condition consisted of two levels. i.e., task (M or MI) and baseline conditions (bM or bMI). A recorded voice guided the participants to execute or imagine movements for the requested time duration. Before each condition, participants familiarized themselves with both actual and imagined movement, performing five repetitions of each.

The instructions for MI included both visual and kinesthetic motor suggestions: *"Please, imagine performing the same movement you did a few minutes ago. You can see your left arm flexing toward your left shoulder while your fingers press one by one on your thumb, from the index finger to the little finger… you can feel the tension in the muscles of your arm, forearm… and fingers… and then, as your forearm extends, the fingers repeat the sequence in reverse, from the little finger to the index finger, returning to the starting position"*.

After MI, participants completed the NASA Task Load Index (NASA TLX, Hart et al., 1988), which consists of 6 subscales measuring the perceived Mental and Physical Demand (how mentally and physically demanding was the task, respectively), Temporal Demand (how hurried or rushed was the pace of the task), Performance (how successful was the task), Effort (how hard the participants worked to perform the task), and Frustration (how insecure, stressed and annoyed the participants were by the task). Each scale score range was between 0 (minimum) and 20 (maximum), except for the Performance subscale, in which the highest score (20) corresponds to experienced failure and the lowest score (0) to perfect performance.

Signal acquisition and analysis

A continuous-wave fNIRS system (Brite fNIRS, Artinis Medical Systems, Einsteinweg, The Netherlands) with a 2 x 12-channel optodes template was used to record changes in oxyhaemoglobin [OHb] and deoxyhaemoglobin [HHb] concentration in the prefrontal and right sensorimotor cortices. Each group of channels included five transmitters operating at 760 and 850 nm and four receivers. The source-detector distance was set at 3 cm. An OxySoft 4.0 (Artinis Medical Systems) device was used for recording, with a sampling rate of 50 Hz. Prefrontal and sensorimotor areas were identified according to the craniocerebral topography within the international 10-20 system and referred to the corresponding Brodmann areas (Koessler et al., 2009). The left and right anterior prefrontal cortex

(lPFC, rPFC), dorsolateral prefrontal cortex (lDLPFC, rDLPFC), and premotor cortex (lPMC, rPMC) were studied. Measures were also performed on the medial prefrontal cortex (mPFC) and the right primary motor (M1) and sensory cortex (S1), which receive blood supply from the anterior and medial cerebral arteries. fNIRS data were processed and analyzed using custom scripts developed in MATLAB (MathWorks Inc., Natick, MA, USA). A third-order low-pass Butterworth filter with a cut-off frequency of 0.1 Hz (Moriarty et al., 2022) was applied to remove motion, cardiac, and respiratory artifacts. Each trial of both levels was normalized by subtracting the average of the first 10 samples from it. Within each channel, both [OHb] and [HHb] time courses were averaged in bM, M, bMI, and MI. The [OHb] and [HHb] mean value and peak amplitude were computed for averaged trials. Metrics were averaged within lPFC, rPFC, lDLPC, rDLPC, mPFC, lPMC, rPMC, right M1 and S1.

Variables

The traits studied were TAS, Betts' V, and Betts' K. The experimental session-related variables included NASA TLX questionnaire scores, mean and peak [OHb] and [HHb] (μM) in the listed cerebral areas.

Statistical analyses

The Statistical Package for the Social Sciences (SPSS 21) was used for the analyses. After assessing the data for normal distribution (Wilcoxon test), univariate ANOVA was used to analyze TAS scores with hypnotizability as a between-subject factor. Separate multivariate ANOVAs were conducted on Betts' V and Betts' K, and on NASA TLX dimensions, with hypnotizability as a between-subject factor. Mean and peak [OHb] and [HHb] concentrations were studied for each area according to a 2 Groups (highs, lows) x 2 Conditions (bM-M, bMI- MI) x 2 Levels [Task (M, MI), baseline (bM, bMI)] design. ANCOVAs were applied to the same variables, controlling for TAS, Betts' V, and Betts' K. Pearson's correlation coefficient was computed to study the association between brain areas' mean [OHb], and partial correlations controlling for TAS, Betts' V, and Betts' K were studied. The level of significance was set at $p = .05$. Complete statistics are reported in Appendix A.

2.1.3. Results

Subjective reports

Univariate ANOVA revealed higher TAS scores ($F(1,18) = 5.35$, $p = .034$, $\eta^2 = .239$, $1 - \beta = .587$) in highs (mean $\pm$ SD); 22.56 $\pm$ 7.52) than in lows (15.10 $\pm$ 6.54). Multivariate ANOVA did not reveal group differences in Betts' V (highs, 3.43 $\pm$ 1.01; lows, 2.93 $\pm$ 1.53) and Betts' K (highs, 3.60 $\pm$ 1.35; lows, 2.95 $\pm$ 1.62). Multivariate ANOVA applied to the NASA TLX questionnaire scores did not reveal a significant group effect.

Functional Near Infrared Spectroscopy

Mean and peak values of [OHb] and [HHb] in aPFC, mPFC, DLPFC, PMC, M1 and S1 during all conditions are reported in **Table S1**.

In prefrontal areas, only lows increased their mean [OHb] during tasks, and [OHb] was higher in highs than in lows in baseline conditions and lower than in lows during tasks

Anterior prefrontal cortex **Table S2**

Repeated measures ANOVA applied to mean [OHb] revealed a significant **Level x Group** interaction ($F(1,18) = 6.82$, $p = .018$, $\eta^2 = .286$, $1 - \beta = .692$) indicating lower [OHb] in highs than in lows during tasks (**Figure 1**), but not in baseline conditions, and higher values during tasks than baseline in lows. All differences were abolished by controlling for TAS**.**

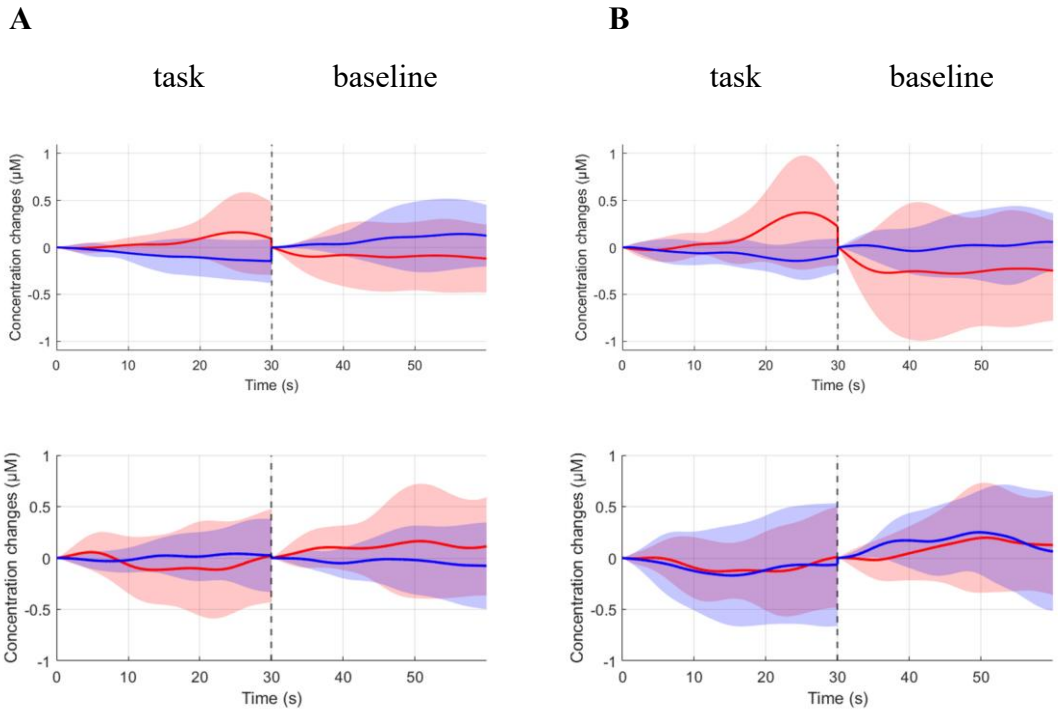

Figure 1. Anterior prefrontal cortex.

[OHb] (red lines) and [HHb] (blue lines) time courses during MI in left (A) and right (B) hemispheres in lows (upper panels) and highs (bottom panels). Exemplificative subject for each group (highs and lows).

For peak [OHb] values (**Table S2**), ANOVA indicated a **Side** effect (left > right, $F(1,18) = 4.95$, p=.04, $\eta^{2=}$ .225, 1 – β= .555) and a significant **Condition x Level x Group** interaction ($F(1,18) = 9.71$, p=.006, $\eta^{2\,=}$ .364, 1 – β = .836). Its decomposition revealed no significant differences in highs, and a higher mean [OHb] during the task compared to baseline in the MI condition in lows; furthermore, the lows' [OHb] was higher during MI than during M. Controlling for TAS and Betts' K abolished the Side effect.

No significant differences were observed for mean [HHb]. Peak [HHb] exhibited a significant **Side** effect (left < right, $F(1,18) = 6.93$, p = .017, $\eta^2 = .290$, 1 - β = .699) and a **Level x Group** interaction ($F(1,18) = 6.12$, p = .024, $\eta^2 = .265$, 1 - β = .645). Its decomposition revealed a significantly higher [HHb] during tasks than rest in highs, and no differences in lows. Highs also exhibited lower values than lows in baseline conditions. Controlling for Betts' K abolished the Side effect.

Medial prefrontal cortex (**Table S3**)

We observed a significant **Level x Group** interaction ($F(1,18) = 9.87$, p = .006, $\eta^2 = .367$, 1 – β= .841) for mean [OHb]. Its decomposition **(Figure 2**) revealed higher [OHb] in highs than in lows in baseline conditions, higher rest than task [OHb] in highs, and no differences in lows. TAS abolished the Level x Group interaction.

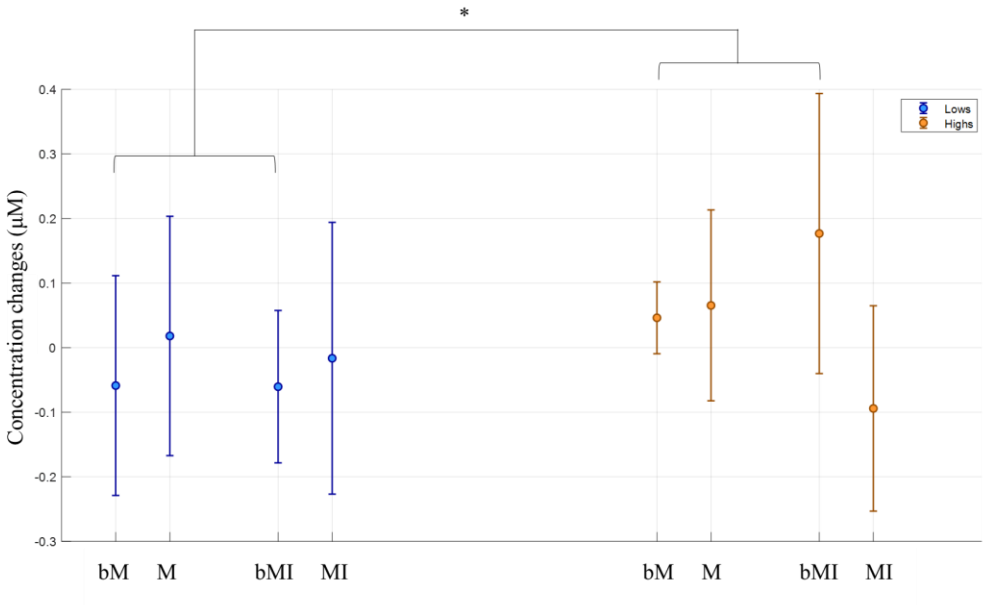

Figure 2. Medial prefrontal cortex.

Mean [OHb] in highs and lows (mean, S.D.). Both lows' baseline values are lower than highs'. *p < .005.

ANOVA applied to peak [OHb] (**Table S3**) revealed a significant **Condition** effect ($F(1,18) = 5.56$, $p = .031$, $\eta^2 = .246$, $1 - \beta = .604$) and significant **Condition x Level x Group** interaction ($F(1,18) = 6.49$, $p = .021$, $\eta^2 = .276$, $1 - \beta = .671$). Its decomposition indicated higher values during both tasks than baseline in lows. The highs' peak [OHb] was greater than the lows during bMI and lower than the lows during MI. Controlling for TAS eliminated the interaction between Condition, Level, and Group.

Mean [HHb] did not differ between groups and tasks. Peak [HHb] showed a significant **Group** effect (highs < lows, $F(1,18) = 5.54$, $p = .031$, $\eta^2 = .246$, $1 - \beta = .603$), which became non-significant controlling for TAS.

Dorsolateral prefrontal cortex (**Table S4**)

Mean values of [OHb] showed a significant **Condition x Side x Level x Group** interaction ($F(1,18) = 9.95$, $p = .006$, $\eta^2 = .369$, $1 - \beta = .844$), whose decomposition revealed task [OHb] lower than baseline only on the left side, and right higher [OHb] than left [OHb] during MI in highs (**Figure 3**). Lows exhibited higher [OHb] levels during tasks compared to baseline conditions on the left side. In the comparison between groups, highs' [OHb] was lower than lows' during MI and higher than lows during bMI on the left side. Controlling for TAS and Betts' V/K did not change the results.

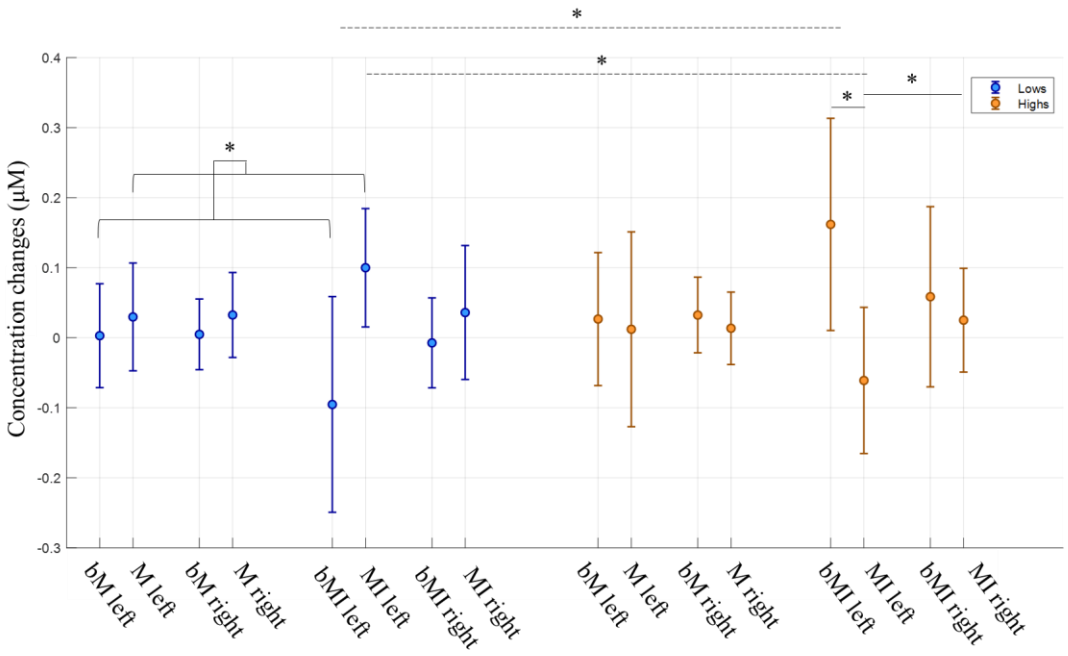

Figure 3. Dorsolateral prefrontal cortex.

Mean [OHb] in highs and lows (mean, S.D.). Continuous lines indicate within-group differences; dotted lines indicate between-group differences. In lows, both baseline values are lower than both tasks. *p < .005.

Peak [OHb] displayed significant **Condition x Level x Group** interaction ($F(1,18) = 8.55$, $p = .009$, $\eta^2 = .335$, $1 - \beta = .787$), consisting of higher [OHb] in task than baseline conditions only in lows. Highs exhibited lower [OHb] than lows during MI and higher [OHb] in baseline conditions (**Table S4**). TAS did not modify the results. Controlling for both Betts' V ($F(1,18) = 8.14$, $p = .012$, $\eta^2 = .337$, $1 - \beta = .764$) and Betts' K ($F(1,18) = 7.75$, $p = .013$, $\eta^2 = .326$, $1 - \beta = .744$) disclosed a significant **Condition x Level x Side x Group** interaction. Both decompositions revealed only higher [OHb] during M than bM on the left side in highs ($F(1,7) = 6.78$, $p = .035$) and lower [OHb] during M than MI ($F(1,8) = 7.95$, $p = .023$) in lows.

Mean and peak [HHb] did not show any difference between tasks and groups. Controlling for TAS disclosed a **Level** effect, with task < baseline ($F(1,18) = 4.64$, $p = .047$, $\eta^2 = .225$, $1 - \beta = .525$).

Both groups mean [OHb] increased during tasks on the left side in PMC. It did not change in the right primary motor and sensory areas during tasks

Premotor cortex

Mean and peak [OHb] did not differ between groups and conditions. Controlling mean [OHb] for Betts' V disclosed a significant **Condition x Level x Side** interaction ($F(1,18) = 9.45$, $p = .007$, $\eta^2 =$

.371, 1 - β = .823). Its decomposition revealed higher values during MI than bMI ($F(1,18) = 4.84$, p = .042) in both groups on the left side (**Figure 4**). Controlling peak [OHb] for TAS, Betts' V, and Betts' K did not modify the results.

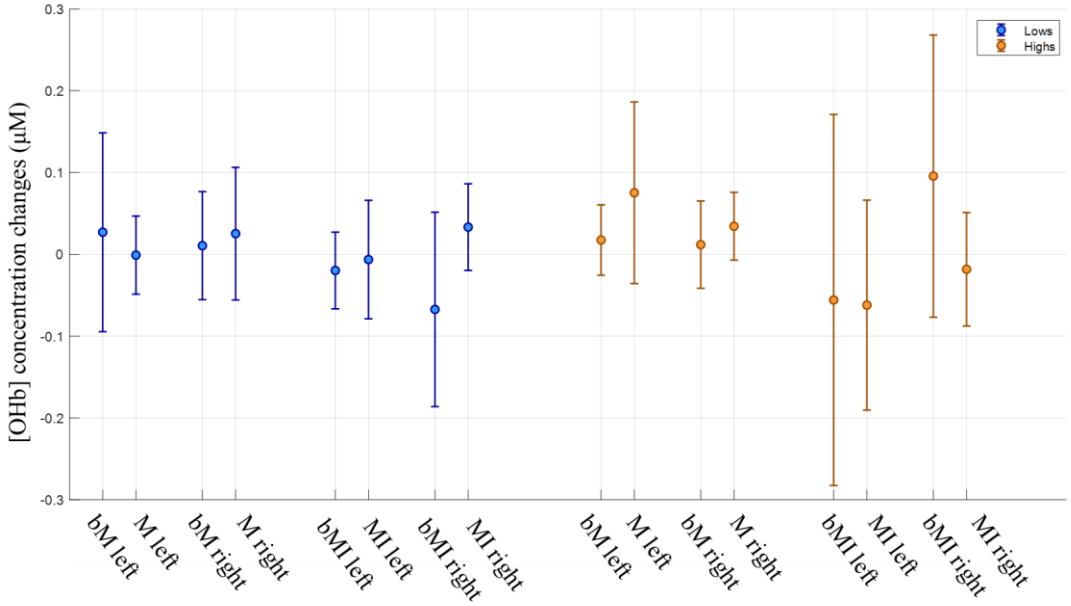

Figure 4. Premotor cortex.

Mean [OHb] in highs and lows (mean, S.D.).

For peak [HHb] we observed a **Condition x Level x Group** interaction ($F(1,18) = 9.08$, p = .008, η^2 = .348, 1 - β = .810). Its decomposition revealed a Condition x Level interaction in lows ($F(1,9)$ = 7.31, p = .024) who exhibited higher values in bM than M ($F(1,9) = 5.23$, p = .048), and no difference in highs. Controlling for TAS, Betts' V, and Betts' K does not modify the results

Right primary motor and sensory cortex (**Table S5**)

No significant differences were observed for mean [OHb] in M1 **(Figure 5**). Controlling for TAS disclosed a **Condition x Level x Group** interaction ($F(1,18) = 5.39$, p = .034, η^2 = .252, 1 - β = .588) sustained by higher values in bM than bMI in highs ($F(1,8) = 5.33$, p = .05) and no difference in lows.

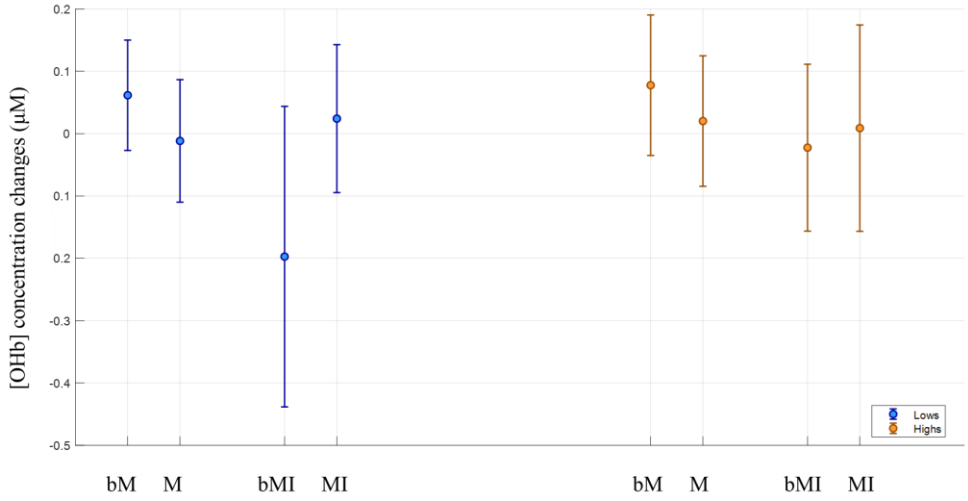

Figure 5. Right primary motor area.

Mean [OHb] in highs and lows (mean, S.D.).

ANOVA revealed a significant **Condition x Level x Group** interaction also for peak [OHb] ($F(1,18) = 6.87$, $p = .018$, $\eta^2 = .288$, $1 - \beta = .699$). Its decomposition revealed significant differences during tasks than baseline conditions in lows ($F(1,9) = 5.56$, $p = .043$). Controlling for TAS, Betts' V, and Betts' K did not modify the results.

No significant differences were observed in the mean values of [HHb]. Controlling for TAS disclosed a **Condition x Level x Group** interaction ($F(1,18) = 5.39$, $p = .034$, $\eta^2 = .252$, $1 - \beta = .588$). Its decomposition revealed a quasi-significant Cond x Level interaction in lows ($F(1,9) = 4.98$, $p = .056$), indicating only higher HHb during bMI than MI in lows ($F(1,9) = 5.26$, $p = .051$). Controlling for TAS, Betts' V, and Betts' K did not modify the results.

In S1, mean and peak values of [OHb] and [HHb] did not show significant differences between baseline and task conditions. Controlling for TAS, Betts' V, and Betts' K did not change the results.

Standard deviation and correlational analysis

No significant between-group differences were observed for standard deviation and were disclosed by controlling for TAS, Betts' V and Betts' K in all areas.

Different correlations, all surviving Bonferroni correction ($p = .01$), were observed during M and MI (**Figure 6)** for mean and peak [OHb]. During M, the rDLPFC mean [OHb] was positively

correlated with lPFC (R = .615, p = .005) and with right M1 (R = .606, p = .006). Partial correlations controlled for SHSS, TAS, Betts' V, and Betts' K did not change the correlation.

During MI, the lDLPFC mean [OHb] was positively correlated with the lPFC (R = .648, p = .003). This correlation was abolished when controlling hypnotizability. The lDLPFC was also correlated with the rPFC (R = .690, p = .001), which survived partial correlation controlled for hypnotizability, TAS, Betts' V, and Betts' K.

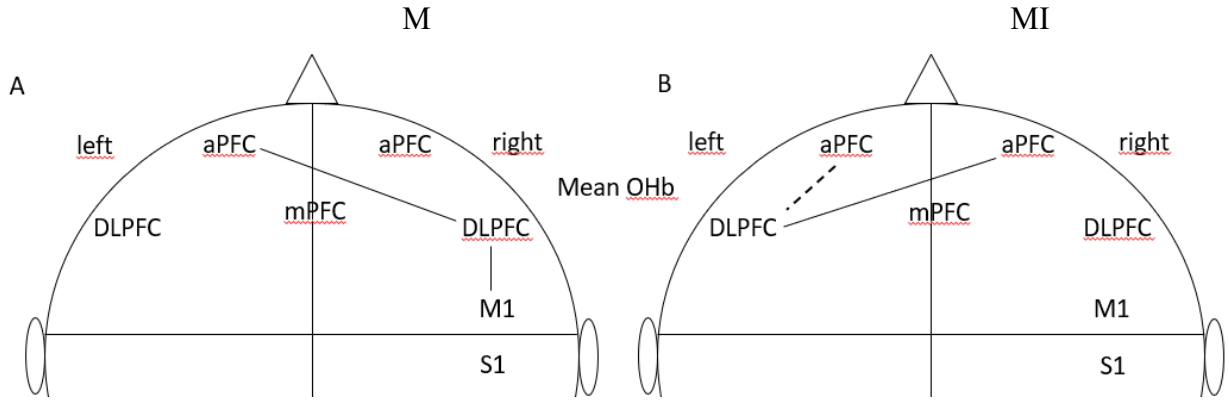

Figure 6. Correlations between mean [OHb] of areas during M (A) and MI (B).

Dotted lines indicate the correlations abolished by controlling for SHSS scores. aPFC, anterior prefrontal cortex, mPFC, medial prefrontal cortex; DLPC, dorsolateral prefrontal cortex; M1, primary motor area; S1, primary sensory area.

2.1.4 Discussion

The study aimed to compare brain oxyhaemoglobin [OHb] and deoxyhaemoglobin [HHb] concentrations in highs and lows under baseline conditions and during actual and imagined sequential movements. The findings support the hypothesis of lower synaptic activity in highs than lows during movement and motor imagery, in line with EEG studies reporting different information processing in highs and lows (Ibanez-Marcelo et al., 2019).

Subjective experience

Preliminary assessment of the participants' cognitive traits indicated higher scores of absorption in highs than in lows, and the absence of hypnotizability-related differences in the scores of visual and kinesthetic abilities, in line with earlier reports mostly indicating higher absorption in highs (Santarcangelo 2024) and no association of Betts' scale scores with the subjective efficacy of imagery (Szrich et al., 2016).

After the experimental session, the NASA questionnaire did not reveal significant group differences in imagery efficacy and effort, despite the lower [OHb] observed in highs than lows during tasks. A similar observation was made for postural control, which is similarly experienced by highs and lows despite the highs' larger sway amplitude and velocity (Santarcangelo et al., 2008).

Functional Near-Infrared Spectroscopy

Motor imagery and execution involve the interaction between prefrontal and sensorimotor regions (Yu et al., 2024; Chen et al., 2025), which are interconnected (Rolls et al., 2023), although they may contribute to executive functions differentially (Panikratova et al., 2020). According to current literature, increases in [OHb] indicate brain activation, while increases in [HHb] indicate deactivation (Kaiser et al., 2018). The observed light, often non-significant changes in [HHb] are in line with other reports describing its minor changes in the presence of substantial modifications in [OHb] (de Roever et al., 2018). Thus, the discussion of the findings will be focused on the mean [OHb].

Prefrontal regions

Overall, the two groups displayed opposite oxygenation patterns during tasks and baseline conditions with higher [OHb] during baseline and lower [OHb] during task in highs compared to lows. In the anterior, medial, and dorsolateral prefrontal areas, only the lows' mean [OHb] increased during tasks, as observed in the general population during motor (Anwar et al., 2016) and cognitive tasks (Jeong et al., 2025). During tasks, highs did not exhibit any [OHb] changes in the anterior PFC. They showed a decreased [OHb] in the medial PFC and in the DLPFC, suggesting that these areas belong to a larger processing network in which small, distributed changes better represent sensorimotor integration. Indeed, despite the slight and scarcely localized brain activities, highs experience less effort than lows due to their functional equivalence between actual and imagined perception/action (Ibanez-Marcelo et al., 2019), more flexible cognitive control (Rubichi et al., 2005; Cojan et al., 2009, 2015), and high absorption ability indicated by TAS scores. Absorption, which involves brain activity across large-scale networks (Linden et al., 2020), accounts for all the differences observed in mean [OHb] in the anterior, medial, and dorsolateral prefrontal regions, where highs exhibit higher activation of the right than left side during motor imagery. Given the role of the right DLPFC in visuo-spatial working memory (Ngetich et al., 2022), as well as in motor preparation and execution, attention allocation, and imagery (Kim et al., 2018; Yang et al., 2025), it is plausible that highs could recruit this region better than lows to manipulate information related to their left arm representation in space. At variance with the other prefrontal areas, the DLPFC changes in peak [OHb] were sustained by visual and kinesthetic abilities (Betts' V and K), which indicates a more complex role for DLPFC in motor

planning (Kim et al., 2018; Yang et al., 2025). The discrepancy between the modifications of mean and peak [OHb] during imagery in this area - no differences in mean [OHb] and increased peak during imagery in highs - can be due to initially increased blood supply leading to vessel diameter autoregulation, which is more efficacious in highs than in lows, as observed during hyperoxyemia, when high oxygen levels reduce the highs' cerebrovascular reactivity (Rashid et al., 2022c). Greater left than right mean [OHb] was observed for both actual and imagined action in the anterior and dorsolateral prefrontal cortex, despite the movement being performed and imagined for the left arm and hand. Indeed, a bilateral representation of imagined movements is often reported, although not consistently (Stinear et al., 2006; Martinez et al., 2019; Wang et al., 2025; Bondi et al., 2025).

Premotor, primary motor, and sensory areas

In the premotor cortex, both groups exhibited greater mean [OHb] during tasks than baseline. In the interplay between sensorimotor areas for movement preparation and execution, this area plays its role in the late part of the process, which is independent of absorption. In contrast, the Side differences in mean [OHb] were masked by the visual imagery ability, which confirms a significant role of sensory information in motor preparation (Egan et al., 2025). Peak levels were not influenced by hypnotizability, absorption, and imagery abilities, in line with the minor involvement of this region in motor planning, compared to prefrontal regions.

Due to the NIRS cap limitations, the primary sensory and motor areas were studied only on the right side, opposite to that of the actual and imagined movements. The absence of M1 activation during actual movement in this region may seem counterintuitive. We hypothesize that this is due to the repetitive characteristics of the sequential movement, which may have reduced motor cortex excitability —a phenomenon known as "cortical adaptation" (He, 2002). In contrast, the absence of activation during motor imagery on the right side was expected, owing to its suppression by the supplementary motor area (Kasess et al., 2008; Yoo et al., 2020). The most relevant difference between M1 and prefrontal regions was that absorption and imagery abilities did not influence mean [OHb], indicating a more stable configuration of the motor preparation and execution network compared to the high modulability of the prefrontal network for motor planning.

Correlations between regions

Prefrontal regions control motor imagery and execution differentially (Ogawa et al., 2022). In the present study, the activity of the right DLPFC mean [OHb] correlated with the ipsilateral primary motor cortex during the execution of left arm/hand movements, as reported by other authors (Hasan et al., 2013; Kim et al., 2018), and with the other executive areas bilaterally during imagery (**Figure**

4, Figure 5). However, blood oxygenation levels can increase bilaterally during the performance of complex motor tasks with the non-dominant arm (Van Impe et al., 2009). The absence of correlation of the primary motor cortex during imagery was expected due to its inhibition by the supplementary motor area. The exclusive left DLPFC participation in motor imagery can be attributed to the role played by the left DLPFC in selective attention, which, in this case, was directed toward the internal visual and proprioceptive memories necessary for mentally reproducing motor execution. Indeed, stimulation of the left DLPFC enhances its role in various executive functions (Vanderhasselt et al., 2006; Hwang et al., 2010; Li et al., 2017). Notably, the observed correlations survived controlling for hypnotizability during actual but not imagined action, indicating a greater relevance of hypnotizability to motor imagery than to actual movement.

Limitations and conclusions

A limitation of the study is the absence of monitoring of the systemic blood pressure, which was not available in the NIRS laboratory. Earlier studies have shown that the highs' cerebrovascular reactivity depends on systemic blood pressure, while the lows' one depends on the respiratory gases partial pressure (Rashid et al., 2022b). Nonetheless, the performed tasks were not expected to modulate vascular and respiratory function significantly. Additionally, more fine-grained signal acquisition may enable better identification of regions.

The present findings indicate significant increases in mean oxygenated haemoglobin during tasks only in lows, thus suggesting a less intense synaptic activity in highs, which accords with their minor EEG changes during actual and imagined action compared to baseline (Ibanez-Marcelo et al., 2019a,b; Ruggirello et al., 2019). The higher absorption capacity can sustain lower cognitive effort and synaptic activity in prefrontal regions during tasks. Imagery abilities were also relevant to the DLPFC's initial response to tasks. The [OHb] in the primary motor cortex was not influenced by hypnotizability, absorption, and imagery abilities, consistent with its role in motor execution only. In conclusion, near-infrared spectroscopy supports the findings previously obtained with electrophysiological methods regarding the highs' and lows' different information processing, which is scarcely localized in highs and more nested in lows during actual and imagined sensorimotor conditions (Ibanez-Marcelo et al., 2019a,b; Ruggirello et al., 2010).

2.2 Study 2. Brain plasticity induced by Motor Imagery Training: Role of cognitive abilities, interoceptive sensibility, and hypnotizability

Abstract

Background

The outcome of imagery-based rehabilitation treatments is variable, but high hypnotizability predicts greater similarity between the cortical correlates of actual and imagined action (functional equivalence, FE). The study investigated whether motor imagery (MI) training (MIT) improves subjective experience, chronometric indices, and the EEG correlates of MI (like physical training), and whether absorption, imagery abilities, and interoceptive sensibility influence the possible improvement.

Methods

Participants with high, medium, and low hypnotizability scores (measured by the Stanford Hypnotic Susceptibility Scale: Form A) participated in a session before MIT (S1) and another session after 15 days of MIT (S2). Each session included baseline condition (B), actual sequential movements of the left arm and hand (M), visual (V), and kinesthetic imagery (K) of the same movements. Time duration of actual and imagined movement was recorded (chronometric index). At the end of each imagery task, participants rated the perceived efficacy of imagery. EEG and EKG were monitored.

Results

After MIT, chronometric indices did not change, whereas the reported efficacy of imagery increased. Offset and exponent of the aperiodic EEG component increased only in highs and lows. Mu/alpha PSD decreased only in lows, low-beta PSD increased in highs and mediums, likely due to practice-related retention mechanisms, and decreased in lows; high-beta PSD decreased in all groups. Highs exhibited stronger FE than lows in low beta. Hypnotizability accounted for the aperiodic component exponent and for spectral changes; interoceptive sensibility accounted for the changes in offset. All groups exhibited improved cortical correlates of MI. Highs displayed neural plasticity in offset, and all groups displayed it in high beta, indicated by the similar changes occurred in baseline and task conditions after training.

Conclusion

MIT can be effective in the general population, although to different extent and through different EEG profiles, being useful for cosmonauts training and neurorehabilitation treatments on Earth.

2.2.1 Background

Motor imagery (MI) refers to the mental simulation of an action without its execution (Finke, 1979; Jeannerod, 1995). It is used to assist neurorehabilitation (Calderone et al., 2025), to counteract the deleterious effects of limb disuse (Debarnot et al., 2021), and to improve sports technical gestures (Frank et al., 2024; McNeil et al., 2025). The subjective efficacy of MI and its physiological correlates depend on sensorimotor conditions, which are impaired in neurological patients (MacIntyre et al., 2018; Scandola et al., 2017; Şekercan et al., 2025), on prior physical activity (Wriessnegger et al., 2018) and on individual traits, including the preferential choice of the visual and kinesthetic modality of imagery and their efficacy (Ahn & Jun, 2015; Guillot et al., 2008; Hanakawa et al., 2016; Ibanez-Marcelo et al., 2019).

A multidimensional approach is considered the best choice to capture the various aspects of MI (Collet et al., 2011), including subjective experience, behavioral indices, cortical activations, and the autonomic correlates of task engagement. The efficacy of imagery is indicated by the chronometric index (Guillot et al., 2012), which represents the difference in duration between the executed and imagined action, and reflects the task difficulty, as imagery time increases for highly demanding tasks (Owen et al., 2024; Dahm and Sachse, 2025).

Moreover, EEG rhythms desynchronize during both actual movement (M) and MI. They encode several MI components (Nakagawa et al., 2011), such as spatial sensorimotor attention, cognitive control (Stoll et al., 2016; Yin et al., 2016; Morrow et al., 2023), action preparation, execution, and termination (Pfurtscheller et al., 2009; Khanna & Carmena, 2015; Yin et al., 2016). Noteworthy, alpha and beta power suppression during MI is modulated by the bodily state, i.e., during the cardiac cycle (Lai et al., 2024), which emphasizes the interaction between sensorimotor and interoceptive signals (Zhang et al., 2024). The aperiodic component of the EEG signal (Donoghue et al., 2020) also differs in different conditions (eyes open/closed, cognitive tasks, resting state), and may indicate individual traits and states (Demuru and Fraschini, 2020; Dziego et al., 2023; Pi et al., 2024). It may also mask oscillatory activities, as occurs for the abolition of the suppression of mu activity during action observation (Harris et al., 2025).

According to the functional equivalence (FE) theory (Finke, 1979; Jeannerod, 1995), the more similar the cortical activities during actual and imagined movements, and/or the less different their durations (Collet et al., 2011), the more efficacious the MI. Stronger FE has been observed in individuals with high levels of hypnotizability (Santarcangelo et al., 2010; Ibanez-Marcelo et al., 2019), a psychophysiological trait indicating the proneness to experience altered perception, memory, and behavior following instructions to imagine contexts different from the actual one (Elkins et al., 2015). Hypnotizability remains stable throughout life (Piccione et al., 1989; Rasch & Cordi, 2024) and is

measured through standardized scales that classify individuals as high hypnotizables (highs), medium hypnotizables (mediums), or low hypnotizables (lows), who are characterized by distinct brain morphofunctional characteristics, behavioral and physiological peculiarities (Santarcangelo, 2024). In particular, beyond stronger FE, highs display greater excitability of the motor cortex during MI (Spina et al., 2020; Cesari et al., 2020) and stronger functional connectivity between the anterior cingulate cortex and the dorsolateral prefrontal cortex in basal and task conditions (Landry et al., 2017) compared to lows, which could account for their greater proneness to ideomotor action (Santarcangelo & Manzoni, 2021). Moreover, they differ in interoception (Craig, 2002; Garfinkel et al., 2015), as the highs' ability to perceive interoceptive signals (interoceptive accuracy) is lower than mediums and lows (Giusti et al., 2024), and their mode of interpreting them (interoceptive sensibility) is more adaptive (Diolaiuti et al., 2019).

In a single experimental session of MI (Malloggi et al., 2024), the hypnotizability-related differences in the absolute power of alpha and beta EEG bands were sustained by individual's proneness to be deeply absorbed in mental and physical tasks ("absorption"), imagery vividness, and interoceptive sensibility.

Predicting the efficacy of MI and assessing whether it can be improved by mental training would be relevant to clinical and sports applications. Thus, the present study aimed to investigate whether motor imagery training (MIT) improves the subjective, chronometric, and physiological correlates of MI in highs, mediums, and lows. Moreover, the study aimed to assess whether the ability to imagine, be deeply absorbed in imagination, and interpret interoceptive information influences the efficacy of MIT.

2.2.2 Methods

Participants

Thirty-four right-handed (according to the Edinburgh Handedness Inventory, Oldfield, 1971) healthy volunteers of both sexes were recruited among students at the University of Pisa for a study consisting of 2 sessions separated by 15 days of MIT. After signing the informed consent approved by the Bioethics Committee of the University of Pisa (n.29/2022), a semi-structured interview ascertained the absence of medical, neurological, psychiatric conditions, sleep and attention disorders, and any current pharmacological therapies. Participants were administered with the Italian version of the Stanford Hypnotic Susceptibility Scale: Form A (SHSS: A, range: 0–12) (Weitzenhoffer & Hilgard, 1959), classifying them as highs (SHSS score $\geq$ 8 out of 12, age: 28.41 $\pm$ 3.17), mediums (SHSS score 5–7, age: 26.33 $\pm$ 2.34), and lows (SHSS score $\leq$ 4, age: 29.54 $\pm$ 3.88). They were 12 highs

(35%, SHSS score: 9.83 ± 1.34; 7 females), 9 mediums (26.4%, SHSS score: 5.89 ± .78, 6 females), and 13 lows (40.6%, SHSS score: 0.46 ± .66, 3 females). They were aware of their hypnotizability score and the experimental procedure, but not of the study's aims. According to G*power (Faul et al., 2007), the minimum number of subjects required to detect main effects and interactions for repeated measures ANOVA for EEG measures (2 sessions, 2 sides, 4 conditions, 3 groups) was N = 15 (with f = .25, α = .05, 1−ß = .80, Malloggi et al., 2024). It was N = 21 for heart rate (4 conditions x 2 sessions x 3 groups), and N = 30 for chronometric indices and subjective efficacy (2 modalities (visual, kinesthetic) x 2 sessions x 3 groups).

Experimental Procedure

Two experimental sessions were conducted at the Department of Translational Research and New Technology in Medicine and Surgery (University of Pisa) at least one month after the hypnotic assessment to prevent the experiment from being influenced by the previous hypnotic assessment. Experiments took place between 9:00 and 12:00 a.m. in a quiet, dim, temperature-controlled room (approximately 21°C). The sessions were S1 (before training) and S2 (after 2 weeks of MIT). In both sessions, participants sat in a comfortable armchair with their eyes closed. On the day of S1, before the experiment, the proneness to be deeply involved in cognitive tasks, the visual and kinesthetic imagery ability, and the interoceptive sensibility were assessed through the Tellegen Absorption Scale (TAS, Tellegen & Atkinson, 1974), the Kinesthetic and Visual scales of the Betts' Questionnaire Upon Mental Imagery (Betts' V and Betts' K, Sheehan, 1973), and the Multidimensional assessment of Interoceptive Awareness (MAIA, Mehling et al., 2012), respectively.

Each session consisted of a 2-minute resting state (baseline, B), followed by two series of actual or imagined sequential movements performed through visual or kinesthetic modality. Before starting the sessions, an experimenter demonstrated the movement that participants had to accomplish and then imagine. The movement consisted of a sequence of ten repetitions of flexion–extension of the left arm and hand, along with finger-to-thumb tapping. An actual movements sequence (M), visually inspected by experimenters, preceded each three-repetition series of the same visually (V) and kinesthetically imagined (K) sequence. Each imagery series was preceded by listening to a 30-second, recorded guided imagery of the movement (**Figure 7**).

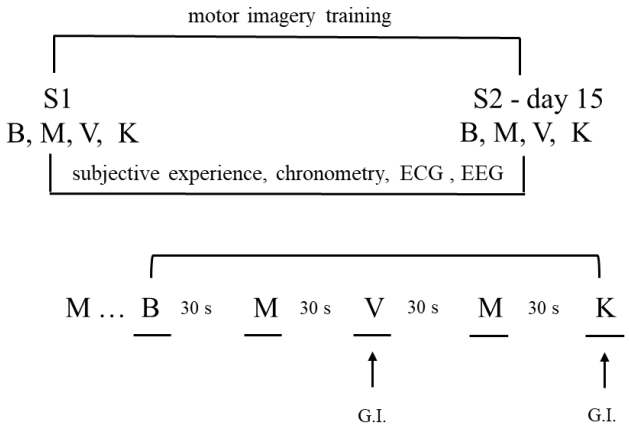

Figure 7. Experimental procedure.

Sessions and variables (upper panel); b) each session procedure (lower panel). G.I., guided imagery. M, actual movement; V, K, imagined movements.

The task conditions (M, V, K) were interspersed with 30-second baseline periods (B). The sequences of visual and kinesthetic imagery were randomized within each group.

To calculate the chronometric visual and kinesthetic indices, each condition was initiated by the experimenter vocal command ("Go") and ended when the subject indicated its end ("Stop"). The experimenter monitored the duration of both actual and imagined movements using a chronometer. At the end of each imagery trial, the participants rated the experienced efficacy of their visual and kinesthetic imagery (range: 0, min –10, max). After S1, a MIT script was recorded and sent to the participants' phones. Participants were instructed to perform MIT twice a day between S1 and S2 (**Figure 7**). A daily notification was scheduled on Google Calendar to remind the participants to perform the training. They were invited to cross it out if they had performed the training. On the day of S2, participants provided the experimenter with the screenshots of Google Calendar to evaluate their compliance with the motor imagery training (range: 0-100).

Imagery training instructions

Each suggestion lasted 30 seconds. For visual imagery, the script read by an experimenter was: "…*Now please imagine doing the same movement you did a few minutes ago. You can see your left arm flexing up to the shoulder…while your fingers touch your thumb one by one from the index to the little finger…*".

For the kinesthetic imagery, the script was: "…*Now, please imagine repeating the same movement you did a few minutes ago. You can feel the tension growing in your left biceps…. as it flexes up to the shoulder… while the muscles in your forearm start contracting and your fingers touch your thumb… one by one from the index to the little finger …*".

Signal acquisition and analysis

The electrocardiogram (EKG) and electroencephalogram (EEG) were acquired with the g.tec' multipurpose wireless biosignal acquisition tool Nautilus (G.tec Medical Engineering, Graz, Austria). An EEG cap with 28 electrodes placed in standardized positions according to the modified 10-10 international system was used (Fp1, Fp2, AF3, AF4, F7, F3, Fz, F4, F8, C3, FC1, FC2, C4, T7, Cz, T8, CP5, CP1, CP2, CP6, P7, P3, Pz, P4, P8, PO3, PO4, Oz). The reference was set at Cz and successively re-referenced to the averaged electrodes. Two additional EKG electrodes were placed according to the D1 standard derivation. The sampling rate was set to 500 Hz, and all impedances were kept below 30 kΩ (which was the best option for our EEG system). EEG pre-processing was performed with the EEGLAB toolbox (Delorme & Makeig, 2004). Signals were band-pass filtered (band pass: 0.5–45 Hz, two-way least-squares FIR filtering, according to the frequency bands analyzed, 8–30 Hz) and visually inspected to reject artifacts (for details, see Malloggi et al., 2024). Bad channels were interpolated by using spherical splines. Signals exceeding 70 μV were discarded. The retained EEG signals were downsampled to 256 Hz.

For every condition (B, M, V, K), the pre-processed EEG signal in F3, Fz, F4, C3, Cz, C4, P3, P4, PO3, and PO4 channels was subjected to fitting Oscillations and One-Over-f (FOOOF) algorithm, which decomposes power spectra into periodic and aperiodic components by parameterizing the power spectral density in log-log space (Donoghue et al., 2020).The aperiodic component is defined by the offset and exponent of the power spectral density, whereas the periodic component is characterized by the center frequency, bandwidth, and relative amplitude of the oscillatory peak. The offset is defined as the intercept of the regression in log10 units, which reflects the overall baseline level of power in the spectrum. The exponent is defined as the negative slope of the regression line, which describes how quickly power decreases as frequency increases (the steepness of the 1/f decay). The periodic component was then derived by subtracting the modeled aperiodic signal from the total PSD, constraining negative values to zero.

From this model, the band-specific Power Spectral Density (PSD) was computed using Welch's method (Welch, 1967). The PSD was integrated over alpha (8–12 Hz), low-beta (13–21 Hz), and high-beta (22–30 Hz) frequency bands and log-transformed. Over μ rhythm (8–12 Hz), PSD was integrated on the frontocentral Fz and Cz sites. PSD was averaged across the three visual imagery trials, the three kinesthetic trials, and two actual movement conditions. Alpha, low-beta, and high-beta PSD from each hemisphere were averaged in each condition (B, M, V, K) to increase the statistical power. Preliminary analysis revealed, however, that the fronto-central PSD was lower than the parieto-occipital one in all conditions and groups (**Table S6**). For mu rhythm, the PSD at Fz and Cz was averaged. The same regions and conditions were studied for aperiodic components, too.

Variables

As a preliminary assessment, we studied absorption (Tellegen Absorption Scale (TAS), measuring the proneness to be deeply involved in cognitive tasks (total score: 0, min –34, max)), the self-reported vividness of visual and kinesthetic imagery (Betts' Questionnaire Upon Mental Imagery; each item score: 1, max – 7, min), and the interoceptive sensibility (Multidimensional Assessment of Interoceptive Awareness (MAIA), consisting of 8 scales (noticing, not distracting, not worrying, attention regulation, emotional awareness, self-regulation, body listening, trusting) (each item range: 1- 5).

In the experimental sessions, we studied the reported efficacy of visual (Ve) and kinesthetic (Ke) imagery (score: 0, min–10, max), chronometric visual and kinesthetic indices (VCI, KCI) computed as [(actual movement duration—imagined movement duration)/actual movement duration], heart rate (HR), HR total (SDNN) and fast (RMSSD) variability in the time domain, the aperiodic 1/f component of the EEG and the oscillatory mu, alpha, low- and high-beta PSD. We also computed the difference between S2 and S1 for each band and condition.

Statistical Analyses

The Statistical Package for the Social Sciences (SPSS, Version 21) was used for the analyses. Univariate ANOVAs were applied to the compliance with the experimental protocol and TAS scores, while separate multivariate ANOVAs were applied to Betts' V and Betts' K dimensions, and to MAIA dimensions, with hypnotizability as a between-subject factor. Chronometric indices and the subjective efficacy of visual and kinesthetic imagery were studied according to a 3 Groups (highs, mediums, lows) x 2 Sessions (S1, S2) x 2 Modalities (V, K) design. HR, SDNN, and RMSSD were analyzed according to a 3 Groups x 2 Sessions x 4 Conditions (B, M, V, K) experimental design. The offset and exponent factors of the aperiodic EEG component and each EEG band PSD were studied according to a 3 Groups × 2 Sessions × 2 Sides (left and right hemispheres) × 4 Conditions (B, M, V, K) design. The Greenhouse-Geisser ε correction was used for non-sphericity. Contrast analyses were performed between conditions. The significance level was set at $p = .05$. After controlling collinearity, stepwise backward regression analysis was applied to the difference between S2 and S1 in each condition for both the aperiodic and oscillatory component to study the contribution of the studied traits to the training effects.

2.2.3 Results

ANOVAs applied to TAS, Betts' V, Betts' K, and MAIA dimensions (**Table S7**) did not reveal significant group differences.

Subjective and behavioral variables

At S2, all participants reported 100% compliance with the imagery training protocol. The subjective efficacy (**Figure 8A**) exhibited significant **Session** (S1 < S2, $F(1,31) = 21.85$, $p = .0001$, $\eta^2 = .413$, 1 - ß = .995) and **Modality** effects (K > V, $F(1,31) = 13.15$, $p = .001$, $\eta^2 = .298$, 1 - ß = .940). Stepwise regression analysis on the increase in S2 to S1 in the subjective experience revealed a significant contribution of MAIA attention regulation (B = -.420, p = .033, adj $R^2 = .108$)

Chronometric indices (**Figure 8B**) did not show significant effects and interactions. Experience and chronometric variables did not correlate with each other.

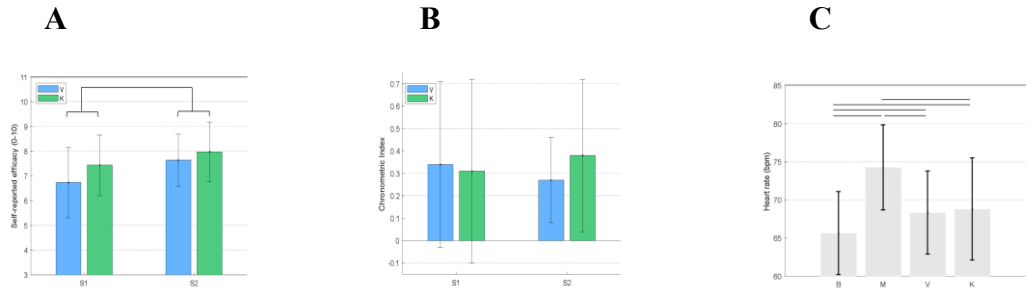

Figure 8. Subjective efficacy (A), chronometric indices (B), and heart rate (C; only Condition effect is represented) (mean and SD).

Lines indicate significant differences (p < .05).

Physiological variables

Heart rate and heart rate variability

HR (**Figure 8C**) exhibited a **Session** (S1 < S2, $F(1,31) = 5.26$, p = .029, $\eta^2 = .145$, 1 - ß = .604) and a **Condition** effect ($F(3,93) = 6.96$, p = .0001, $\eta^2 = .544$, 1 - ß = .999). The latter indicated lower HR in B than M ($F(1,31) = 85.96$, p = .0001), V ($F(1,31) = 10.93$, p = .002) and K ($F(1,31) = 15.95$, p = .0001). Moreover, HR was higher during M than V ($F(1,31) = 10.93$, p = .002) and K ($F(1,31) = 37.07$, p = .0001). Stepwise regression analysis on the difference in HR between S2 and S1 (adj $R^2 = .161$) revealed significant contribution of MAIA *attention regulation* (B = .415, p = .015, adj $R^2 = .147$)

SDNN and RMSSD (**Table S8**) did not show significant differences between sessions, conditions and groups.

EEG aperiodic component

Both exponent and offset 1/f components increased after training. The former was mostly accounted for by hypnotizability, the latter only by interoceptive sensibility.

Offset

In the frontocentral midline region, ANOVA revealed significant **Session** ($F(1,31) = 10.73$, $p = .03$, $\eta^2 = .257$, $1 - ß = .887$) and **Condition** effects ($F(3,93) = 19.46$, $p = .0001$, $\eta^2 = .386$, $1 - ß = .999$) and a **Session x Condition x Group** interaction ($F(6,93) = 2.75$, $p = .046$, $\eta^2 = .151$, $1 - ß = .854$). Its decomposition did not reveal any session and condition effects in mediums. S1 values were lower than S2 in lows ($F(1,12) = 4.89$, $p = .047$), and lower values were observed in M than B ($F(1,12) = 8.01$, $p = .015$). Highs exhibited lower values in S1 than S2 in all conditions except for M, and significantly higher values in B than in M in S1. In S2 higher values were observed in B than M, K, and V, and lower values in M than V and K. No differences were observed among groups. **Table 1** (section A) summarizes the significant differences sustaining Session x Condition x Group interaction. **Table S9** also reports non-significant differences.

Table 1. Offset differences in the (A) fronto-central midline and (B) hemispheric regions.

Session x Condition x Group interaction

A				B		
group		**F**	**p**		**F**	**p**
highs (df = 1,11)						
	B S1 < S2	15.60	.002	B S1 < S2	18.55	.001
	V S1 < S2	5.31	.042	V S1 < S2	8.11	.016
	K S1 < S2	6.67	.025			
	S1 B > M	12.10	.005	S1 condition	2.14	.11
	M < V	5.70	.036			
	S2 B > M	17.45	.002	S2 B > M	16.83	.002
	B > V	13.51	.004	B > V	13.00	.004
	B > K	21.83	.001	B > K	16.67	.002
	M < V	8.35	.015	M < V	6.46	.027
	M < K	4.98	.047	M < K	4.60	*.055*
mediums (df = 1,8)	session	.14	.71	B > M	11.19	.010
	condition	2.63	.073	B > K	7.66	.024
				M < V	13.45	.006
				M = K	3.77	.088
lows (df = 1,12)	S1 < S2	4.89	.047	S1 < S2	5.69	.034
	B > M	8.01	.015	B > M	9.53	.009
				M < K	9.41	.010
				V < K	7.36	.019

B, baseline; *df*, degrees of freedom; *K*, kinesthetic; *M*, movement; *S1*, first session; *S2*, second session; *V*, visual.

In hemispheric regions (FC-PO), we observed significant **Session** ($F(1,31) = 15.77$, p = .0001, η^2 = .337, 1 - ß = .970) and **Condition** effects ($F(3,93) = 17.70$, p = .0001, η^2 = .364, 1 - ß = .999) and a significant **Session x Condition x Group** interaction ($F(6,93) = 3.55$, p = .003, η^2 = .186, 1 - ß = .939). Its decomposition (**Table 1, section B**) revealed, in highs, higher values in S2 than S1 in baseline conditions and during V, and no differences for M and K. Within each session, there were significant differences between conditions only in S2, with B values higher than M, K, and V. M values were quasi-significantly lower than K and significantly lower than V. In mediums, a significant condition effect consisted of higher values of B compared to M and K. Lows exhibited higher values in S2 compared to S1, and a condition effect only consisting of higher values in B than M. No differences were observed between groups.

Figure 9 represents between-session aperiodic differences in highs and lows in fronto-central midline regions.

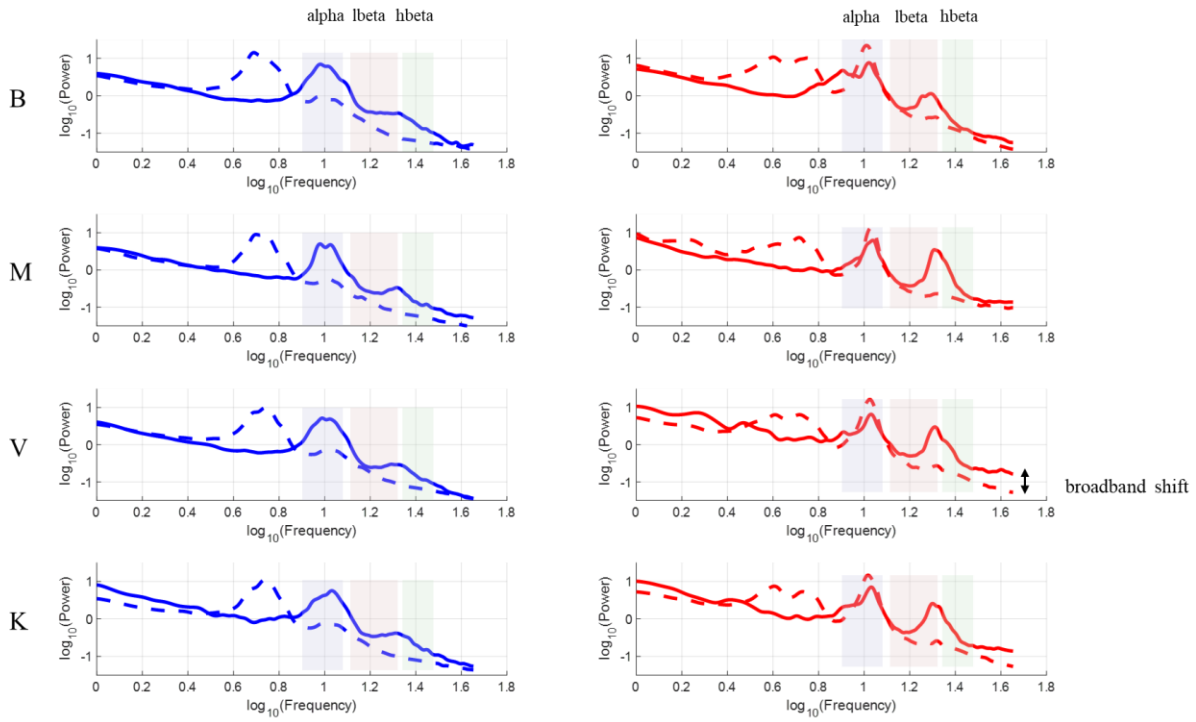

Figure 9. Power Spectra.

Lows (blue), highs (red). Continuous lines indicate the first session, dotted lines indicate the second session. The arrow indicates the changes in the aperiodic component offset. B, baseline; M, movement; V, visual imagery; K, kinesthetic imagery.

Exponent

In the frontocentral midline region, ANOVA revealed a significant **Condition** effect ($F(3,93) = 7.81$, $p = .001$, $\eta^2 = .201$, $1 - ß = .943$), and significant **Session x Group** ($F(1,31) = 9.39$, $p = .001$, $\eta^2 = .377$, $1 - ß = .967$) and **Session x Condition** interactions ($F(3,93) = 7.43$, $p = .004$, $\eta^2 = .193$, $1 - ß = .865$). Decomposition of the former revealed lower values in S1 than S2 in highs ($F(1,11) = 23.86$, $p = .0001$) and mediums ($F(1,8) = 5.71$, $p = .044$), and no differences between sessions in lows ($F(1,12) = 3.92$, $p = .071$). Groups did not differ between each other ($F = .58$, $p = .57$). Decomposition of the latter revealed significant differences between conditions only in S2 (B > K, $F(1,33) = 8.06$, $p = .008$; B > V ($F(1,33) = 7.90$, $p = .008$; B > M ($F(1,33) = 16.90$, $p = .0001$); M < K ($F = 8.99$, $p = .05$); M < V ($F = 11.04$, $p = .002$). No significant differences between sessions were observed (B: $F(1,33) = 3.63$, $p = .065$; M: $F(1,33) = 1.43$, $p = .24$; V: $F(1,33) = .12$, $p = .73$; K: $F(1,33) = .23$, $p = .63$).

In hemispheric regions, ANOVA revealed significant **Session x Group** ($F(2,31) = 10.79$, $p = .0001$, $\eta^2 = .411$, $1 - ß = .983$) and **Session x Condition** interactions ($F(3,93) = 3.53$, $p = .052$, $\eta^2 = .102$, $1 - ß = .537$). Decomposition of the former revealed lower values in S1 than S2 in highs ($F(1,11) = 23.57$, $p = .001$) and in lows ($F(1,12) = 4.80$, $p = .049$), but not in mediums.

No group differences were observed in S1, and higher values were observed in highs than in lows in S2 (p = .001). Decomposition of session x condition interaction revealed significant differences only between B and M in S2 ($F(1,33) = 8.79$, p = .06).

Table 2 reports the regression analysis of SHSS scores on the differences between S2 and S1 aperiodic components. It shows that hypnotizability accounts for the 1/f exponent, but not offset, whereas MAIA offered a scattered contribution to both components, and Betts' V and K to the exponent (**Table S10**).

Table 2. Regression analysis of SHSS on the 1/f exponent changes between sessions

	SHSS		
	B	p	adj R2
FzCz exponent			
ΔB	.374	.019	.361
ΔM	.594	.0001	.333
ΔV	.551	.001	.282
ΔK	.503	.002	.229
FCPO exponent			
left			
ΔB	.341	.034	.337
ΔM	.417	.009	.349
ΔV	.590	.0001	.328
ΔK	.420	.009	.345
right			
ΔB	.471	.004	.342
ΔM	.544	.0001	.435
ΔV	.530	.001	.340
ΔK	.407	.012	.321

adj R^2 , adjusted R^2; *B*, standardized beta; *Δ*, difference between S2 and S1 in baseline conditions (B), actual movement (M), visual (V) and kinesthetic (K) imagery; *FzCz*, frontocentral midline region; *FCPO*, fronto-central parieto-occipital region; *SHSS*, Stanford Hypnotic Susceptibility Scale.

EEG oscillatory components

Imagery was effective in all groups, but highs exhibited stronger FE than mediums and lows (low beta). High beta showed PSD changes independent of hypnotizability after training. PSD changes occurred after training also in baseline conditions, which reveal neural plasticity.

Mu PSD decreased in S2 compared to S1 (**Session**, $F(1,31) = 6.13$, p = .019, $\eta^2 = .165$, 1 - ß = .670) and exhibited a significant **Condition** effect ($F(3,93) = 20.19$, p = .0001, $\eta^2 = .394$, 1 - ß = .999) consisting of higher PSD in B than in M ($F(1,31) = 39.08$, p = .0001) K ($F(1,31) = 10.52$, p = .003, and V ($F(1,31) = 8.88$, p = .006). PSD was lower in M than in K ($F(1,31) = 20.77$, p = .0001)

and V (F(1,31) = 21.69, p = .0001), with V exhibiting the same PSD as K. ANOVA also revealed a significant **Session x Group** interaction (F(2,31) = 5.63, p = .008, η^2 = .266, 1 - ß = .824). Its decomposition did not reveal any differences between sessions in highs and mediums and a significantly higher PSD in S1 than S2 in lows (F(1,12) = 17.31, p = .002). Highs exhibited greater PSD than lows in S2 (p = .002).

Alpha PSD exhibited significant **Session** (S2 < S1, F(1,31) = 6.43, p = .016, η^2 = .172, 1-ß = .691) and **Condition** effects (F(3,93) = 23.22, p = .0001, η^2 = .428, 1-ß = .999), and significant **Session x Group** (F(2,31) = 4.69, p = .017, η^2 = .232, 1 - ß = .745) and **Session x Side x Condition** interaction (F(3,93) = 2.89, p = .040, η^2 = .085, 1 - ß = .673).

The former's decomposition (**Figure 10**) did not reveal significant session differences in highs and mediums, and greater PSD in S1 than S2 in lows (F(1,12) = 16.58, p = .002). Highs exhibited greater PSD than lows in S2 (p = .006).

Decomposition of the Session x Side x Condition revealed significant side differences in S1 baseline condition (left < right, F(1,33) = 4.27, p = .047) and no differences in S2. **Table S11** reports the significant differences between conditions in S1, revealing significantly lower PSD values in V than B on the left and the right side for both V and K; in S2, both K and V values were lower than B on both sides. Furthermore, the values of all conditions were lower in S2 than in S1.

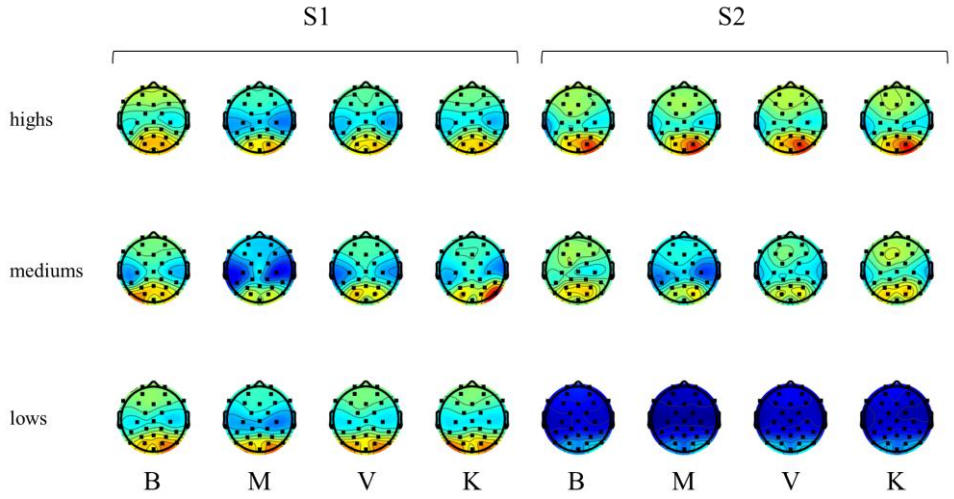

Figure 10. Topographical distribution of alpha PSD.

S1 (first session) and S2 (second session) in baseline condition, and during actual (M), visually (V), and kinesthetically imagined (K) action across groups. Decomposition of the Session x Condition x Group interaction not shown. Raw data.

Low-beta PSD (**Figure 11**) exhibited significant **Group** (F(2,31) = 10.52, p = .0001, η^2 = .404, 1 - ß = .981) and **Condition** effects (F(3,93) = 42.48, p = .0001, η^2 = .578, 1 - ß = .999), and **Session x Group** (F(2,31) = 10.17, p = .0001, η^2 = .396, 1 - ß = .977), **Condition x Group** (F(6,93) = .3.36, p = .005, η^2 = .178, 1 - ß = .924), and **Session x Side x Condition** (F(3, 93) = 3.37, p = .022,

η^2 = .098, 1-ß = .747) interactions. Decomposition of the Session x Group interaction revealed greater PSD in S1 than S2 only in lows (F(1,12) = 30.88, p = .0001), lower PSD in S1 than S2 in highs (F(1,11) = 7.29, p = .021), and no difference between sessions in mediums. Highs (p = .0001) and mediums (p = .002) displayed higher PSD values compared to lows only in S2.

Table 3. Low-beta Condition x Group interaction

		df	F	p
highs	B > M	1,11	30.38	.0001
	B > V	1,11	22.94	.001
	B > K	1,11	14.44	.003
	M = V			
	M = K			
mediums	B > M	1,8	64.89	.0001
	B > V	1,8	18.44	.003
	B > K	1,8	6.44	.035
	M < V	1,8	38.60	.0001
	M < K	1,8	17.44	.003
lows	B > M	1,12	37.31	.0001
	B > V	1,12	25.61	.0001
	B = K			
	M < V	1,12	6.86	.022

B, baseline; *df*, degrees of freedom; *K*, kinesthetic; *M*, movement; *V*, visual.

Decomposition of the **Condition x Group** interaction revealed than PSD was greater in highs than lows in B (p = .0001), M (p = .002), V (p = .001) and K (p = .005); mediums PSD was greater than lows in B (p = .002), M (p = .040), V (p = .005) and K (p = .031). **Table 3** reports lower values during M, K and V than B, with M not displaying different values from K and V in highs. In mediums, M, V, and K exhibited greater PSD than B, but M differed significantly from both K and V. In lows, only M and V exhibited lower PSD than B, and M values were lower than V. Decomposition of Session x Side x Condition is reported in **Table S12**.

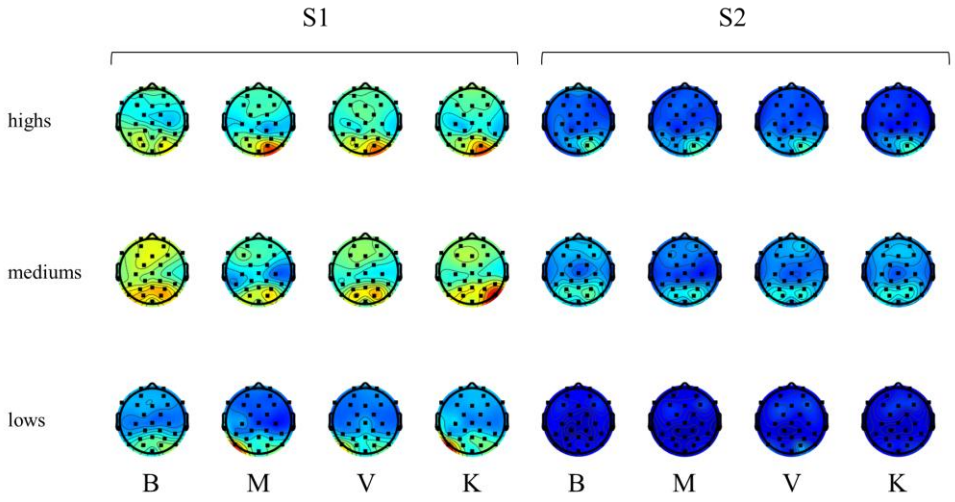

Figure 11. Topographical distribution of low-beta PSD.

S1 and S2 in baseline condition, and during actual (M), visually (V), and kinesthetically imagined (K) action across groups. Side differences not illustrated. Raw data.

For high beta, we observed significant **Session** ($F(1,31) = 108.37$, $p = .0001$, $\eta^2 = .778$, 1-ß = .999), with S1 > S2, and **Condition** effects ($F(3,93) = 3.60$, $p = .026$, $\eta^2 = .104$, 1 - ß = .694), and a **Session x Condition** interaction ($F(3,93) = 3.93$, $p = .033$, $\eta^2 = .113$, 1 - ß = .628). Its decomposition revealed that PSD was greater in S1 than in S2 in all conditions (p = .0001); B ($F(1,33) = 104.33$; M ($F(1,33) = 71.97$); V ($F(1,33) = 72.26$); K ($F(1,33) = 111.57$). In S1, PSD was lower only during M than B ($F(1,33) = 9.48$, $p = .004$). No differences were observed in S2 between conditions (**Figure 12**).

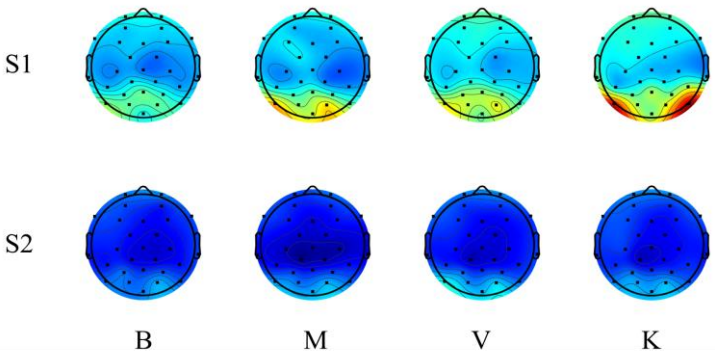

Figure 12. Topographical distribution of high-beta PSD.

S1 and S2 in baseline condition, and during actual (M), visually (V), and kinesthetically imagined (K) action. Raw data.

Regression analyses on the changes occurred between S1 and S2 in the EEG oscillatory components revealed significant hypnotizability contribution of SHSS to alpha and low-beta changes (**Table 4**),

whereas the contribution of some MAIA dimensions (not distracting, noticing, trusting) and Betts' V scores were limited to ΔK in the mu band (**Table S13**). TAS did not contribute at all.

Table 4. SHSS contribution to changes in oscillatory components

						SHSS					
mu	**B**	**p**	**adj R2**	**alpha**	**B**	**p**	**adj R2**	**low beta**	**B**	**p**	**adj R2**
ΔB	.659	.0001	.401	left				left			
ΔM	.512	.002	.239	ΔB	.581	.001	.389	ΔB	.572	.0001	.306
ΔV	.524	.001	.252	ΔM	.454	.007	.181	ΔM	.570	.0001	.397
ΔK	.617	.0001	.400	ΔV	.457	.007	.184	ΔV	.597	.0001	.477
				ΔK	.438	.010	.167	ΔK	.580	.0001	.315
				right				right			
				ΔB	.432	.005	.392	ΔB	.556	.0001	.371
				ΔM	.441	.009	.169	ΔM	.563	.0001	.398
				ΔV	.523	.002	.262	ΔV	.619	.0001	.364
				ΔK	.553	.001	.301	ΔK	.591	.0001	.329

adj R^2, adjusted R^2; *B*, standardized beta; *Δ*, difference between S2 and S1 in baseline conditions (B), actual movement (M), visual (V) and kinesthetic (K) imagery; *SHSS*, Stanford Hypnotic Susceptibility Scale.

2.2.4 Discussion

The study aimed to assess whether the efficacy of imagery in participants with low to medium hypnotizability scores may benefit from motor imagery training, which would extend the applicability of motor imagery to space flights and neurorehabilitation treatments from highs to the general population. The findings support this hypothesis, as they show that imagery training induces brain plasticity (Buckner & Vincent 2007; Guerra-Carrillo et al. 2014), like physical training (Amad et al. 2017), and indicate that interoceptive sensibility cooperates with hypnotizability in sustaining the training effects.

Subjective and chronometric variables

The efficacy of both imageries increased after training, and the kinesthetic modality was more effective than the visual one, which accords with the different functional connectivity reported for them (Yang et al., 2021), although the related cortical activations overlap almost entirely with each other (Kilintari et al., 2016; Filgueiras et al., 2018). The better effectiveness of the kinesthetic modality could be due to its deeper relation with the body schema, whose neural underpinnings are associated with the motor system, that is, with the premotor cortex and intraparietal sulcus (Parsons et al., 1995; Ehrsson et al., 2005), which are activated during kinesthetic imagery (Kasai et al., 1997; Liang et al., 2007; Bhattacharjee et al., 2021; Barhoun et al., 2022). On the contrary, visual imagery

primarily activates the primary visual cortex (Ragni et al., 2020; Park et al., 2022), although the areas of activation largely overlap (Ridderinkhof & Bras, 2015; Filgueiras et al., 2018). The training effects on subjective variables depended on MAIA *attentional regulation*, in line with the role played by interoceptive sensibility in a single imagery session (Malloggi et al., 2024).

Chronometry was not sensitive to training, supporting the independence of most imagery measures from one another (Collet et al., 2011; Williams et al., 2015). We might argue that the temporal equivalence between actual and imagined movements does not necessarily represent an index of overall performance accuracy and may fail to capture all aspects of motor imagery quality. Indeed, a single reliable index has not been found, and we agree with Collet and colleagues (2011) on the necessity of a multidimensional evaluation of motor imagery. On the contrary, subjective measures are in line with physiological findings.

Physiological variables

Participants did perform mental imagery, as evidenced by the increased heart rate during tasks in both sessions, which reflects an enhanced sympathetic/decreased parasympathetic tone (Dallaway et al., 2022) independent from the task content (Kim et al., 2018). The heart rate increase was sustained by MAIA *attentional regulation,* in line with the cardiac effects associated with cognitive engagement/effort (Forte et al., 2019), and with the role of interoceptive sensibility in motor imagery (Malloggi et al., 2024).

EEG aperiodic 1/f component

Both the oscillatory and aperiodic components of the EEG signal have been associated with cognitive abilities (Dziego et al., 2023) and cognitive styles (Pi et al., 2024). After training, both midline and hemispheric EEG aperiodic components increased in highs, indicating a modified balance between arousal and rest, shifting towards a more relaxed state. Of note, also mediums and lows showed training-induced aperiodic changes, but not for all components; indeed, lows increased their 1/f midline and hemispheric offset and their hemispheric exponent, while mediums increased the exponent on the hemispheric regions, suggesting a greater relevance of this component to both sensorimotor representation and attentional processes in the general population represented by mediums (De Pascalis et al., 2000). Nonetheless, offset differed between baseline and actual movement, whereas the changes in exponent were sustained by hypnotizability, in line with the observation of its difference between highs and lows, earlier observed in resting conditions (Landry et al., 2024). The offset component was independent from hypnotizability, and more sensitive to interoceptive sensibility. Its increase, together with exponent increase in highs and lows after training,

could be accounted for by reduced attention demand associated with greater recruitment of inhibitory GABAergic neural pathways, rather than excitatory glutamatergic pathways (Gao et al., 2017). However, only highs modulated tasks differentially after training, displaying functional equivalence between actual and kinesthetically-imagined movement for hemispheric offset, thus their performance was better than mediums and lows. Modulation of EEG aperiodic components have been associated with levels of consciousness (Widmann et al., 2025), cognitive function (Frelih et al., 2024) and various neurological diseases (Martínez-Cañada et al., 2023). Reduced level of consciousness during deep sleep, anesthesia, and coma are associated with 1/f steeper slope and higher broadband power, whereas high arousal conditions like attention exhibit 1/f decreased exponent and offset (Montemurro et al., 2024; Rosenblum et al., 2025; Zhao et al., 2025; Borah et al., 2025). Thus, based on the aperiodic component, we argue that, after training, the attention request was lower than before it.

EEG Power Spectral Density

In the present study, we consider imagery as effective if the visual and/or kinesthetic imagery conditions exhibit a PSD lower than baseline conditions, and highly effective if actual and imagined movements share the same PSD, which indicates functional equivalence (Finke, 1979; Jeannerod, 1995).

The PSD reduction observed in high beta supports the fact that the participants became more engaged in the tasks after training (Calmels et al., 2006; Yi et al., 2016; Garro et al., 2025). The hypnotizability-related differences between sessions in mu and alpha, observed only in lows, indicate that this group required more attentional effort (Bressler et al., 2015; Magosso et al., 2019) than highs and mediums, who did not modulate these rhythms.

The highs' and mediums' increase in low-beta PSD after training contrasts to all other bands and can be attributed to practice-related mechanisms of motor skill retention (Nelson et al., 2017), which induce better top-down control after perceptual learning training for motor sequences (Theves et al., 2020; Dyck & Klaes, 2024). Indeed, both physiological and experimental cortical stimulation favors cortical plasticity (Kweon et al., 2023). This mechanism could have been not effective in lows due to their motor cortex lower excitability (Spina et al., 2021) In low beta, highs exhibited functional equivalence between the actual and imagined movements, thus their performance was better than mediums, exhibiting a less strong similarity between the two conditions, and lows, who displayed only effective visual imagery. The lows' more effective visual than kinesthetic performance accords with earlier reports describing their preferential choice of the visual modality of imagery (Santarcangelo et al., 2010). The mediums' results indicate imagery-dependent changes only on the

right side, contralateral to movements, during kinesthetic imagery. In the general population, inconsistent findings have been reported about contralateral or bilateral movement representation in the general population (Stinear et al., 2006; Martinez et al., 2019; Wang et al., 2025). The sample composition might account for inconsistencies. High-beta PSD decreased in the second session during both imagery tasks independently of hypnotizability. The similar high-beta PSD observed in highs, mediums and lows during imagery tasks suggests that this rhythm, which encodes both cognitive and motor aspects of imagery (Stoll et al., 2016) and increases during high-demanding tasks (Kamiński et al., 2012), may reflect a different balance between attentional engagement and mode of action representation in the three groups. The hypnotizability-related differences in this rhythm were masked by interoceptive sensibility, which indicates a cooperation between these two traits in high-beta modulation.

Most of the observed EEG changes after training were sustained by hypnotizability and interoceptive sensibility. Trait imagery abilities appeared less relevant to the EEG correlates of imagery, in fact they were not expected to predict functional equivalence between actual and imagined action (Srzich et al., 2016). Side differences were present only in mediums, and only for low-beta PSD. They indicate greater activation on the right side during actual and kinesthetically imagined action, in line with what is expected for left movements in the general population. However, both contralateral and bilateral activations have been reported for motor imagery (Stinear et al., 2006; Martinez et al., 2019; Wang et al., 2025). The asymmetry observed for actual and kinesthetically imagined movement, but not for visually imagined movement, suggests a significant role for proprioception in the representation of complex movement. Indeed, kinesthetic imagery is associated with greater corticospinal excitability compared to visual imagery and produces better results than visual imagery (Lebon et al., 2018), likely due to a more extensive control network (Kraeutner et al., 2014).

Finally, it is noteworthy that the decreases in high-beta PSD in all groups and in aperiodic offset component in highs were observed after training also in baseline conditions, indicating training-induced plasticity. Indeed, resting state neuroplasticity is considered an effective measure of plasticity, and fMRI studies show that resting-state is modulated like the trained-task-related regions (Buckner & Vincent 2007; Guerra-Carrillo et al., 2014). Thus, MI training effects could persist after training interruption, in line with the consolidation processes observed after motor practice (Amad et al., 2017).

Limitations and Conclusion

A limitation of the study is that the EEG signals were averaged across each hemisphere, which may mask potential differences in the efficacy of the visual and kinesthetic modalities of imagery. However, subjective experience, heart rate, and EEG findings suggest that imagery training improves motor imagery in the general population. Additionally, absorption did not differ between groups, which aligns with recent findings (Scacchia & De Pascalis, 2020), but contrasts with earlier evidence (Santarcangelo, 2024). Finally, the absence of group difference between MAIA dimensions must be attributed to the sample size, which should have been much larger to be able to replicate the previous findings of more adaptive interoceptive sensibility in highs than in mediums and lows (Diolaiuti et al., 2019).

In conclusion, 15-day motor imagery training is efficacious in all groups, although to different extent and with different changes in the aperiodic and oscillatory EEG components, with highs performing better than mediums and lows. Neural plasticity indicated by modifications in both baseline and task conditions were observed in all groups. Absorption and interoceptive sensibility sustain the effects on the subjective experience and physiological variables, which emphasizes the role of these traits based on "inwardly focused" cognitive style in motor imagery (Kvamme et al., 2024), and on the close relationship between motor and interoceptive systems (Lai et al., 2024). Further research should assess whether the effects of motor imagery training persist beyond the interruption of training. Clinical trials are required to extend present findings to medical practice. For patients, mental imagery training may represent an easy, non-time-consuming, and cheap tool to enhance the effects of neuro-rehabilitative treatments. Also, the aforementioned findings can be applied to tailor motor and cognitive training interventions for adaptation to extreme conditions like microgravity during spaceflights.

2.3 Study 3. Interplay between cognitive conditions and individual traits in voluntary apnea

Abstract

Background

Apnea is employed to enhance performance in diving and other sports due to its specific physiological correlates. Its duration can be enhanced through training and the use of specific cognitive strategies and can be influenced by individual traits. Hypnotizability might be one of them, as it is associated with interoceptive sensibility and imagery abilities. The study investigates whether these traits affect apnea duration during imagery of normal breathing (motor imagery, MI, a cognitively incongruent condition) and while focusing attention on apnea sensations (internally focused attention, IFA, a cognitively congruent condition) in participants with different hypnotizability scores.

Methods

Hypnotizability was assessed in healthy participants, classified as low-to-medium (med-lows, N = 16) and medium-to-high hypnotizables (med-highs, N = 17), according to the Stanford Hypnotic Susceptibility Scale: Form A. They completed the Multidimensional Assessment of Interoceptive Awareness and the Movement Imagery Questionnaire-3 to assess interoceptive sensibility and trait imagery abilities. They performed three apnea trials for IFA and MI in counterbalanced order. During baseline and apnea conditions, heart rate and skin conductance were monitored. The vividness and easiness of MI and IFA tasks were reported.

Results

Apnea duration increased across trials independently of the cognitive condition and hypnotizability ($p = .032$). Heart rate increased during MI more than during IFA ($p = .002$), skin conductance decreased quasi-significantly during both tasks in both groups ($p = .054$). ANCOVA with imagery abilities and interoceptive sensibility as covariates indicated that these traits masked hypnotizability-related differences in the tasks' subjective experience, heart rate, and the increase in apnea duration across trials.

Conclusion

Hypnotizability, imagery abilities, and interoceptive sensibility jointly contribute to increase apnea duration across trials and to the associated subjective experience and autonomic response.

2.3.1 Background

Voluntary apnea, also known as breath-hold, represents a specific physiological state characterized by coordinated autonomic responses, including bradycardia, increased mean arterial blood pressure, peripheral vasoconstriction (Ferrigno & Lundgren, 2003), and reduced haemoglobin saturation (Ichinose et al., 2017). These changes reflect the diving reflex, an oxygen-conserving response that aims to maintain cerebral and cardiac perfusion under hypoxic stress. Breath-holding time is determined by the increase in CO_2 and lung volume (Godfrey et al., 1969; Godfrey & Campbell, 1969; Kelman & Wann, 1971) and by the preceding oxygenation rate (Bruce et al., 2021). The reported urge to breathe is positively correlated with the magnitude of the thoracic and abdominal expansion (Decavèle et al., 2025).

Apnea elicits a maximal autonomic response, as the change in blood pressure is not sensitive to additional cold stimulation (Matsutake et al., 2025). Adenosine is likely involved in its adaptive cardiovascular response because of its vasodilating and bradycardic properties (Marlinge et al., 2021). Apnea performance can be trained, as observed in swimmers and divers who can hold their breath for over 10 minutes and exhibit marked increases in cerebral blood flow (Arce-Álvarez et al., 2021; Bain et al., 2018). Cognitive factors also modulate apnea duration, including time perception and mental tasks such as imagery of normal breathing and deep absorption in the apnea-related sensation (Vigran et al., 2019; Kanthack et al., 2019).

Motor imagery, hypnotizability and interoception

Motor imagery (MI) refers to the mental simulation of a movement without overt motor output (Decety, 1996) and is used in sports to enhance performance (McNeil et al., 2025). It can be experienced either through internal visual imagery from a first-person perspective or through kinesthetic imagery, which involves vivid sensations of movement (Munzert et al., 2009). MI is characterized by subjective, behavioral and physiological variables that are influenced by imagery abilities (Guillot et al., 2009), motor conditions (Di Rienzo et al., 2022) and interoceptive sensibility (Malloggi et al., 2024). The latter represents the experience and interpretation of internal bodily signals (Critchley & Garfinkel, 2017) and is measured by questionnaires (Mehling et al., 2018; Porges, 1994). MI is also influenced by hypnotizability, a psychophysiological trait measured by scales that evaluate the ability to experience cognitive and physical states different from the actual ones (Santarcangelo, 2024). High hypnotizability is associated with greater functional equivalence between actual and imagined perception/action, that is, more similar cortical activations and connections during the two conditions (Ibanez-Marcelo et al., 2019 a,b), and the greater excitability

of their motor cortex during imagery (Spina et al., 2020; Cesari et al., 2020). Also, hypnotizability levels display different "adaptive" interoceptive sensibility (Diolaiuti et al., 2020), and interoceptive accuracy (Giusti et al., 2024), that is the ability to accurately detect interoceptive information, likely due to hypnotizability-related variations in the insula grey matter volume (Landry et al., 2017; Picerni et al., 2019).

Aim of the study

In the general population, apnea duration is influenced by the concomitant cognitive context, with longer durations observed during MI of normal breathing compared to IFA (Kanthack et al., 2019). Since imagery abilities, interoceptive sensibility, and hypnotizability are interrelated (Zelič et al., 2023), the present study aimed to expand the findings of Kanthack et al. (2019) about apnea duration in cognitively congruent and incongruent conditions by examining the role of these individual traits in modulating apnea duration during both conditions.

2.3.2 Methods

Participants

Thirty-three healthy sedentary volunteers (age mean $\pm$ SD): 27.2 $\pm$ 8.5; 15 females) were recruited among the students at the University of Pisa. After signing an informed consent approved by the Pisa University Bioethics Committee (n.29/2022), a semi-structured interview ascertained the absence of cardiovascular, respiratory, neurological, psychiatric conditions, sleep and attention disorders, and any current pharmacological therapies. Participants were administered with the Italian version of the Hypnotic Susceptibility Scale: Form A (SHSS: A, range 0–12) (Weitzenhoffer & Hilgard, 1959), classifying them in highs (score $\geq$ 8 out of 12), mediums (score 5–7) and lows (score $\leq$ 4). In the general population, mediums represent 70%, while highs and lows represent 15% each (De Pascalis et al., 2000). Owing to the small number of recruited mediums, a group of medium-to-highs (med-highs including 2 mediums, 8 females, SHSS score (mean $\pm$ SD): 8.88 $\pm$ 1.32) and a group of medium-to-lows (med-lows, including 3 mediums, 7 females, SHSS score: 2.88 $\pm$ 1.82) were studied.

For a preliminary assessment of the participants' psychophysiological traits, they completed the Multidimensional Assessment of Interoceptive Awareness (MAIA; Mehling et al., 2018) and the Motor Imagery Questionnaire-3 (MIQ-3; Williams et al., 2012). The MAIA questionnaire includes 8

scales (noticing, not distracting, not worrying, attention regulation, emotional awareness, self-regulation, body listening, trusting; range 0-5), while the MIQ-3 includes three modalities (external visual, MIQEVI; internal visual, MIQIVI; kinesthetic imagery, MIQKI; total range 0 - 28). For experiential and behavioral variables, which were studied during tasks, G*power (Faul et al., 2007) indicated a minimum number of 20 subjects to obtain significant main effects and interactions for experiential and behavioral variables, and a minimum number of 14 subjects for physiological variables with $f = .25$, $p = .05$, and $1-\beta = .80$.

Experimental procedure

The experiment was performed at least one week after the hypnotic assessment. The participants were asked to refrain from caffeine and alcohol for the three hours preceding the session, which was conducted in a sound and light-attenuated room. Before starting the experimental procedure, participants completed the State Anxiety Questionnaire (STAI-Y1; cut off for clinical anxiety = 52; Spielberger, 1983). Before undergoing the experimental conditions, participants performed a familiarization trial of apnea until their breaking point, without cognitive instructions.

The experimental closed-eye session included 2-minute baseline intervals (spontaneous, non-controlled breaths), following every trial of IFA (B1) and MI (B2) to let physiological signals return to baseline. Three maximal breath-hold trials were performed for IFA and MI in a seated position, with knees at 90° and with hands and forearms placed on the thighs. Before the breath-hold tasks (apnea), participants were instructed to take a deep breath. The inspiratory act was considered acceptable if its depth was at least one and a half times the normal breath, as controlled online by a Compumedics Summit IP® Inductive Respiratory Effort System (Compumedics, Newton, PA, USA). The duration of the breath hold was measured with a chronometer and controlled online by visualizing the respiratory signal. Participants were blinded to their maximal breath-hold duration.

In the IFA condition, participants were instructed to focus on the bodily sensations that emerge during breath-holding. The experimenter provided guidance using instructions such as: *"Focus on the sensations associated with the effort of voluntary breath-holding. Feel the muscle contractions pressing against your lungs and the tension in your chest as it remains still. Notice the absence of movement in your respiratory tract and the growing urge to breathe."*. In the MI condition, performed while imagining normal breathing, participants were instructed to engage in both visual and kinesthetic imagery of natural respiration. They were guided with instructions such as: *"Imagine the*

sensations associated with breathing. Feel the air entering your nose and the pressure changes in your lungs and chest. Sense the muscular contractions and stretches accompanying inhalation and exhalation, as if you were breathing." After each apnea trial, the participants were invited to rate the vividness and easiness of their IFA and MI experience.

IFA and MI were randomly administered to the participants. After each apnea trial, the participants were invited to rate the vividness and easiness of their IFA and MI experience.

Signal acquisition and analysis

Electrocardiogram (EKG) and skin conductance level (SCL) were monitored by a Psylab device (Contact Precision Instrument) and stored for offline analysis. For EKG acquisition, disposable electrodes (https://www.fiab.it/it/index.php) were placed according to the standard DI configuration. SCL was recorded using two similar electrodes placed on the middle phalanges of the index and middle fingers of the dominant hand. A common reference electrode was used for both EKG and SCL signals. A band-pass filter (0.5 Hz - 20 Hz) was applied to the EKG signal, and HR was computed as 60/mean RR interval for each condition (B1, B2, IFA, MI). Heart rate variability (HRV) was estimated using the root mean square of successive differences (RMSSD), a time-domain index reflecting short-term parasympathetic modulation. RMSSD values were interpreted in consideration of normative data for short-term resting conditions (Nunan et al., 2010). Notably, total HRV (SDNN) could not be studied due to the short duration of the studied conditions (Shaffer et al., 2017). For SCL, the signal was detrended, and its mean value was subtracted from the entire signal as baseline removal. A fourth-order low-pass butter filter was applied with a cut-off frequency set at 0.5 Hz. Then, a Savitzky-Golay smoothing filter was applied (Savitzky & Golay, 1964). Breath-hold trials were averaged during IFA and MI, respectively, as well as baseline intervals. The mean value of HRV and SCL was computed for each condition.

Variables

For the assessment of interoceptive sensibility and motor imagery abilities, we studied MAIA and MIQ-3 scales. The variables studied during the experimental session were experiential (state anxiety, STAI-Y1, Spielberger, 1983, vividness and easiness of IFA and MI, range 1 min - 7 max), behavioral (apnea duration, s), and autonomic (heart rate (HR, bpm), HR fast variability (RMSSD, ms), and skin

conductance level (SCL, μS)). A reduced number of participants (N = 21, 10 med-highs and 11 med-lows) agreed to undergo the assessment of HR and SCL.

Statistical analyses

The statistical Package SPSS 15 was used for all analyses. For the preliminary assessment, separate multivariate analyses of variance (MANOVAs) were conducted on the MAIA and MIQ-3 scales. For the experimental session, univariate ANOVA was applied to STAI-Y1 scores. Repeated measures ANOVAs were applied to apnea duration, vividness, and easiness of the cognitive tasks, according to a 2 groups (med-highs, med-lows) x 2 Tasks (IFA, IM) x 3 Trials (T1, T2, T3) design.

Repeated measures ANOVAs were applied to HR, RMSSD, and SCL following a 2 Group (med-highs, med-lows) x 3 Trial (T1, T2, T3) x 2 Task (IFA, MI) x 2 Level (baseline, task). The Greenhouse-Geisser ε correction was used for non-sphericity. Contrast analysis between levels was performed. ANCOVAs were applied to apnea duration, vividness, easiness, HR, RMSSD, and SCL, controlling MIQ-3 and MAIA dimensions.

In addition, linear backward regression analysis was performed to detail the magnitude of the effects of hypnotizability, MAIA and MIQ scores, HR, and SCL on the apnea duration.

2.3.3 Results

Questionnaires

MIQ-3 scores (Cronbach's alpha = .63) were not significantly different between groups (**Figure 13A**). MAIA scales (Cronbach's alpha = .89) did not exhibit a significant group effect. Nonetheless, not worrying ($F(1,30) = 4.42$, $p = .044$), self-regulation ($F(1,30) = 7.81$, $p = .009$) and body listening ($F(1,30) = 4.63$, $p = .040$) differed between med-highs and med-lows (**Figure 13B**).

STAI-Y1 scores did not differ between groups (mean $\pm$ SD; med-highs, 31.59 $\pm$ 8.96; med-lows, 33.18 $\pm$ 8.41) and were in the normality range (< 52).

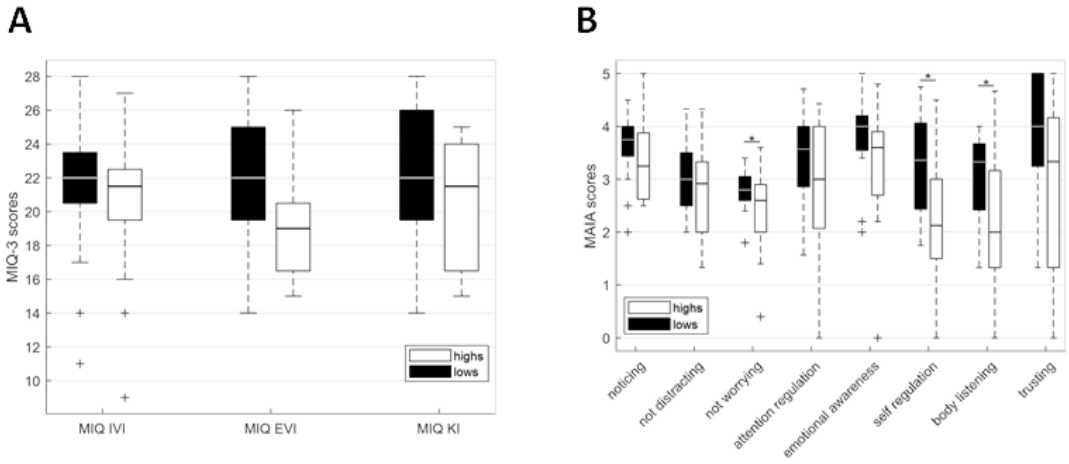

Figure 13. Imagery abilities and interoceptive scores (mean, SD).

A) MIQ; MIQIVI, internal visual imagery, MIQ EVI, external visual imagery; MIQKI, Kinesthetic imagery. B) MAIA scales. b) Lines indicate significant differences between groups (* $p < .05$).

Apnea duration

Repeated measures ANOVA revealed only a significant **Trial** effect ($F(2,38) = 3.79$, $p = .032$, $\eta^2 = .166$, $1 - ß = .656$) indicating increasing apnea duration across consecutive trials (T1 < T3, $(F(1,19) = 8.21$, $p = .010$; T2 < T3 ($F(1,19) = 4.13$, $p = .056$) independently from tasks and hypnotizability (**Figure 14A**). Both imagery abilities and interoceptive sensibility accounted for these learning effects, as controlling for MAIA and MIQ-3 dimensions separately abolished the Trial effect.

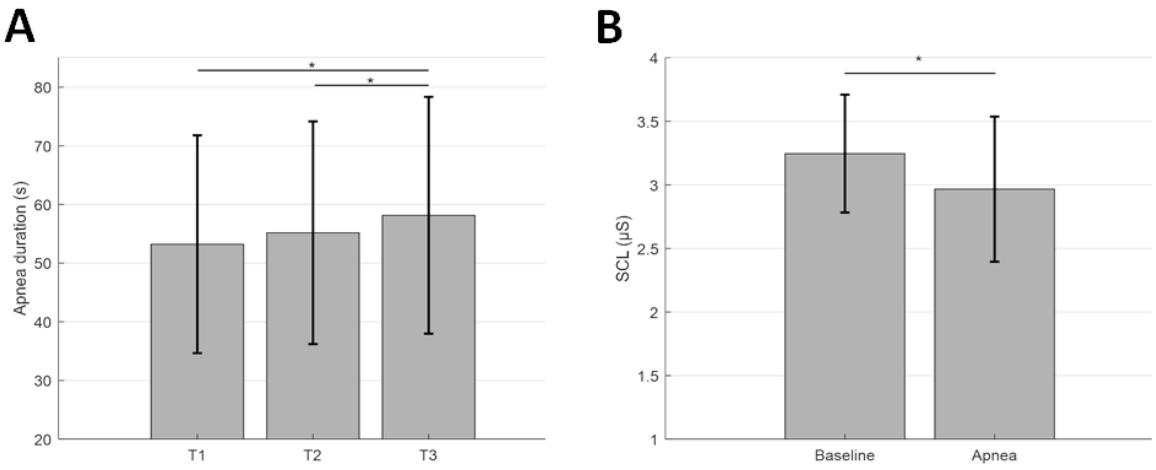

Figure 14. Apnea duration and SCL (mean, SD).

A) Apnea duration (s) in each trial independently from conditions; B) SCL level (µS) during baseline and apnea, independently from condition. Lines indicate significant differences (* $p < .05$).

Self-reported easiness and vividness of IFA and MI

The reported easiness (IFA (mean ± SD): 5.29 ± 1.09; MI: 4.41 ± 1.47) of the tasks exhibited a significant **Task** effect ($F(1,31) = 7.17$, $p = .012$, $\eta^2 = .188$, $1 - ß = .737$), indicating greater easiness to perform IFA than MI. Controlling ANOVA for MIQIVI disclosed a **Trial** effect ($F(2,60) = 3.49$, $p = .037$, $\eta^2 = .104$, $1 - ß = .631$), with T2 < T3 ($F(1,30) = 7.85$, $p = .009$). Controlling it for MIQKI disclosed a **Task x Group** interaction ($F(1,30) = 4.14$, $p = .051$, $\eta^2 = .121$, $1 - ß = .504$). Its decomposition revealed that med-highs report greater easiness than med-lows for MI ($F(1,31) = 6.56$, $p = .015$). Controlling ANOVA for all MAIA dimensions, except for not worrying, abolished the Task effect.

The reported vividness (IFA, mean ± SD: 5.20 ± 1.21; MI: 4.45 ± 1.48) differed between **Trials** ($F(2,62) = 5.10$, $p = .009$, $\eta^2 = .141$, $1 - ß = .804$) and increased from T1 to T3 (T1 = T2, T2 < T3 ($F(1,31) = 11.04$, $p = .002$; T1 < T3 ($F(1,31) = 5.70$, $p = .023$), and indicated greater vividness for IFA than MI (**Task** effect, $F(1,31) = 8.67$, $p = .006$, $\eta^2 = .219$, $1 - ß = .813$). Controlling for MAIA noticing, not distracting, attention regulation, trusting, MIQEVI, and MIQIVI abolished both effects. Controlling for not worrying, emotional awareness, and self-regulation abolished only the Trial effect. Controlling for MIQKI abolished both effects and disclosed a **Task x Group** interaction ($F(1,30) = 4.88$, $p = .035$, $\eta^2 = .140$, $1 - ß = .571$). Its decomposition revealed a difference between tasks only in med-lows who exhibited higher vividness for IFA than MI ($F(1,15) = 8.21$, $p = .012$).

Physiological variables

HR did not exhibit any significant differences between groups and tasks (mean ± SD; baseline: 72.74 ± 11.21; task: 71.88 ± 11.41). Controlling for MAIA *not distracting* disclosed a **Task x Level** interaction ($F(1,18) = 7.58$, $p = .013$, $\eta^2 = .296$, $1 - ß = .739$), whose decomposition revealed lower HR during IFA than MI ($F(1,19) = 13.29$, $p = .002$) in the presence of a non-different baseline.

RMSSD (ms) did not exhibit significant effects and interactions (mean ± SD; B: 92.78 ± 70.13; task: 146.72 ± 162.98).

Mean SCL exhibited a significant **Trial** effect ($F(2,38) = 3.16$, $p = .054$, $\eta^2 = .143$, $1 - ß = .571$), with T1= T2, T1 < T3 ($F(1,19) = 4.52$, $p = .047$), and T2 = T3. The **Level** effect ($F(1,19) = 6.11$, $p = .023$, $\eta^2 = .243$, $1 - ß = .650$) consisted only of higher SCL in B than in tasks independently

from the cognitive condition (**Figure 14B**). Controlling for all MAIA dimensions abolished all effects. Controlling for MIQIVI and MIQEVI abolished all effects. MIQKI abolished all effects and disclosed a **Trial x Task x Level x Group** interaction ($F(2,36) = 3.90$, $p = .029$, $\eta^2 = .178$, $1 - ß = .667$). Its decomposition revealed a Level effect in med-highs ($F(1,8) = 7.12$, $p = .028$), with B > Task. In med-lows it revealed a Level x Task interaction ($F(1,9) = 12.03$, $p = .007$), with B > IFA in T1 ($F(1,9) = 15.60$, $p = .003$), and no significant effects in T2 and T3.

Regression analysis of SHSS and MAIA scores, and physiological variables on apnea duration

After controlling collinearities, linear backward regression of MAIA and MIQ dimensions, HR, and SCL on apnea duration is reported in **Table 5**. It indicates the role of a few MAIA dimensions in apnea duration in the first trial of both IFA and MI, and an increasing role of MAIA dimensions and autonomic variables in the successive trials during IFA, but not during MI.

Table 5. Linear backward regression

Apnea duration	IFA				MI			
	R^2		B	p	R^2		B	p
T1	.198	noticing	-.468	.045	.241	noticing	-.604	.014
		trusting	.484	.039		attention regulation	.486	.043
T2	.526	SHSS	-.797	.003				
		noticing	-1.09	.0001				
		emotional awareness	.710	.009				
		body listening	.984	.001				
		SCL	-.886	.002				
T3	.362	noticing	-.587	.013				
		attention regulation	.743	.004				
		RMSSD	-.453	*.052*				
		HR	-.539	.026				

Adj R^2, adjusted R^2; *B*, standardized beta; *HR*, heart rate; *IFA*, internal focus apnea; *MI*, motor imagery apnea; R^2, adjusted R^2; *RMSSD*, heart rate fast variability; *SCL*, skin conductance level; *SHSS*, Stanford Hypnotic Susceptibility Scale; *T1, T2, T3*, first, second, and third trial.

2.3.4 Discussion

The present study was designed to explore how hypnotizability, imagery abilities, and interoceptive sensibility influence breath-hold performance in different cognitive conditions. Our findings indicate that apnea duration did not significantly differ between the cognitively congruent and incongruent conditions. Additionally, attention to apnea sensation (congruent with the physical state) and motor imagery of normal breathing (incongruent with it) are differentially associated with experiential and physiological variables.

The findings reveal a dissociation between subjective experience and apnea duration, as interoceptive sensibility and autonomic markers are more strongly associated with apnea duration in the congruent cognitive condition than in the incongruent condition. Additionally, hypnotizability influences subjective experience, but not apnea duration. Interoceptive sensibility and motor imagery abilities account for most of the differences between the two conditions, and masked hypnotizability-related differences.

Subjective Experience

The study did not demonstrate significant hypnotizability-related differences in the self-reported scores of trait imagery abilities (measured by the Betts' questionnaire), in line with the observation that questionnaire scores do not always correlate with hypnotizability (Srzich et al., 2016) and functional equivalence between actual and imagined perception/action (Ibanez-Marcelo et al., 2019).

Med-highs and med-lows reported different experiences in cognitively congruent and incongruent apnea conditions. The higher vividness of the congruent than the incongruent experience observed in both groups suggests that the former was easier than the latter. In contrast, the greater easiness of the cognitively incongruent task in med-highs was masked by the trait kinesthetic ability of imagery, which compensated for the med-lows' lower imagery ability and weaker functional equivalence (Ibanez-Marcelo et al., 2019). Two non-alternative hypotheses can account for the groups' different experiences. One can be based on the highs' flexible functional connections between the salience and executive systems (Hoeft et al., 2012), the other can be sustained by the highs' lower ability to represent bodily signals accurately (Giusti et al., 2024).

Interoceptive sensibility contributed to the difference in task easiness. The ability to allocate attention (attention regulation) and adaptively modulate internal bodily sensations of discomfort (self-

regulation), together with emotional awareness, likely induced a more vivid experience during the cognitively congruent apnea condition. Enhanced vividness also depends on the association between respiratory sensations and emotional processes (Harrison et al., 2021), making them more easily accessible or meaningful during imagery in emotionally resonant contexts such as apnea.

Apnea Duration

Hypnotizability did not influence apnea duration in both cognitive conditions and in both groups, despite the highs' lower interoceptive accuracy (Giusti et al., 2024), which was expected to positively influence apnea duration when attention was focused on the apnea-related sensations, and their stronger functional equivalence between actual and imagined normal breathing, which was expected to increase apnea duration during imagination of normal breathing. The absence of behavioral hypnotizability-related differences between groups contrasts with their subjective experiences, as earlier observed for other functions, such as postural control, which was quite different between highs and lows, but was similarly reported (Santarcangelo et al., 2008).

In contrast to the study by Kanthack et al. (2019), we did not find a significant difference in apnea duration between the cognitively congruent (IFA) and incongruent (MI) conditions. A possible explanation for this discrepancy lies in the composition of the two samples. While Kanthack et al.'s participants were recruited from the general population through a sports science department and were all physically active individuals engaged in regular sporting practices, our sample consisted of non-athletes with no systematic physical training. It is plausible that athletes are more familiar with motor imagery, either through formal practice or embodied experience, which may enhance the effectiveness of MI in extending apnea duration. This hypothesis aligns with the well-established role of motor imagery in sports performance and motor learning (Desai et al., 2024). In contrast, our sample's limited familiarity with MI, and its composition comprising many med-lows, which differs from the general population (De Pascalis et al., 2000), may have reduced the efficacy of MI (Ibanez-Marcelo et al., 2019).

In line with earlier reports (Kanthack et al., 2019), the duration of apnea increased across trials. In our study, both interoceptive sensibility and imagery abilities contributed to this effect, which can be attributed to the observed cooperation of interoceptive sensibility in the cortical representation of both actual and imagined movements (Malloggi et al., 2024). Interestingly, no correlation emerged between apnea duration and the subjective experience of the two tasks, suggesting that performance

improvements may have been more strongly influenced by arousal or emotional regulation than by cognitive engagement (Maric et al., 2020; Harrison et al., 2021).

Physiological variables

In the general population, heart rate decreases during 30-60 seconds of normoxic apnea (O'Croinin et al., 2024). In this condition, earlier findings do not reveal significant differences in heart rate between apnea with instructions and with attention focused on bodily sensations (Kanthack et al., 2019), which could be attributed to the low cognitive effort required by the congruent condition. In the more demanding, cognitively incongruent condition, in contrast to earlier reports (Kanthack et al., 2019), we observed an increase in heart rate compared to baseline, consistent with the increase in the sympathetic/parasympathetic ratio observed during demanding cognitive tasks (Chang & Huang, 2012). The MAIA not distracting dimension, not measured in the earlier study (Kanthack et al., 2019), may have masked the difference. The parasympathetic, fast heart rate variability (RMSSD) did not differ between tasks and hypnotizability groups, likely due to the different contributions to its regulation by multiple components, such as apnea, cognitive effort, emotion, and arousal, which may balance each other. Indeed, apnea is associated with both sympathetic and parasympathetic activation (Bain et al., 2018).

Our results also showed a reduction in skin conductance during apnea compared to baseline. While both physical and cognitive load are typically associated with increased skin conductance due to elevated sympathetic nervous system activity (Critchley, 2002; Boucsein, 2012; Chang & Huang, 2012), voluntary breath-holding constitutes a unique autonomic condition. It triggers the diving reflex, a physiological response characterized by bradycardia, peripheral vasoconstriction, and reduced blood flow to the extremities of the limbs (Ferrigno & Lundgren, 2003), which potentially leads to reduced skin conductance despite an elevated central sympathetic drive (Heusser et al., 2009). It is noteworthy that interoceptive sensibility sustained the observed SCL differences, supporting the idea that it modulates autonomic activity during challenging bodily states such as apnea.

Limitations and conclusions

Limitations of the study are the sample's scarce representativeness of the general population (De Pascalis et al., 2000) and the classification of highs, mediums, and lows based on their total

hypnotizability scores rather than on a more accurate categorization based on motor inhibition, hallucination, and dissociation (Terhune et al., 2011). Another limitation is not having acquired, but only monitored online, the respirogram. Its acquisition could have allowed for the correlation of the amplitudes of maximal inspiration with the experiential, behavioral, and autonomic results, as different thorax enlargements correspond to different interoceptive conditions. However, the sample was substantially composed of females of comparable age who did not practice sports; thus, large differences between groups were not expected. Furthermore, the addition of a neutral apnea condition without employing cognitive strategies could have represented a control condition.

In conclusion, the results support the view that, in healthy participants, interoceptive sensibility and trait imagery abilities are relevant to apnea duration and that hypnotizability contributes to its subjective and physiological correlates. The complexity of the interaction between these variables in regulating the effects of cognitive conditions on the physiological state of apnea suggests that assessing interoceptive and imagery abilities could be beneficial for sports performers who may benefit from training in voluntary apnea (Bouten et al., 2024).

3. General Discussion

This thesis examined the role played by hypnotizability and interoception in the neural and behavioral correlates of motor imagery, and the effects of motor imagery training in the general population represented by mediums, which is relevant to spaceflights. Three experimental studies were conducted: study 1 monitored brain oxygenation during movement and motor imagery in highs and lows, study 2 investigated motor imagery training effects on the cortical activity, experiential and behavioral correlates in highs, mediums and lows, study 3 assessed the apnea duration when attention was focused on breath-hold-related sensations and during imagery of normal breathing in highs and lows. Taken together, the studies confirm that highs exhibit stronger mind–body coupling and more efficient imagery processes than mediums and lows, that mental training can increase motor imagery-related plasticity across all individuals, and that extreme interoceptive conditions can be experienced by highs and lows differentially.

3.1 Summary of Findings

In Study 1, oxygenation responses during actual and imagined movements were compared between highs and lows using functional near-infrared spectroscopy. Lows showed greater task-related synaptic activity than highs, indicated by increased oxyhaemoglobin concentration in prefrontal and premotor regions during both executed and imagined movements. Subjectively, both groups reported the same imagery efficacy, despite their physiological differences indicating lower synaptic activity/cortical effort in highs. Thus, highs rely on more efficient neural recruitment, confirming and extending prior EEG evidence of distributed activation patterns in highs (Ibanez-Marcelo et al., 2019).

Study 2 investigated whether a two-week motor imagery training could improve imagery efficacy and cortical markers in the general population, represented by mediums, and in lows. Chronometric index did not change after training, whereas self-reported motor imagery efficacy and EEG markers improved. However, the temporal equivalence between actual and imagined movements may fail to capture all aspects of motor imagery quality. Indeed, a multidimensional evaluation of motor imagery has been recommended (Collet et al., 2011). Specifically, after motor imagery training, highs reported higher imagery efficacy and exhibited increases in the values of both midline and hemispheric EEG aperiodic components. This indicates a modified balance between arousal and rest (Donoghue et al., 2020; Gyurkovics et al., 2021; Frelih et al., 2025) in favor of greater recruitment of inhibitory

GABAergic neural pathways rather than excitatory glutamatergic pathways (Gao et al., 2017), thus suggesting a lower cognitive effort after training. Of note, also mediums and lows showed training-induced EEG aperiodic changes, but not for both components, and only highs modulated the tasks-related EEG differentially, displaying functional equivalence between actual and kinesthetically imagined movement for the hemispheric offset.

Regarding the EEG oscillatory component, only lows showed training-induced reduction in the frontal midline and hemispheric alpha PSD, indicating greater cognitive effort (not observed in highs due to their better functional equivalence). Low-beta PSD increased after training in highs and mediums, in contrast to lows. Such PSD increases can be due to practice-related mechanisms of motor skill retention observed for sequential movements (Nelson et al., 2017; Theves et al., 2020; Dyck & Klaes, 2024), and indicate better performance compared to lows. Highs also displayed stronger functional equivalence between actual and both visually- and kinesthetically imagined movements, thus exhibiting better performance compared to mediums and lows. High-beta PSD, reflecting sensorimotor function, decreased in all groups after training.

Of note, the same changes observed after training in the regions involved in the proposed tasks were observed in basal conditions for the aperiodic offset component in highs and for alpha and high-beta PSD in all groups, which indicates neural plasticity (Amad et al., 2017; Kweon et al., 2023).

In Study 3, participants performed repeated voluntary breath-hold under two cognitive conditions: focusing attention internally on apnea sensations (congruent condition) and mentally imagining normal breathing (incongruent condition). Apnea duration increased over trials for all groups, confirming a training effect on breath-hold capacity independently from the cognitive condition. Skin conductance decreased during both tasks compared to baseline, in line with the autonomic changes associated with apnea. While both physical and cognitive load are typically associated with increased skin conductance due to elevated sympathetic nervous system activity (Critchley, 2002; Boucsein, 2012; Chang & Huang, 2012), voluntary breath-holding constitutes a unique autonomic condition characterized by bradycardia, peripheral vasoconstriction, and reduced blood flow to the extremities of the limbs (Ferrigno & Lundgren, 2003), which potentially leads to reduced skin conductance (Heusser et al., 2009). Autonomic, experiential and behavioral variables were mostly modulated by imagery and interoceptive sensibility abilities rather than by hypnotizability *per se*, highlighting a possible role of these traits in bearing challenging, extreme conditions. However, hypnotizability was relevant to the perceived easiness of the more difficult condition of imagining normal breath during apnea.

Altogether, the present studies indicate that hypnotic assessment may assist in space flights and staying and in neurorehabilitation as well. It predicts the ability of individuals to live in microgravity and may assist in enhancing the astronauts' quality of life in space by mental imagery training, which can be efficacious also in non-highly hypnotizable participants.

3.2 Somatic Marker Hypothesis and the As-If Body Loop

The somatic marker hypothesis (Bechara & Damasio, 2005; Damasio, 1996) posits that bodily signals, such as heartbeats and visceral sensations, become linked to experiences and guide decisions, while the as-if body loop allows the brain to re-create those bodily states internally without actual sensory input (Damasio, 1996). In the present experimental studies, highs appear to utilize a stronger as-if body loop during cognitive tasks, as they displayed higher motor imagery vividness and stronger functional equivalence, specifically for the kinesthetic imagery modality – for which functional equivalence was reached for the offset of the aperiodic component too –, whose neural underpinnings, indeed, are closely linked to those of body representation. This suggests that, although mediums and lows also display neural plasticity after mental imagery practice (significant modulation of aperiodic and periodic components after training), highs can better internally simulate bodily states to achieve motor plans. Indeed, their changes in low-beta PSD and aperiodic component offset indicate stronger functional equivalence between both imagery modalities and movement for low-beta, and between actual and kinesthetically-imagined movement. During imagery, highs may generate vivid kinesthetic and interoceptive sensations that mirror real movement, effectively associating those simulations with the expected somatic feedback. In contrast, lows, who have higher interoceptive accuracy but less vivid imagery, may depend more on actual sensory feedback and less on internal simulation, making them less efficient at maintaining performance when external cues are absent.

The highs' enhanced "as-if" looping may also explain the lower cortical oxygenation observed during tasks. Indeed, by simulating rather than physically enacting a response, highs may engage motor networks less intensely and rely on internal anticipatory signals. In Study 1, the absence of task-related activation in prefrontal cortices in highs may reflect a widely distributed signal elaboration compared to lows, who show a nested integration mode (Ibanez-Marcelo et al., 2019). Specifically, regarding the medial prefrontal cortex, the aforementioned findings revealed a task-related deactivation in highs during motor imagery, while lows did not show this modulation. Given that this structure is a central node of the Default Mode Network, associated with self-referential and internally focused processes, its downregulation in highs likely reflects a more effective suppression of task-

irrelevant information. This interpretation aligns with previous neuroimaging studies indicating reduced Default Mode Network activity during flow states (Dietrich 2004) and suggests that highs can flexibly shift resources from self-oriented to task-relevant processing. This is also in line with previous literature reporting highs to display greater absorption abilities (Tellegen & Atkinson, 1974), that is the tendency to experience states of strong engagement in tasks. Therefore, vivid internal imagery, being facilitated by greater absorption and interference inhibition abilities, might allow highs relying on a robust somatic marker system, binding bodily anticipation to cognition that facilitates action under sensory deprivation, thus with less activation and energetic expenditure.

3.3 Motor imagery training effects on brain activity

Motor imagery training produced dissociable effects on the aperiodic and periodic components of the EEG, with important consequences for the conceptualization of how brain assets reorganize across different hypnotizability groups. Specifically, study 2 reports that highs and lows share similar profiles in the aperiodic domain, whereas mediums did not exhibit training-induced EEG aperiodic changes. Thus, the general population represented by mediums (De Pascalis et al., 2000) does not shift the global brain activation after training.

Attention/motor-related rhythms (mu, alpha, low-beta) (Debnath et al., 2018; Chen et al., 2021) were largely similar between highs and mediums. They did not display significant training-induced modulation in mu and alpha PSD, likely due to lower cognitive effort, and showed a post-training increase of low-beta PSD, possibly indicating higher neural efficiency and practice-related mechanisms of motor skill retention compared to lows (Nelson et al., 2017; Theves et al., 2020; Dyck & Klaes, 2024). These findings suggest that the general population, represented by mediums, may benefit from mental imagery training, despite the mediums' lack of changes in the aperiodic EEG component. In lows, MI training produced an increase of the aperiodic component, indicating a modulation of cortical recruitment and inhibitory-excitatory balance (Frelih et al., 2024; Donoghue et al., 2024). At the same time, their desynchronization of mu, alpha and low-beta oscillations likely reflect increased cortical engagement during imagery. Thus, lows perform mental imagery through background dynamics adjustment that facilitates oscillatory modulation compatible with a compensatory increase in task-related neural effort.

In sum, different types of cortical reorganization have been shown as a function of hypnotizability: both highs and lows display training-induced modulation of cortical recruitment and inhibitory-

excitatory balance (EEG aperiodic component increases), although lows display a different profile compared to highs regarding the oscillatory component; on the contrary, mediums do not modulate their aperiodic components, although showing oscillatory profile similar to highs. Neural plasticity was observed for alpha and high-beta PSD in all groups, indicated by the similar activation observed in baseline and task conditions after training. Modulation of excitation–inhibition balance and changes in network recruitment (aperiodic component) might require longer-lasting mental training in mediums. Furthermore, findings show that hypnotizability predicts training-induced changes in oscillatory power and in the aperiodic exponent, but not in offset; conversely, interoceptive sensibility accounts for both offset and exponent modulation.

3.4 Implications for Microgravity Adaptation and Future Perspectives

The findings have important implications for spaceflights, as highs could better adapt to diminished proprioceptive, interoceptive and vestibular inputs through their stronger functional equivalence, potentially stabilizing motor control when sensory cues are unreliable. Nevertheless, MI training induces neural plasticity in all groups, suggesting the possibility to enhance functional equivalence and cortical plasticity through guided tailored motor imagery practice in the general population. Moreover, findings show that coping with extreme, challenging interoceptive conditions, such as apnea, can be successfully obtained in highs and lows, as a function of interoceptive sensibility.

In future research, astronauts could be screened for hypnotizability to personalize countermeasures that help modulate sensorimotor and autonomic functions. Hypnotizability-related training might also protect against microgravity's long-term risks, such as oxidative stress and impaired sensorimotor and vascular functions (Zelic et al., 2025). Understanding how interoception and imagery interact in microgravity could help design facilities to provide countermeasures such as mental training and sensory augmentation. Studies in microgravity are required to support the findings of the present research.

In conclusion, our integrated findings support an embodied cognition model in which highs exhibit better mind–body integration allowing to confront challenging contexts such as microgravity, although training-induced cortical modulation occurs also in lows and mediums. Thus, astronauts selection and training may improve human experience and performance in altered gravity.

Acknowledgements

This doctoral thesis was carried out within the Space It Up project and received funding from the ASI and the MUR – Contract n. 2024-5-E.0 - CUP n. I53D24000060005. Study 3 was partially conducted at Université Claude Bernard Lyon 1, Laboratoire Interuniversitaire de Biologie de la Motricité under the supervision of Prof. Ursula Debarnot.

It was produced by Eleonora Malloggi while attending the Ph.D. program in Space Science and Technology at the University of Trento, Cycle XXXVIII, with the support of a scholarship financed by the Ministerial Decree no. 352 of 9 April 2022, based on the NRRP—funded by the European Union—NextGenerationEU—Mission 4 “Education and Research”, Component 1 “Enhancement of the offer of educational services: from nurseries to universities”—Investment 4.1 “Extension of the number of research doctorates and innovative doctorates for public administration and cultural heritage”.

References

Ahn, M., & Jun, S.C. (2015). Performance variation in motor imagery brain–computer interface: A brief review. *Journal of Neuroscience Methods, 243*, 103–110. https://doi.org/10.1016/j.jneumeth.2015.01.033.

Amad, A., Seidman, J., Draper, S.B., Bruchhage, M.M.K., Lowry, R.G., Wheeler, J., Robertson, A., Williams, S.C.R., Smith, M.S. (2017). Motor Learning Induces Plasticity in the Resting Brain—Drumming Up a Connection, *Cerebral Cortex*, 27(3), 2010–2021, https://doi.org/10.1093/cercor/bhw048.

Anwar, A. R., Muthalib, M., Perrey, S., Galka, A., Granert, O., Wolff, S., Heute, U., Deuschl, G., Raethjen, J., & Muthuraman, M. (2016). Effective Connectivity of Cortical Sensorimotor Networks During Finger Movement Tasks: A Simultaneous fNIRS, fMRI, EEG Study. *Brain topography*, *29*(5), 645–660. https://doi.org/10.1007/s10548-016-0507-1.

Arce-Álvarez, A., Veliz, C., Vazquez-Muñoz, M., et al. (2021). Hypoxic respiratory chemoreflex control in young trained swimmers. *Front Physiol, 12*: 632603. https://doi.org/10.3389/fphys.2021.632603.

Bain, A. R., Drvis, I., Dujic, Z., MacLeod, D. B., & Ainslie, P. N. (2018). Physiology of static breath holding in elite apneists. *Experimental physiology*, *103*(5), 635–651. https://doi.org/10.1113/EP086269.

Barhoun, P., Fuelscher, I., Do, M., He, J. L., Cerins, A., Bekkali, S., & Hyde, C. (2022). The role of the primary motor cortex in motor imagery: A theta burst stimulation study. *Psychophysiology, 59*, e14077. https://doi.org/10.1111/psyp.14077.

Bechara, A., & Damasio, A. R. (2005). *The somatic marker hypothesis: A neural theory of economic decision.* Games and Economic Behavior, 52(2), 336–372. https://doi.org/10.1016/j.geb.2004.06.010.

Bhattacharjee, S., Kashyap, R., Abualait, T., Chen, S. H. A., Yoo, W. K., & Bashir, S. (2021). The role of primary motor cortex: More than movement execution. *Journal of Motor Behavior, 53*(2), 258–274. https://doi.org/10.1080/00222895.2020.1738992.

Bondi, E., Ding, Y., Zhang, Y., Maggioni, E., He, B. (2025). Investigating the neurovascular coupling across multiple motor execution and imagery conditions: a whole-brain EEG-informed fMRI analysis. *Neuroimage, 15*, 317:121311. doi: 10.1016/j.neuroimage.2025.121311.

Borah, R.M., Pathak, A., Banerjee, A. (2025). Inhibition of thalamic relay nuclei scales the aperiodic and alpha band oscillations associated with arousal during naturalistic stimulus viewing. *Imaging Neurosci (Camb), 23*, 3:imag_a_00451. doi: 10.1162/imag_a_00451.

Boucsein, W. (2012). *Electrodermal activity* (2nd ed.). Springer.

Bouten, J., Declercq, L., Boone, J. et al. (2024). Apnoea as a novel method to improve exercise performance: A current state of the literature. *Exp Physiol*, 10.1113/EP091905. Advance online publication. https://doi.org/10.1113/EP091905.

Bressler, S. L., & Richter, C. G. (2015). Interareal oscillatory synchronization in top-down neocortical processing. *Current Opinion in Neurobiology, 31*, 62–66. https://doi.org/10.1016/j.conb.2014.08.010.

Bruce, C. D., Vanden Berg, E. R., Pfoh, J. R., et al. (2021). Prior oxygenation, but not chemoreflex responsiveness, determines breath-hold duration during voluntary apnea. *Physiological Reports, 9*(1), e14664. https://doi.org/10.14814/phy2.14664.

Buckner, R. L., & Vincent, J. L. (2007). Unrest at rest: Default activity and spontaneous network correlations. *NeuroImage, 37*(4), 1091–1096; discussion 1097–1099. https://doi.org/10.1016/j.neuroimage.2007.01.010.

Calderone, A., Manuli, A., Arcadi, F. A., Militi, A., Cammaroto, S., Maggio, M. G., Pizzocaro, S., Quartarone, A., De Nunzio, A. M., & Calabrò, R. S. (2025). The impact of visualization on stroke rehabilitation in adults: A systematic review of randomized controlled trials on guided and motor imagery. *Biomedicines, 13*(3), 599. https://doi.org/10.3390/biomedicines13030599.

Calmels, C., Holmes, P., Jarry, G., et al. (2006). Cortical activity before, and during, observation and execution of sequential finger movements. *Brain Topography, 19*(2), 77–88. https://doi.org/10.1007/s10548-006-0014-x.

Carli, G., Rendo, C., Sebastiani, L., & Santarcangelo, E. L. (2006). Suggestions of altered balance: Possible equivalence of imagery and perception. *The International Journal of Clinical and Experimental Hypnosis, 54*(2), 206–223. https://doi.org/10.1080/00207140500528455.

Cavallaro, F. I., Cacace, I., Del Testa, M., Andre, P., Carli, G., De Pascalis, V., Rocchi, R., & Santarcangelo, E. L. (2010). Hypnotizability-related EEG alpha and theta activities during visual and somesthetic imageries. *Neuroscience Letters, 470*(1), 13–18. https://doi.org/10.1016/j.neulet.2009.12.044.

Cebolla, A., Petieau, M., Dan, B., et al. (2016). Cerebellar contribution to visuo-attentional alpha rhythm: Insights from weightlessness. *Scientific Reports, 6*, 37824. https://doi.org/10.1038/srep37824.

Cesari, P., Modenese, M., Benedetti, S., Emadi Andani, M., & Fiorio, M. (2020). Hypnosis-induced modulation of corticospinal excitability during motor imagery. *Scientific Reports, 10*, 16882. https://doi.org/10.1038/s41598-020-74020-0.

Chang, Y. C., & Huang, S. L. (2012). The influence of attention levels on psychophysiological responses. *International Journal of Psychophysiology, 86*(1), 39–47. https://doi.org/10.1016/j.ijpsycho.2012.09.001.

Chen, W., Yan, C., & Wang, C. (2021). Neural correlates of motor imagery training: A meta-analysis of functional neuroimaging studies. *Frontiers in Human Neuroscience, 15*, 742520. https://doi.org/10.3389/fnhum.2021.742520.

Chen, L., Zhang, L., Wang, Z., Li, Q., Gu, B., & Ming, D. (2025). Task-related reconfiguration patterns of frontoparietal network during motor imagery. *Neuroscience, 579*, 302–311. https://doi.org/10.1016/j.neuroscience.2025.05.035.

Clement, G., & Ngo-Anh, J. T. (2013). Space physiology II: Adaptation of the central nervous system to space flight—Past, current, and future studies. *European Journal of Applied Physiology, 113*, 1655–1672.

Cojan, Y., Piguet, C., & Vuilleumier, P. (2015). What makes your brain suggestible? Hypnotizability is associated with differential brain activity during attention outside hypnosis. *NeuroImage, 117*, 367–374. https://doi.org/10.1016/j.neuroimage.2015.05.076.

Cojan, Y., Waber, L., Schwartz, S., Rossier, L., Forster, A., & Vuilleumier, P. (2009). The brain under self-control: Modulation of inhibitory and monitoring cortical networks during hypnotic paralysis. *Neuron, 62*(6), 862–875. https://doi.org/10.1016/j.neuron.2009.05.021.

Collet, C., Guillot, A., Lebon, F., MacIntyre, T., & Moran, A. (2011). Measuring motor imagery using psychometric, behavioral, and psychophysiological tools. *Exercise and Sport Sciences Reviews, 39*(2), 85–92. https://doi.org/10.1097/JES.0b013e31820ac5e0.

Craig, A. D. (2002). How do you feel? Interoception: The sense of the physiological condition of the body. *Nature Reviews Neuroscience, 3*(8), 655–666. https://doi.org/10.1038/nrn894.

Critchley, H. D. (2002). Electrodermal responses: What happens in the brain. *The Neuroscientist, 8*(2), 132–142.

Critchley, H., & Garfinkel, S. N. (2017). Interoception and emotion. *Current Opinion in Psychology, 17*, 7–14. https://doi.org/10.1016/j.copsyc.2017.04.020.

Cruz-Sanabria, F., Faraguna, U., Panu, C., Tommasi, L., Bruno, S., Bazzani, A., Sebastiani, L., & Santarcangelo, E. L. (2024). Hypnotizability-related risky experience and behavior. *Neuroscience Letters, 821*, 137625. https://doi.org/10.1016/j.neulet.2024.137625.

Dahm, S. F., & Sachse, P. (2025). Let's do it: Response times in Mental Paper Folding and its execution. *Quarterly Journal of Experimental Psychology, 78*(4), 731–743. https://doi.org/10.1177/17470218241249727.

Dallaway, N., Lucas, S. J. E., & Ring, C. (2022). Cognitive tasks elicit mental fatigue and impair subsequent physical task endurance: Effects of task duration and type. *Psychophysiology, 59*(12), e14126. https://doi.org/10.1111/psyp.14126.

Damasio, A. R. (1996). The somatic marker hypothesis and the possible functions of the prefrontal cortex. *Philosophical Transactions of the Royal Society B: Biological Sciences, 351*(1346), 1413–1420. https://doi.org/10.1098/rstb.1996.0125.

De Pascalis, V., Bellusci, A., & Russo, P. M. (2000). Italian norms for the Stanford Hypnotic Susceptibility Scale, Form C. *International Journal of Clinical and Experimental Hypnosis, 48*(3), 315–323. https://doi.org/10.1080/00207140008415249.

de Roever, I., Bale, G., Mitra, S., Meek, J., Robertson, N. J., & Tachtsidis, I. (2018). Investigation of the pattern of the hemodynamic response as measured by functional near-infrared spectroscopy (fNIRS) studies in newborns, less than a month old: A systematic review. *Frontiers in Human Neuroscience, 12*, 371. https://doi.org/10.3389/fnhum.2018.00371.

Debarnot, U., Perrault, A. A., Sterpenich, V., Legendre, G., Huber, C., Guillot, A., & Schwartz, S. (2021). Motor imagery practice benefits during arm immobilization. *Scientific Reports, 11*, 8928. https://doi.org/10.1038/s41598-021-88142-6.

Debnath, R., Buzzell, G. A., Morales, S., Bowers, M. E., Leach, S. C., & Fox, N. A. (2018). The development of mu rhythm desynchronization during action observation and execution from infancy

to adulthood. *Developmental Cognitive Neuroscience, 30*, 11–22. https://doi.org/10.1016/j.dcn.2018.01.011.

Decavèle, M., Nierat, M. C., Laviolette, L., et al. (2025). Multimodal physiological correlates of dyspnea ratings during breath-holding in healthy humans. *European Journal of Applied Physiology, 125*(3), 729–737. https://doi.org/10.1007/s00421-024-05627-8.

Decety, J. (1996). The neurophysiological basis of motor imagery. *Behavioural Brain Research, 77*(1–2), 45–52. https://doi.org/10.1016/0166-4328(95)00225-1.

Delorme, A., & Makeig, S. (2004). EEGLAB: An open-source toolbox for analysis of single-trial EEG dynamics including independent component analysis. *Journal of Neuroscience Methods, 134*(1), 9–21. https://doi.org/10.1016/j.jneumeth.2003.10.009.

Demuru, M., & Fraschini, M. (2020). EEG fingerprinting: Subject-specific signature based on the aperiodic component of power spectrum. *Computers in Biology and Medicine, 120*, 103748. https://doi.org/10.1016/j.compbiomed.2020.103748.

Desai, V., Stambulic, T., Grounds, R., et al. (2025). A scoping review of mental practice in athletes: How can surgeons learn? *Journal of Surgical Education, 82*(1), 103336. https://doi.org/10.1016/j.jsurg.2024.103336.

Di Rienzo, F., Joassy, P., Ferreira Dias Kanthack, T., et al. (2022). Stabilometric correlates of motor and motor imagery expertise. *Frontiers in Human Neuroscience, 15*, 741709. https://doi.org/10.3389/fnhum.2021.741709.

Dietrich, A. (2004). Neurocognitive mechanisms underlying the experience of flow. *Consciousness and Cognition, 13*(4), 746–761. https://doi.org/10.1016/j.concog.2004.07.002.

Dijkstra, N., Bosch, S. E., & van Gerven, M. A. J. (2019). Shared neural mechanisms of visual perception and imagery. *Trends in Cognitive Sciences, 23*(5), 423–434. https://doi.org/10.1016/j.tics.2019.02.004.

Diolaiuti, F., Tramonti Fantozzi, M., Di Galante, M., et al. (2020). Association of hypnotizability and deep sleep: Any role for interoceptive sensibility? *Experimental Brain Research, 238*(9), 1937–1943. https://doi.org/10.1007/s00221-020-05853-4.

Diolaiuti, F., Huber, A., Ciaramella, A., Santarcangelo, E. L., & Sebastiani, L. (2019). Hypnotisability-related interoceptive awareness and inhibitory/activating emotional traits. *Archives Italiennes de Biologie, 157*(4), 111–119. https://doi.org/10.12871/00039829202042.

Donoghue, T., Haller, M., Peterson, E. J., Varma, P., Sebastian, P., Gao, R., et al. (2020). Parameterizing neural power spectra into periodic and aperiodic components. *Nature Neuroscience, 23*(12), 1655–1665. https://doi.org/10.1038/s41593-020-00744-x.

Dyck, S., & Klaes, C. (2024). Training-related changes in neural beta oscillations associated with implicit and explicit motor sequence learning. *Scientific Reports, 14*(1), 6781. https://doi.org/10.1038/s41598-024-57285-7.

Dziego, C. A., Bornkessel-Schlesewsky, I., Jano, S., Chatburn, A., Schlesewsky, M., Immink, M. A., Sinha, R., Irons, J., Schmitt, M., Chen, S., & Cross, Z. R. (2023). Neural and cognitive correlates of performance in dynamic multi-modal settings. *Neuropsychologia, 180*, 108483. https://doi.org/10.1016/j.neuropsychologia.2023.108483.

Egan, J. M., Gomez-Ramirez, M., Foxe, J. J., O'Connell, R. G., & Kelly, S. P. (2025). Distinct audio and visual accumulators co-activate motor preparation for multisensory detection. *Nature Human Behaviour*. Advance online publication. https://doi.org/10.1038/s41562-025-02280-9.

Ehrsson, H. H., Kito, T., Sadato, N., Passingham, R. E., & Naito, E. (2005). Neural substrate of body size: Illusory feeling of shrinking of the waist. *PLoS Biology, 3*(12), e412. https://doi.org/10.1371/journal.pbio.0030412.

Elkins, G. R., Barabasz, A. F., Council, J. R., & Spiegel, D. (2015). Advancing research and practice: The revised APA Division 30 definition of hypnosis. *The International Journal of Clinical and Experimental Hypnosis, 63*(1), 1–9. https://doi.org/10.1080/00207144.2014.961870.

Estévez-Rodríguez, M., Sánchez-Garrido Campos, G., Zafra, Á. M., Cordones, I., & Márquez-Ruiz, J. (2025). Modulating excitation/inhibition balance through transcranial electrical stimulation: Physiological mechanisms in animal models. *Frontiers in Neuroscience, 19*, 1609679. https://doi.org/10.3389/fnins.2025.1609679.

Faul, F., Erdfelder, E., Lang, A.-G., & Buchner, A. (2007). G*Power 3: A flexible statistical power analysis program for the social, behavioral, and biomedical sciences. *Behavior Research Methods, 39*, 175–191. https://doi.org/10.3758/bf03193146.

Ferrigno, M., & Lundgren, C. E. G. (2003). Breath-hold diving. In A. O. Brubakk & T. Neuman (Eds.), *Bennett and Elliott's physiology and medicine of diving* (pp. 153–180). Saunders.

Filgueiras, A., Quintas Conde, E. F., & Hall, C. R. (2018). The neural basis of kinesthetic and visual imagery in sports: An ALE meta-analysis. *Brain Imaging and Behavior, 12*(5), 1513–1523. https://doi.org/10.1007/s11682-017-9813-9.

Finke, R. A. (1979). The functional equivalence of mental images and errors of movement. *Cognitive Psychology, 11*(2), 235–264. https://doi.org/10.1016/0010-0285(79)90011-2.

Forte, G., Favieri, F., & Casagrande, M. (2019). Heart rate variability and cognitive function: A systematic review. *Frontiers in Neuroscience, 13*, 710. https://doi.org/10.3389/fnins.2019.00710.

Frank, C., Guillot, A., & Vogt, S. (2024). Imagery and motor learning: A special issue on the neurocognitive mechanisms of imagery and imagery practice of motor actions. *Psychological Research, 88*(6), 1785–1789. https://doi.org/10.1007/s00426-024-01982-5.

Frelih, T., Matkovič, A., Mlinarič, T., Bon, J., & Repovš, G. (2025). Modulation of aperiodic EEG activity provides sensitive index of cognitive state changes during working memory task. Preprint. https://doi.org/10.1101/2024.05.13.593835.

Gao, R., Peterson, E. J., & Voytek, B. (2017). Inferring synaptic excitation/inhibition balance from field potentials. *NeuroImage, 158*, 70–78. https://doi.org/10.1016/j.neuroimage.2017.06.078.

Garfinkel, S. N., Seth, A. K., Barrett, A. B., Suzuki, K., & Critchley, H. D. (2015). Knowing your own heart: Distinguishing interoceptive accuracy from interoceptive awareness. *Biological Psychology, 104*, 65–74. https://doi.org/10.1016/j.biopsycho.2014.11.004.

Garro, F., Fenoglio, E., Laffranchi, M., Garcia-Hernandez, N. V., & Semprini, M. (2025). Neurophysiological correlates of user engagement in mixed reality exergames. *Journal of Neural Engineering*. Advance online publication. https://doi.org/10.1088/1741-2552/addae7.

Giusti, G., Zelič, Ž., Callara, A. L., et al. (2024). Interoception as a function of hypnotizability during rest and a heartbeat counting task. *Psychophysiology, 61*(6), e14535. https://doi.org/10.1111/psyp.14535.

Godfrey, S., Edwards, R. H., & Warrell, D. A. (1969). The influence of lung shrinkage on breath holding time. *Quarterly Journal of Experimental Physiology and Cognate Medical Sciences, 54*, 129–140.

Godfrey, S., & Campbell, E. (1969). Mechanical and chemical control of breath holding. *Quarterly Journal of Experimental Physiology and Cognate Medical Sciences, 54*, 117–128.

Guerra-Carrillo, B., Mackey, A. P., & Bunge, S. A. (2014). Resting-state fMRI: A window into human brain plasticity. *The Neuroscientist, 20*(5), 522–533. https://doi.org/10.1177/1073858414524442.

Guillot, A., Collet, C., Nguyen, V. A., et al. (2009). Brain activity during visual versus kinesthetic imagery: An fMRI study. *Human Brain Mapping, 30*(7), 2157–2172. https://doi.org/10.1002/hbm.20658.

Guillot, A., Collet, C., Nguyen, V. A., Malouin, F., Richards, C., & Doyon, J. (2008). Functional neuroanatomical networks associated with expertise in motor imagery. *NeuroImage, 41*(4), 1471–1483. https://doi.org/10.1016/j.neuroimage.2008.03.042.

Guillot, A., Hoyek, N., Louis, M., & Collet, C. (2012). Understanding the timing of motor imagery: Recent findings and future directions. *International Review of Sport and Exercise Psychology, 5*(1), 3–22. https://doi.org/10.1080/1750984X.2011.623787.

Gyurkovics, M., Clements, G. M., Low, K. A., Fabiani, M., & Gratton, G. (2021). The impact of 1/f activity and baseline correction on the results and interpretation of time-frequency analyses of EEG/MEG data: A cautionary tale. *NeuroImage, 237*, 118192. https://doi.org/10.1016/j.neuroimage.2021.118192.

Hanakawa, T., Dimyan, M. A., & Hallett, M. (2008). Motor planning, imagery, and execution in the distributed motor network: A time-course study with functional MRI. *Cerebral Cortex, 18*(12), 2775–2788. https://doi.org/10.1093/cercor/bhn036.

Hanakawa, T. (2016). Organizing motor imageries. *Neuroscience Research, 104*, 56–63. https://doi.org/10.1016/j.neures.2015.11.003.

Harris, A. M., Denaro, C. M., & Reed, C. L. (2025). Aperiodic activity masks sensorimotor mu suppression during human action observation. *Social Cognitive and Affective Neuroscience, 20*(1), nsaf059. https://doi.org/10.1093/scan/nsaf059.

Harrison, O. K., Köchl, K., Marino, S., et al. (2021). Interoception of breathing and its relationship with anxiety. *Neuron, 109*(24), 4080–4093.e8. https://doi.org/10.1016/j.neuron.2021.09.045.

Hart, S. G., & Staveland, L. E. (1988). Development of NASA-TLX (Task Load Index): Results of empirical and theoretical research. In P. A. Hancock & N. Meshkati (Eds.), *Human mental workload* (pp. 139–183). North Holland Press.

Hasan, A., Galea, J. M., Casula, E. P., Falkai, P., Bestmann, S., & Rothwell, J. C. (2013). Muscle- and timing-specific functional connectivity between the dorsolateral prefrontal cortex and the primary motor cortex. *Journal of Cognitive Neuroscience, 25*(4), 558–570. https://doi.org/10.1162/jocn_a_00338.

He, J. (2002). Learning and adaptation in cortical control of arm movement. *Proceedings of the 2002 American Control Conference (IEEE Cat. No.CH37301)*, 2323–2328 vol. 3. https://doi.org/10.1109/ACC.2002.1023987.

Henschke, J. U., & Pakan, J. M. P. (2023). Engaging distributed cortical and cerebellar networks through motor execution, observation, and imagery. *Frontiers in Systems Neuroscience, 17*, 1165307. https://doi.org/10.3389/fnsys.2023.1165307.

Hétu, S., Grégoire, M., Saimpont, A., et al. (2013). The neural network of motor imagery: An ALE meta-analysis. *Neuroscience & Biobehavioral Reviews, 37*(5), 930–949. https://doi.org/10.1016/j.neubiorev.2013.03.017.

Heusser, K., Dzamonja, G., Tank, J., et al. (2009). Cardiovascular regulation during apnea in elite divers. *Hypertension, 53*(4), 719–724.

Hoeft, F., Gabrieli, J. D., Whitfield-Gabrieli, S., et al. (2012). Functional brain basis of hypnotizability. *Archives of General Psychiatry, 69*(10), 1064–1072. https://doi.org/10.1001/archgenpsychiatry.2011.2190.

Hwang, J. H., Kim, S. H., Park, C. S., Bang, S. A., & Kim, S. E. (2010). Acute high-frequency rTMS of the left dorsolateral prefrontal cortex and attentional control in healthy young men. *Brain Research, 1329*, 152–158. https://pubmed.ncbi.nlm.nih.gov/20226772.

Ibáñez-Marcelo, E., Campioni, L., Manzoni, D., Santarcangelo, E. L., & Petri, G. (2019a). Spectral and topological analyses of the cortical representation of the head position: Does hypnotizability matter? *Brain and Behavior, 9*(6), e01277. https://doi.org/10.1002/brb3.1277.

Ibáñez-Marcelo, E., Campioni, L., Phinyomark, A., et al. (2019b). Topology highlights mesoscopic functional equivalence between imagery and perception: The case of hypnotizability. *NeuroImage, 200*, 437–449. https://doi.org/10.1016/j.neuroimage.2019.06.044.

IBM Corp. (2023). *IBM SPSS Statistics for Windows, Version 29.0*.

Ichinose, M., Matsumoto, M., Fujii, N., et al. (2018). Voluntary apnea during dynamic exercise activates the muscle metaboreflex in humans. *American Journal of Physiology-Heart and Circulatory Physiology, 314*(3), H434–H442. https://doi.org/10.1152/ajpheart.00367.2017.

Immink, M. A., Cross, Z. R., Chatburn, A., Baumeister, J., Schlesewsky, M., & Bornkessel-Schlesewsky, I. (2021). Resting-state aperiodic neural dynamics predict individual differences in

visuomotor performance and learning. *Human Movement Science, 78*, 102829. https://doi.org/10.1016/j.humov.2021.102829.

Jambrik, Z., Chunzeng, L., Santarcangelo, E. L., Sebastiani, L., Ghelarducci, B., & Picano, E. (2004b). Traditional acupuncture does not modulate the endothelial dysfunction induced by mental stress. *The International Journal of Cardiovascular Imaging, 20*(5), 357–362. https://doi.org/10.1023/b:caim.0000041939.61963.b0.

Jambrik, Z., Santarcangelo, E. L., Ghelarducci, B., Picano, E., & Sebastiani, L. (2004a). Does hypnotizability modulate the stress-related endothelial dysfunction? *Brain Research Bulletin, 63*(3), 213–216. https://doi.org/10.1016/j.brainresbull.2004.01.011.

Jeannerod, M. (1995). Mental imagery in the motor context. *Neuropsychologia, 33*(11), 1419–1432. https://doi.org/10.1016/0028-3932(95)00073-C.

Jeong, S., Hong, J. S., & Han, D. H. (2025). Brain activation in response to literature-related activities. *Psychiatry Investigation, 22*(5), 574–582. https://doi.org/10.30773/pi.2025.0035.

Kaiser, V., Bauernfeind, G., Kreilinger, A., Kaufmann, T., Kübler, A., Neuper, C., & Müller-Putz, G. R. (2014). Cortical effects of user training in a motor imagery based brain-computer interface measured by fNIRS and EEG. *NeuroImage, 85*(Pt 1), 432–444. https://doi.org/10.1016/j.neuroimage.2013.04.097.

Kamiński, J., Brzezicka, A., Gola, M., & Wróbel, A. (2012). β band oscillations engagement in the human alertness process. *International Journal of Psychophysiology, 85*(1), 125–128. https://doi.org/10.1016/j.ijpsycho.2011.11.006.

Kanthack, T. F. D., Guillot, A., Sabou, D., et al. (2019). Breathing with the mind: Effects of motor imagery on breath-hold performance. *Physiology & Behavior, 208*, 112583. https://doi.org/10.1016/j.physbeh.2019.112583.

Kasai, T., Kawai, S., Kawanishi, M., & Yahagi, S. (1997). Evidence for facilitation of motor evoked potentials (MEPs) induced by motor imagery. *Brain Research, 744*(1), 147–150. https://doi.org/10.1016/s0006-8993(96)01101-8.

Kasess, C. H., Windischberger, C., Cunnington, R., Lanzenberger, R., Pezawas, L., & Moser, E. (2008). The suppressive influence of SMA on M1 in motor imagery revealed by fMRI and dynamic causal modeling. *NeuroImage, 40*(2), 828–837. https://doi.org/10.1016/j.neuroimage.2007.11.040.

Keogh, R., Bergmann, J., & Pearson, J. (2020). Cortical excitability controls the strength of mental imagery. *eLife, 9*, e50232. https://doi.org/10.7554/eLife.50232.

Khanna, P., & Carmena, J. M. (2015). Neural oscillations: Beta band activity across motor networks. *Current Opinion in Neurobiology, 32*, 60–67. https://doi.org/10.1016/j.conb.2014.11.010.

Kilintari, M., Narayana, S., Babajani-Feremi, A., Rezaie, R., & Papanicolaou, A. C. (2016). Brain activation profiles during kinesthetic and visual imagery: An fMRI study. *Brain Research, 1646*, 249–261. https://doi.org/10.1016/j.brainres.2016.06.009.

Kim, H. G., Cheon, E. J., Bai, D. S., Lee, Y. H., & Koo, B. H. (2018). Stress and heart rate variability: A meta-analysis and review of the literature. *Psychiatry Investigation, 15*(3), 235–245. https://doi.org/10.30773/pi.2017.08.17.

Kim, Y. K., Park, E., Lee, A., Im, C. H., & Kim, Y. H. (2018). Changes in network connectivity during motor imagery and execution. *PLoS ONE, 13*(1), e0190715. https://doi.org/10.1371/journal.pone.0190715.

Koessler, L., Maillard, L., Benhadid, A., Vignal, J. P., Felblinger, J., Vespignani, H., & Braun, M. (2009). Automated cortical projection of EEG sensors: Anatomical correlation via the international 10-10 system. *NeuroImage, 46*(1), 64–72. https://doi.org/10.1016/j.neuroimage.2009.02.006.

Koppelmans, V., Pasternak, O., Bloomberg, J. J., Dios, Y. E., Wood, S. J., Riascos, R., Reuter-Lorenz, P. A., Kofman, I. S., Mulavara, A. P., & Seidler, R. D. (2017). Intracranial fluid redistribution but no white matter microstructural changes during a spaceflight analog. *Scientific Reports, 7*(1), 3154. https://doi.org/10.1038/s41598-017-03311-w.

Kraeutner, S., Gionfriddo, A., Bardouille, T., & Boe, S. (2014). Motor imagery-based brain activity parallels that of motor execution: Evidence from magnetic source imaging of cortical oscillations. *Brain Research, 1588*, 81–91. https://doi.org/10.1016/j.brainres.2014.09.001.

Kuldavletova, O., Navarro Morales, D. C., Quarck, G., Denise, P., & Clément, G. (2023). Spaceflight alters reaction time and duration judgment of astronauts. *Frontiers in Physiology, 14*, 1141078. https://doi.org/10.3389/fphys.2023.1141078.

Kvamme, T. L., Sandberg, K., & Silvanto, J. (2024). Mental imagery as part of an 'inwardly focused' cognitive style. *Neuropsychologia, 204*, 108988. https://doi.org/10.1016/j.neuropsychologia.2024.108988

Kweon, J., Vigne, M. M., Jones, R. N., Carpenter, L. L., & Brown, J. C. (2023). Practice makes plasticity: 10-Hz rTMS enhances LTP-like plasticity in musicians and athletes. *Frontiers in Neural Circuits, 17*, 1124221. https://doi.org/10.3389/fncir.2023.1124221.

Lai, G., Landi, D., Vidaurre, C., Bhattacharya, J., & Herrojo Ruiz, M. (2024). Cardiac cycle modulates alpha and beta suppression during motor imagery. *Cerebral Cortex, 34*(11), bhae442. https://doi.org/10.1093/cercor/bhae442.

Landry, M., Lifshitz, M., & Raz, A. (2017). Brain correlates of hypnosis: A systematic review and meta-analytic exploration. *Neuroscience & Biobehavioral Reviews, 81*, 75–98. https://doi.org/10.1016/j.neubiorev.2017.02.020.

Lebon, F., Horn, U., Domin, M., & Lotze, M. (2018). Motor imagery training: Kinesthetic imagery strategy and inferior parietal fMRI activation. *Human Brain Mapping, 39*(4), 1805–1813. https://doi.org/10.1002/hbm.23956.

Li, Y., Wang, L., Jia, M., Guo, J., Wang, H., & Wang, M. (2017). The effects of high-frequency rTMS over the left DLPFC on cognitive control in young healthy participants. *PLoS ONE, 12*(6), e0179430. https://doi.org/10.1371/journal.pone.0179430.

Liang, N., Murakami, M., Niu, X., & Nakazawa, K. (2007). The effects of motor imagery are dependent on motor strategies. *NeuroReport, 18*(12), 1241–1245. https://doi.org/10.1097/WNR.0b013e3282202707.

Linden, J. H. (2020). Relationship factors in the theater of the imagination: Hypnosis with children and adolescents. *The American Journal of Clinical Hypnosis, 62*(1-2), 60–73. https://doi.org/10.1080/00029157.2019.1568961.

MacIntyre, T. E., Madan, C. R., Moran, A. P., Collet, C., & Guillot, A. (2018). Motor imagery, performance, and motor rehabilitation. *Progress in Brain Research, 240*, 141–159. https://doi.org/10.1016/bs.pbr.2018.09.010.

Magosso, E., De Crescenzio, F., Ricci, G., Piastra, S., & Ursino, M. (2019). EEG alpha power is modulated by attentional changes during cognitive tasks and virtual reality immersion. *Computational Intelligence and Neuroscience, 2019*, 7051079. https://doi.org/10.1155/2019/7051079.

Malloggi, E., Zelič, Ž., & Santarcangelo, E. L. (2024). The role of interoceptive sensitivity and hypnotizability in motor imagery. *Brain Sciences, 14*(8), 832. https://doi.org/10.3390/brainsci14080832.

Maric, V., Ramanathan, D., & Mishra, J. (2020). Respiratory regulation & interactions with neuro-cognitive circuitry. *Neuroscience & Biobehavioral Reviews, 112*, 95–106. https://doi.org/10.1016/j.neubiorev.2020.02.001.

Marlinge, M., Chefrour, M., Billaut, F., Zavarro, M., Rostain, J. C., Coulange, M., Guieu, R., & Joulia, F. (2021). Blood adenosine increase during apnea in spearfishermen reinforces the efficiency of the cardiovascular component of the diving reflex. *Frontiers in Physiology, 12*, 743154. https://doi.org/10.3389/fphys.2021.743154.

Martinez, J. A., Wittstein, M. W., Folger, S. F., & Bailey, S. P. (2019). Brain activity during unilateral physical and imagined isometric contractions. *Frontiers in Human Neuroscience, 13*, 413. https://doi.org/10.3389/fnhum.2019.00413.

Mateos-Aparicio, P., & Rodríguez-Moreno, A. (2019). The impact of studying brain plasticity. *Frontiers in Cellular Neuroscience, 13*, 66. https://doi.org/10.3389/fncel.2019.00066.

Matsutake, R., Fujimoto, T., Ichinose, M., et al. (2025). The blood flow and vascular responses in dynamically exercising skeletal muscles evoked by combination of cold stimulation and voluntary apnea in humans. *European Journal of Applied Physiology, 125*(4), 1179–1190. https://doi.org/10.1007/s00421-024-05643-8.

McFarland, D. J., Miner, L. A., Vaughan, T. M., & Wolpaw, J. R. (2000). Mu and beta rhythm topographies during motor imagery and actual movements. *Brain Topography, 12*(3), 177–186. https://doi.org/10.1023/a:1023437823106.

McNeil, D. G., Lindsay, R. S., Worn, R., Spittle, M., & Gabbett, T. J. (2025). Could motor imagery training provide a novel load management solution for athletes? Recommendations for sport medicine and performance practitioners. *Sports Health, 17*(1), 156–163. https://doi.org/10.1177/19417381241297161.

Mehling, W. E., Acree, M., Stewart, A., Silas, J., & Jones, A. (2018). The Multidimensional Assessment of Interoceptive Awareness, Version 2 (MAIA-2). *PLOS ONE, 13*(12), e0208034. https://doi.org/10.1371/journal.pone.0208034.

Menzocchi, M., Mecacci, G., Zeppi, A., Carli, G., & Santarcangelo, E. L. (2015). Hypnotizability and performance on a prism adaptation test. *The Cerebellum, 14*(6), 699–706. https://doi.org/10.1007/s12311-015-0671-y.

Montemurro, S., Borek, D., Marinazzo, D., Zago, S., Masina, F., Napoli, E., Filippini, N., & Arcara, G. (2024). Aperiodic component of EEG power spectrum and cognitive performance are modulated by education in aging. *Scientific Reports, 14*(1), 15111. https://doi.org/10.1038/s41598-024-66049-2.

Moriarty, T., Johnson, A., Thomas, M., Evers, C., Auten, A., Cavey, K., Dorman, K., & Bourbeau, K. (2022). Acute aerobic exercise-induced motor priming improves piano performance and alters motor cortex activation. *Frontiers in Psychology, 13*, 825322. https://doi.org/10.3389/fpsyg.2022.825322.

Morrow, A., Elias, M., & Samaha, J. (2023). Evaluating the evidence for the functional inhibition account of alpha-band oscillations during preparatory attention. *Journal of Cognitive Neuroscience, 35*(8), 1195–1211. https://doi.org/10.1162/jocn_a_02009.

Munzert, J., Lorey, B., & Zentgraf, K. (2009). Cognitive motor processes: The role of motor imagery in the study of motor representations. *Brain Research Reviews, 60*(2), 306–326. https://doi.org/10.1016/j.brainresrev.2008.12.024.

Nakagawa, K., Aokage, Y., Fukuri, T., Kawahara, Y., Hashizume, A., Kurisu, K., & Yuge, L. (2011). Neuromagnetic beta oscillation changes during motor imagery and motor execution of skilled movements. *NeuroReport, 22*(5), 217–222. https://doi.org/10.1097/WNR.0b013e328344b480.

Naraindas, A. M., Moreno, M., & Cooney, S. M. (2023). Beyond gender: Interoceptive sensibility as a key predictor of body image disturbances. *Behavioral Sciences (Basel, Switzerland), 14*(1), 25. https://doi.org/10.3390/bs14010025.

Nelson, A. B., et al. (2017). Beta oscillatory changes and retention of motor skills during practice in healthy subjects and in patients with Parkinson's disease. *Frontiers in Human Neuroscience, 11*, 104. https://doi.org/10.3389/fnhum.2017.00104.

Newman, E. A. (2013). Functional hyperemia and mechanisms of neurovascular coupling in the retinal vasculature. *Journal of Cerebral Blood Flow and Metabolism, 33*(11), 1685–1695. https://doi.org/10.1038/jcbfm.2013.145.

Ngetich, R., Jin, D., Li, W., Song, B., Zhang, J., Jin, Z., & Li, L. (2022). Enhancing visuospatial working memory performance using intermittent theta-burst stimulation over the right dorsolateral

prefrontal cortex. *Frontiers in Human Neuroscience, 16*, 752519. https://doi.org/10.3389/fnhum.2022.752519.

Nunan, D., Sandercock, G. R., & Brodie, D. A. (2010). A quantitative systematic review of normal values for short-term heart rate variability in healthy adults. *Pacing and Clinical Electrophysiology, 33*(11), 1407–1417. https://doi.org/10.1111/j.1540-8159.2010.02841.x.

O'Croinin, B. R., Young, D. A., Maier, L. E., et al. (2024). Influence of hypercapnia and hypercapnic hypoxia on the heart rate response to apnea. *Physiological Reports, 12*(11), e16054. https://doi.org/10.14814/phy2.16054.

Obrig, H., Israel, H., Kohl-Bareis, M., Uludag, K., Wenzel, R., Müller, B., Arnold, G., & Villringer, A. (2002). Habituation of the visually evoked potential and its vascular response: Implications for neurovascular coupling in the healthy adult. *NeuroImage, 17*(1), 1–18. https://doi.org/10.1006/nimg.2002.1177.

Obrig, H., & Villringer, A. (2003). Beyond the visible—Imaging the human brain with light. *Journal of Cerebral Blood Flow and Metabolism, 23*(1), 1–18. https://doi.org/10.1097/01.WCB.0000043472.45775.29.

Ogawa, T., Shimobayashi, H., Hirayama, J. I., & Kawanabe, M. (2022). Asymmetric directed functional connectivity within the frontoparietal motor network during motor imagery and execution. *NeuroImage, 247*, 118794. https://doi.org/10.1016/j.neuroimage.2021.118794.

Oldfield, R. C. (1971). The assessment and analysis of handedness: The Edinburgh inventory. *Neuropsychologia, 9*(1), 97–113. https://doi.org/10.1016/0028-3932(71)90067-4.

Owen, R., Wakefield, C. J., & Roberts, J. W. (2024). Online corrections can occur within movement imagery: An investigation of the motor-cognitive model. *Human Movement Science, 95*, 103222. https://doi.org/10.1016/j.humov.2024.103222.

Padilla-Castaneda, M. A., Castellani, E., Frisoli, A., Bergamasco, M., & Santarcangelo, E. L. (2015). Hypnotizability and the position sense: Proprioceptive localization of the hand. *Archives Italiennes de Biologie, 153*(1), 46–55. https://doi.org/10.4449/aib.v153i1.3736.

Panikratova, Y. R., Vlasova, R. M., Akhutina, T. V., Korneev, A. A., Sinitsyn, V. E., & Pechenkova, E. V. (2020). Functional connectivity of the dorsolateral prefrontal cortex contributes to different components of executive functions. *International Journal of Psychophysiology, 151*, 70–79. https://doi.org/10.1016/j.ijpsycho.2020.02.013.

Papalia, E., Manzoni, D., & Santarcangelo, E. L. (2014). Stabilizing posture through imagery. *The International Journal of Clinical and Experimental Hypnosis, 62*(3), 292–309. https://doi.org/10.1080/00207144.2014.901080.

Park, S., & Serences, J. T. (2022). Relative precision of top-down attentional modulations is lower in early visual cortex compared to mid- and high-level visual areas. *Journal of Neurophysiology, 127*(2), 504–518. https://doi.org/10.1152/jn.00300.2021.

Parsons, L. M., Fox, P. T., Downs, J. H., Glass, T., Hirsch, T. B., Martin, C. C., Jerabek, P. A., & Lancaster, J. L. (1995). Use of implicit motor imagery for visual shape discrimination as revealed by PET. *Nature, 375*, 54–58. https://doi.org/10.1038/375054a0.

Pfurtscheller, G., & Solis-Escalante, T. (2009). Could the beta rebound in the EEG be suitable to realize a "brain switch"? *Clinical Neurophysiology, 120*, 24–29. https://doi.org/10.1016/j.clinph.2008.09.027.

Pi, Y., Yan, J., Pscherer, C., Gao, S., Mückschel, M., Colzato, L., Hommel, B., & Beste, C. (2024). Interindividual aperiodic resting-state EEG activity predicts cognitive-control styles. *Psychophysiology, 61*(8), e14576. https://doi.org/10.1111/psyp.14576.

Piccione, C., Hilgard, E. R., & Zimbardo, P. G. (1989). On the degree of stability of measured hypnotizability over a 25-year period. *Journal of Personality and Social Psychology, 56*(2), 289–295. https://doi.org/10.1037/0022-3514.56.2.289.

Picerni, E., Santarcangelo, E. L., Laricchiuta, D., et al. (2019). Cerebellar structural variations in subjects with different hypnotizability. *Cerebellum, 18*(1), 109–118. https://doi.org/10.1007/s12311-018-0965-y.

Porges, S. W. (1993). *Body perception questionnaire*. Laboratory of Developmental Assessment: University of Maryland.

Pusil, S., Zegarra-Valdivia, J., Cuesta, P., Laohathai, C., Cebolla, A. M., Haueisen, J., Fiedler, P., Funke, M., Maestú, F., & Cheron, G. (2023). Effects of spaceflight on the EEG alpha power and functional connectivity. *Scientific Reports, 13*(1), 9489. https://doi.org/10.1038/s41598-023-34744-1.

Quivira-Lopesino, A., Sevilla-García, M., Cuesta, P., Pusil, S., Bruña, R., Fiedler, P., Cebolla, A. M., Cheron, G., Funke, M., & Maestú, F. (2025). Changes of EEG beta band power and functional connectivity during spaceflight: A retrospective study. *Scientific Reports, 15*(1), 13399. https://doi.org/10.1038/s41598-025-96897-5.

Ragni, F., Tucciarelli, R., Andersson, P., & Lingnau, A. (2020). Decoding stimulus identity in occipital, parietal and inferotemporal cortices during visual mental imagery. *Cortex, 127*, 371–387. https://doi.org/10.1016/j.cortex.2020.02.020.

Rannaud Monany, D., Barbiero, M., Lebon, F., Babič, J., Blohm, G., Nozaki, D., & White, O. (2022). Motor imagery helps updating internal models during microgravity exposure. *Journal of Neurophysiology, 127*(2), 434–443. https://doi.org/10.1152/jn.00214.2021.

Rasch, B., & Cordi, M. J. (2024). The influence of experience and modality of presentation (online vs. offline) on hypnotizability. *Frontiers in Psychology, 14*, 1293070. https://doi.org/10.3389/fpsyg.2023.1293070.

Rashid, A., Santarcangelo, E. L., & Roatta, S. (2022a). Cerebral blood flow in healthy subjects with different hypnotizability scores. *Brain Sciences, 12*(5), 558. https://doi.org/10.3390/brainsci12050558.

Rashid, A., Santarcangelo, E. L., & Roatta, S. (2022b). Cerebrovascular reactivity during visual stimulation: Does hypnotizability matter? *Brain Research, 1794*, 148059. https://doi.org/10.1016/j.brainres.2022.148059.

Rashid, A., Santarcangelo, E. L., & Roatta, S. (2022c). Does hypnotizability affect neurovascular coupling during cognitive tasks? *Physiology & Behavior, 257*, 113915. https://doi.org/10.1016/j.physbeh.2022.113915.

Ridderinkhof, K. R., & Brass, M. (2015). How kinesthetic motor imagery works: A predictive-processing theory of visualization in sports and motor expertise. *Journal of Physiology-Paris, 109*(1–3), 53–63. https://doi.org/10.1016/j.jphysparis.2015.02.003.

Roberts, D. R., Ramsey, D., Johnson, K., Kola, J., Ricci, R., Hicks, C., Borckardt, J. J., Bloomberg, J. J., Epstein, C., & George, M. S. (2010). Cerebral cortex plasticity after 90 days of bed rest: Data from TMS and fMRI. *Aviation, Space, and Environmental Medicine, 81*(1), 30–40. https://doi.org/10.3357/asem.2532.2009.

Rolls, E. T., Deco, G., Huang, C. C., & Feng, J. (2023). Prefrontal and somatosensory-motor cortex effective connectivity in humans. *Cerebral Cortex, 33*(8), 4939–4963. https://doi.org/10.1093/cercor/bhac391.

Rubichi, S., Ricci, F., Padovani, R., & Scaglietti, L. (2005). Hypnotic susceptibility, baseline attentional functioning, and the Stroop task. *Consciousness and Cognition, 14*(2), 296–303. https://doi.org/10.1016/j.concog.2004.08.003.

Ruffino, C., Papaxanthis, C., & Lebon, F. (2017). Neural plasticity during motor learning with motor imagery practice: Review and perspectives. *Neuroscience, 341*, 61–78. https://doi.org/10.1016/j.neuroscience.2016.11.023.

Ruggirello, S., Campioni, L., Piermanni, S., Sebastiani, L., & Santarcangelo, E. L. (2019). Does hypnotic assessment predict the functional equivalence between motor imagery and action? *Brain and Cognition, 136*, 103598. https://doi.org/10.1016/j.bandc.2019.103598.

Santarcangelo, E. L., & Manzoni, D. (2022). Hypnotisability and the cerebellum: Hypotheses and perspectives. *Cerebellum, 21*(6), 1025–1028. https://doi.org/10.1007/s12311-021-01292-1.

Santarcangelo, E. L., Scattina, E., Carli, G., Macerata, A., & Manzoni, D. (2008). Hypnotizability-dependent modulation of postural control: Effects of alteration of the visual and leg proprioceptive inputs. *Experimental Brain Research, 191*(3), 331–340. https://doi.org/10.1007/s00221-008-1526-2.

Santarcangelo, E. L. (2024). Physiological correlates of hypnotizability. In J. H. Linden, G. De Benedittis, L. I. Sugarman, & K. Varga (Eds.), *The Routledge international handbook of clinical hypnosis* (1st ed.). Routledge. https://doi.org/10.4324/9781003449126.

Santarcangelo, E. L., & Scattina, E. (2016). Complementing the latest APA definition of hypnosis: Sensory-motor and vascular peculiarities involved in hypnotizability. *The International Journal of Clinical and Experimental Hypnosis, 64*(3), 318–330. https://doi.org/10.1080/00207144.2016.1171093.

Santarcangelo, E. L., Cavallaro, E., Mazzoleni, S., Marano, E., Ghelarducci, B., Dario, P., Micera, S., & Sebastiani, L. (2005). Kinematic strategies for lowering of upper limbs during suggestions of heaviness: A real-simulator design. *Experimental Brain Research, 162*(1), 35–45. https://doi.org/10.1007/s00221-004-2112-x.

Santarcangelo, E. L., Scattina, E., Carli, G., Ghelarducci, B., Orsini, P., & Manzoni, D. (2010). Can imagery become reality? *Experimental Brain Research, 206*(3), 329–335. https://doi.org/10.1007/s00221-010-2412-2.

Savitzky, A., & Golay, M. J. E. (1964). Smoothing and differentiation of data by simplified least squares procedures. *Analytical Chemistry, 36*(8), 1627–1639. https://doi.org/10.1021/ac60214a047.

Scacchia, P., & De Pascalis, V. (2020). Effects of prehypnotic instructions on hypnotizability and relationships between hypnotizability, absorption, and empathy. *American Journal of Clinical Hypnosis, 62*(3), 231–266. https://doi.org/10.1080/00029157.2019.1586639.

Scandola, M., Aglioti, S. M., Pozeg, P., Avesani, R., & Moro, V. (2017). Motor imagery in spinal cord injured people is modulated by somatotopic coding, perspective taking, and post-lesional chronic pain. *Journal of Neuropsychology, 11*(3), 305–326. https://doi.org/10.1111/jnp.12098.

Schuster, C., Hilfiker, R., Amft, O., Scheidhauer, A., Andrews, B., Butler, J., Kischka, U., & Ettlin, T. (2011). Best practice for motor imagery: A systematic literature review on motor imagery training elements in five different disciplines. *BMC Medicine, 9*, 75. https://doi.org/10.1186/1741-7015-9-75.

Şekercan, G., Fil, A., Yetkin, M. F., Karabudak, R., Tuncer, A., & Salcı, Y. (2025). Evaluating motor imagery capabilities in fatigued versus non-fatigued individuals with multiple sclerosis without cognitive impairment. *Neurorehabilitation and Neural Repair.* Advance online publication. https://doi.org/10.1177/15459683251331594.

Shaffer, F., & Ginsberg, J. P. (2017). An overview of heart rate variability metrics and norms. *Frontiers in Public Health, 5*, 258. https://doi.org/10.3389/fpubh.2017.00258.

Sheehan, P. W. (1967). A shortened form of Betts' questionnaire upon mental imagery. *Journal of Clinical Psychology, 23*(3), 386–389. https://doi.org/10.1002/1097-4679(196707)23:3<386::AID-JCLP2270230328>3.0.CO;2-S.

Spielberger, C. D. (1983). *Manual for the State-Trait Anxiety Inventory.* Consulting Psychologists Press. (Citato in: Rachman, S., 2004).

Spina, V., Chisari, C., & Santarcangelo, E. L. (2020). High motor cortex excitability in highly hypnotizable individuals: A favourable factor for neuroplasticity? *Neuroscience, 430*, 125–130. https://doi.org/10.1016/j.neuroscience.2020.01.042.

Srzich, A. J., Byblow, W. D., Stinear, J. W., Cirillo, J., & Anson, J. G. (2016). Can motor imagery and hypnotic susceptibility explain Conversion Disorder with motor symptoms? *Neuropsychologia, 89*, 287–298. https://doi.org/10.1016/j.neuropsychologia.2016.06.030.

Stahn, A. C., Bucher, D., zu Eulenburg, P., et al. (2023). Paving the way to better understand the effects of prolonged spaceflight on operational performance and its neural bases. *npj Microgravity, 9*, 59. https://doi.org/10.1038/s41526-023-00295-y.

Stinear, C. M., Fleming, M. K., & Byblow, W. D. (2006). Lateralization of unimanual and bimanual motor imagery. *Brain Research, 1095*(1), 139–147. https://doi.org/10.1016/j.brainres.2006.04.008.

Stoll, F. M., Wilson, C. R. E., Faraut, M. C. M., Vezoli, J., Knoblauch, K., & Procyk, E. (2016). The effects of cognitive control and time on frontal beta oscillations. *Cerebral Cortex, 26*(4), 1715–1732. https://doi.org/10.1093/cercor/b.

Tellegen, A., & Atkinson, G. (1974). Openness to absorbing and self-altering experiences ("absorption"), a trait related to hypnotic susceptibility. *Journal of Abnormal Psychology, 83*(3), 268–277. https://doi.org/10.1037/h0036681.

Terhune, D. B., Cardeña, E., & Lindgren, M. (2011). Dissociative tendencies and individual differences in high hypnotic suggestibility. *Cognitive Neuropsychiatry, 16*(2), 113–135. https://doi.org/10.1080/13546805.2010.503048.

The MathWorks, Inc. (2024). *MATLAB (Version R2024a)*. Natick, MA: The MathWorks Inc.

Theves, S., Chan, J. S., Naumer, M. J., & Kaiser, J. (2020). Improving audio-visual temporal perception through training enhances beta-band activity. *NeuroImage, 206*, 116312. https://doi.org/10.1016/j.neuroimage.2019.116312.

Ulrich, M., Keller, J., Hoenig, K., Waller, C., & Grön, G. (2014). Neural correlates of experimentally induced flow experiences. *NeuroImage, 86*, 194–202. https://doi.org/10.1016/j.neuroimage.2013.08.019.

Van Impe, A., Coxon, J. P., Goble, D. J., Wenderoth, N., & Swinnen, S. P. (2009). Ipsilateral coordination at preferred rate: Effects of age, body side and task complexity. *NeuroImage, 47*, 1854–1862. https://doi.org/10.1016/j.neuroimage.2009.06.027.

Vanderhasselt, M. A., De Raedt, R., Baeken, C., Leyman, L., & D'Haenen, H. (2006). The influence of rTMS over the left dorsolateral prefrontal cortex on Stroop task performance. *Experimental Brain Research, 169*(2), 279–282. https://pubmed.ncbi.nlm.nih.gov/16418843.

Vigran, H. J., Kapral, A. G., Tytell, E. D., et al. (2019). Manipulating the perception of time affects voluntary breath-holding duration. *Physiological Reports, 7*(23), e14309. https://doi.org/10.14814/phy2.14309.

Wang, J., Jia, X., Song, J., Qin, Z., Cao, M., & Chen, J. (2025). Motor cortex activation patterns in both hemispheres induced by motor imagery in patients with right- and left-sided cerebral infarction: An fNIRS study. *The European Journal of Neuroscience, 61*(7), e70079. https://doi.org/10.1111/ejn.70079.

Weitzenhoffer, A. M., & Hilgard, E. R. (1959). *Stanford hypnotic susceptibility scales*. Stanford, CA: Consulting Psychologists Press.

Welch, P. D. (1967). The use of Fast Fourier Transform for the estimation of power spectra: A method based on time averaging over short, modified periodograms. *IEEE Transactions on Audio and Electroacoustics, AU-15*(2), 70–73. https://doi.org/10.1109/TAU.1967.1161901.

Whittier, T. T., Patrick, C. M., & Fling, B. W. (2023). Somatosensory information in skilled motor performance: A narrative review. *Journal of Motor Behavior, 55*(5), 453–474. https://doi.org/10.1080/00222895.2023.2213198.

Williams, S., Cumming, J., Ntoumanis, N., et al. (2012). Further validation and development of the movement imagery questionnaire. *Journal of Sport & Exercise Psychology, 34

Wriessnegger, S. C., Brunner, C., & Müller-Putz, G. R. (2018). Frequency specific cortical dynamics during motor imagery are influenced by prior physical activity. *Frontiers in Psychology, 9*, 1976. https://doi.org/10.3389/fpsyg.2018.01976.

Wu, S., Li, J., Gao, L., Chen, C., & He, S. (2018). Suppressing systemic interference in fNIRS monitoring of the hemodynamic cortical response to motor execution and imagery. *Frontiers in Human Neuroscience, 12*, 85. https://doi.org/10.3389/fnhum.2018.00085.

Yang, J., Zhang, G., Gao, X., Cheng, X., Hao, Z., Ma, J., Lin, N., Fu, R., Leung, W., Lo, A., Li, Y., Xie, H., Liang, Z., Chen, X., Yu, Q., & Wang, C. (2025). Role of dorsolateral prefrontal cortex during motor preparation on anticipatory postural adjustments. *Brain Topography, 38*(4), 44. https://doi.org/10.1007/s10548-025-01120-3.

Yang, Y. J., Jeon, E. J., Kim, J. S., & Chung, C. K. (2021). Characterization of kinesthetic motor imagery compared with visual motor imageries. *Scientific Reports, 11*(1), 3751. https://doi.org/10.1038/s41598-021-82241-0.

Yi, W., Qiu, S., Wang, K., et al. (2016). EEG oscillatory patterns and classification of sequential compound limb motor imagery. *Journal of NeuroEngineering and Rehabilitation, 13*, 11. https://doi.org/10.1186/s12984-016-0119-8.

Yin, S., Liu, Y., & Ding, M. (2016). Amplitude of sensorimotor mu rhythm is correlated with BOLD from multiple brain regions: A simultaneous EEG-fMRI study. *Frontiers in Human Neuroscience, 10*, 364. https://doi.org/10.3389/fnhum.2016.00364.

Yoo, P. E., Oxley, T. J., Hagan, M. A., John, S., Ronayne, S. M., Rind, G. S., Brinded, A. M., Opie, N. L., Moffat, B. A., & Wong, Y. T. (2020). Distinct neural correlates underlie inhibitory mechanisms

of motor inhibition and motor imagery restraint. *Frontiers in Behavioral Neuroscience, 14*, 77. https://doi.org/10.3389/fnbeh.2020.00077.

Youssofzadeh, V., Roy, S., Chowdhury, A., Izadysadr, A., Parkkonen, L., Raghavan, M., & Prasad, G. (2023). Mapping and decoding cortical engagement during motor imagery, mental arithmetic, and silent word generation using MEG. *Human Brain Mapping, 44*(8), 3324–3342. https://doi.org/10.1002/hbm.26284.

Yu, Y., Shen, X., Hong, Y., & Wang, F. (2024). Characteristic brain functional activation and connectivity during actual and imaginary right-handed grasp. *Brain Research, 1844*, 149141. https://doi.org/10.1016/j.brainres.2024.149141.

Zabicki, A., de Haas, B., Zentgraf, K., Stark, R., Munzert, J., & Krüger, B. (2019). Subjective vividness of motor imagery has a neural signature in human premotor and parietal cortex. *NeuroImage, 197*, 273–283. https://doi.org/10.1016/j.neuroimage.2019.04.073.

Zelič, Ž., Sebastiani, L., & Santarcangelo, E. L. (2023). Association of hypnotizability, interoception, and emotion. *International Journal of Clinical and Experimental Hypnosis, 71*(3), 250–262. https://doi.org/10.1080/00207144.2023.2226188.

Zelič, Ž., Giusti, G., & Santarcangelo, E. L. (2025). Emotion regulation: The role of hypnotizability and interoception. *Consciousness and Cognition, 131*, 103856. https://doi.org/10.1016/j.concog.2025.103856.

Zhao, Y., Wang, A., Zhao, W., Hu, N., Laureys, S., & Di, H. (2025). The neural correlates of consciousness: A spectral exponent approach to diagnosing disorders of consciousness. *Brain Sciences, 15*(4), 377. https://doi.org/10.3390/brainsci15040377.

APPENDIX A

Study 1

Table S1. Mean and peak [OHb] and [HHb] values of aPFC, mPFC, DLPFC, PMC, M1 and S1 during movement, motor imagery and rest

	HIGHS		LOWS	
Movement		**laPFC task**		
	Mean	S.D.	Mean	S.D.
mean OHb	-0,054	0,263	0,068	0,11
peak OHb	0,124	0,13	0,219	0,17
mean HHb	-0,024	0,024	-0,038	0,097
peak HHb	-0,066	0,04	-0,082	0,108
		lDLPFC task		
mean OHb	0,012	0,139	0,03	0,077
peak OHb	0,23	0,227	0,176	0,204
mean HHb	-0,006	0,131	-0,028	0,07
peak HHb	-0,104	0,088	-0,102	0,097
		mPFC task		
mean OHb	0,065	0,148	0,018	0,185
peak OHb	0,101	0,068	0,184	0,128
mean HHb	0,003	0,079	-0,021	0,076
peak HHb	-0,107	0,121	-0,065	0,101
		lPMC task		
mean OHb	0,075	0,111	-0,001	0,048
peak OHb	0,154	0,139	0,115	0,117
mean HHb	0,046	0,256	0,023	0,148
peak HHb	-0,238	0,299	-0,138	0,197
		M1 task		
mean OHb	0,02	0,105	-0,012	0,098
peak OHb	0,137	0,093	0,067	0,045
mean HHb	0,038	0,096	-0,043	0,107
peak HHb	-0,12	0,168	-0,179	0,205
		S1 task		
mean OHb	0,016	0,169	0,033	0,137
peak OHb	0,129	0,085	0,231	0,372
mean HHb	-0,015	0,169	-0,069	0,165
peak HHb	-0,058	0,069	-0,233	0,248
		laPFC rest		
mean OHb	0,012	0,091	0,03	0,141
peak OHb	0,104	0,113	0,181	0,143
mean HHb	-0,002	0,046	-0,011	0,034
peak HHb	-0,066	0,056	-0,058	0,047
		lDLPFC rest		
mean OHb	0,027	0,095	0,003	0,074
peak OHb	0,166	0,144	0,115	0,114
mean HHb	-0,107	0,152	-0,003	0,034
peak HHb	-0,154	0,128	-0,057	0,045
		lPMC rest		
mean OHb	0,017	0,043	0,027	0,122
peak OHb	0,091	0,079	0,057	0,059
mean HHb	0,031	0,372	0,06	0,177
peak HHb	-0,312	0,486	-0,055	0,101
		mPFC rest		
mean OHb	0,046	0,056	-0,059	0,17
peak OHb	0,214	0,228	0,105	0,08
mean HHb	-0,056	0,074	-0,009	0,023
peak HHb	-0,148	0,141	-0,038	0,033
		M1 rest		
mean OHb	0,078	0,113	0,062	0,088
peak OHb	0,145	0,1	0,185	0,11
mean HHb	0,046	0,152	0,035	0,065
peak HHb	-0,101	0,117	-0,061	0,083
		S1 rest		
mean OHb	0,075	0,195	0,071	0,233
peak OHb	0,189	0,123	0,144	0,094
mean HHb	0,012	0,101	-0,004	0,161
peak HHb	-0,114	0,117	-0,105	0,122
Motor imagery		**laPFC task**		
mean OHb	-0,003	0,06	0,126	0,112
peak OHb	0,142	0,154	0,343	0,19
mean HHb	0,02	0,064	-0,023	0,056
peak HHb	-0,053	0,058	-0,093	0,062
		lDLPFC task		
mean OHb	-0,061	0,104	0,1	0,084
peak OHb	0,093	0,034	0,315	0,147
mean HHb	-0,064	0,123	0,007	0,098
peak HHb	-0,106	0,106	-0,099	0,081
		mPFC task		
mean OHb	-0,094	0,159	-0,016	0,21
peak OHb	0,1	0,08	0,225	0,163
mean HHb	-0,039	0,127	-0,013	0,044
peak HHb	-0,137	0,132	-0,065	0,06
		lPMC task		
mean OHb	-0,062	0,128	-0,006	0,072
peak OHb	0,097	0,133	0,116	0,121
mean HHb	-0,021	0,071	-0,008	0,088
peak HHb	-0,101	0,106	-0,139	0,244
		M1 task		
mean OHb	0,009	0,166	0,024	0,119
peak OHb	0,073	0,064	0,184	0,137
mean HHb	-0,058	0,103	0,012	0,103
peak HHb	-0,177	0,185	-0,087	0,104
		S1 task		
mean OHb	0,011	0,141	0,033	0,08
peak OHb	0,147	0,121	0,238	0,102
mean HHb	0,022	0,082	-0,012	0,126
peak HHb	-0,193	0,174	-0,299	0,289
		laPFC rest		
mean OHb	0,03	0,183	-0,074	0,113
peak OHb	0,189	0,201	0,096	0,094
mean HHb	0,048	0,201	0,025	0,064
peak HHb	-0,09	0,086	-0,049	0,04
		lDLPFC rest		
mean OHb	0,162	0,151	-0,095	0,154
peak OHb	0,239	0,1	0,081	0,099
mean HHb	0,054	0,167	-0,001	0,067
peak HHb	-0,07	0,067	-0,103	0,118
		mPFC rest		
mean OHb	0,177	0,217	-0,06	0,118
peak OHb	0,49	0,384	0,11	0,128
mean HHb	-0,084	0,188	0,003	0,032
peak HHb	-0,101	0,061	-0,046	0,029
		lPMC rest		
mean OHb	-0,056	0,227	-0,02	0,469
peak OHb	0,157	0,125	0,365	0,953
mean HHb	0,018	0,062	-0,084	0,152
peak HHb	-0,039	0,055	-0,269	0,523
		M1 rest		
mean OHb	-0,022	0,134	-0,197	0,441
peak OHb	0,118	0,105	0,103	0,108
mean HHb	0,01	0,216	0,015	0,037
peak HHb	-0,034	0,043	-0,062	0,063
		S1 rest		
mean OHb	-0,012	0,141	-0,225	1,034
peak OHb	0,191	0,104	0,391	0,785
mean HHb	0,068	0,266	-0,025	0,201
peak HHb	-0,115	0,102	-0,238	0,278

	HIGHS		LOWS	
Movement		**raPFC task**		
	Mean	S.D.	Mean	S.D.
mean OHb	0,015	0,039	0,053	0,16
peak OHb	0,075	0,065	0,159	0,149
mean HHb	-0,005	0,015	-0,026	0,058
peak HHb	-0,049	0,03	-0,064	0,065
		rDLPFC task		
mean OHb	0,013	0,052	0,033	0,061
peak OHb	0,116	0,063	0,147	0,084
mean HHb	0,015	0,071	-0,007	0,047
peak HHb	-0,071	0,075	-0,077	0,087
mean OHb				
peak OHb				
mean HHb				
peak HHb				
		rPMC task		
mean OHb	0,034	0,041	0,025	0,081
peak OHb	0,126	0,105	0,135	0,079
mean HHb	0,06	0,125	-0,044	0,121
peak HHb	-0,09	0,107	-0,271	0,256
mean OHb				
peak OHb				
mean HHb				
peak HHb				
mean OHb				
peak OHb				
mean HHb				
peak HHb				
		raPFC rest		
mean OHb	-0,004	0,077	0,022	0,097
peak OHb	0,08	0,089	0,165	0,109
mean HHb	-0,011	0,021	0,003	0,026
peak HHb	-0,083	0,088	-0,036	0,029
		rDLPFC rest		
mean OHb	0,032	0,054	0,005	0,05
peak OHb	0,11	0,099	0,113	0,067
mean HHb	-0,033	0,036	0	0,038
peak HHb	-0,084	0,07	-0,071	0,05
		rPMC rest		
mean OHb	0,012	0,053	0,011	0,066
peak OHb	0,091	0,083	0,091	0,086
mean HHb	-0,043	0,119	0,028	0,179
peak HHb	-0,132	0,122	-0,091	0,07
mean OHb				
peak OHb				
mean HHb				
peak HHb				
mean OHb				
peak OHb				
mean HHb				
peak HHb				
mean OHb				
peak OHb				
mean HHb				
peak HHb				
Motor imagery		**raPFC task**		
mean OHb	0,002	0,059	0,07	0,059
peak OHb	0,089	0,063	0,271	0,115
mean HHb	0,016	0,03	-0,02	0,031
peak HHb	-0,025	0,024	-0,06	0,038
		rDLPFC task		
mean OHb	0,025	0,074	0,036	0,096
peak OHb	0,152	0,108	0,22	0,111
mean HHb	0,007	0,062	-0,006	0,046
peak HHb	-0,086	0,056	-0,07	0,042
mean OHb				
peak OHb				
mean HHb				
peak HHb				
		rPMC task		
mean OHb	-0,018	0,069	0,033	0,053
peak OHb	0,089	0,071	0,188	0,097
mean HHb	-0,117	0,193	-0,025	0,088
peak HHb	-0,134	0,129	-0,114	0,079
mean OHb				
peak OHb				
mean HHb				
peak HHb				
mean OHb				
peak OHb				
mean HHb				
peak HHb				
		raPFC rest		
mean OHb	0,069	0,128	-0,044	0,065
peak OHb	0,146	0,186	0,108	0,137
mean HHb	-0,021	0,034	0,016	0,03
peak HHb	-0,069	0,059	-0,027	0,02
		rDLPFC rest		
mean OHb	0,059	0,129	-0,007	0,064
peak OHb	0,189	0,126	0,114	0,077
mean HHb	0,047	0,108	-0,006	0,019
peak HHb	-0,068	0,047	-0,082	0,042
mean OHb				
peak OHb				
mean HHb				
peak HHb				
		rPMC rest		
mean OHb	0,096	0,172	-0,067	0,119
peak OHb	0,244	0,191	0,077	0,06
mean HHb	0,113	0,291	-0,045	0,085
peak HHb	-0,067	0,081	-0,171	0,196
mean OHb				
peak OHb				
mean HHb				
peak HHb				
mean OHb				
peak OHb				
mean HHb				
peak HHb				

Table S2. Anterior prefrontal region. Significant interactions for [OHb]

mean	**d.f.**	**F**	**p**	**η^2**	**1 - ß**
level x group	1,18	6.82	.018	.286	.692
highs					
level			n.s.		
lows					
level: task > rest	1,9	5.57	.043		
highs vs lows					
task: highs < lows	1,18	5.81	.027		
rest: highs = lows					
peak					
group, highs < lows	1,18	5.26	.035	.236	.581
side, left > right	1,18	4.95	.04	.225	.555
cond x level x group	1,18	9.71	.006	.364	.836
highs					
cond, level			n.s.		
lows					
cond x level	1,9	10.63	.010		
M			n.s.		
MI: task > rest	1,9	19.18	.002		
task: M < MI	1,9	15.87	.003		
rest			n.s.		

d.f., degrees of freedom; *M*, movement; *MI*, motor imagery; *n.s.*, not significant.

Table S3. Medial prefrontal region. Significant interactions for [OHb]

mean	**df**	**F**	**p**	**η^2**	**1 - ß**
level x group	1,18	9.87	.006	.367	.841
highs					
level: task < rest	1,8	8.26	.021		
lows					
level			n.s.		
highs vs lows					
task			n.s.		
rest: highs > lows	1,18	12.09	.003		
peak					
cond	1,18	5.56	.031	.246	.604
cond x level x group	1,18	6.49	.021	.276	.671
highs					
cond x level	1,8	9.90	.014		
M: task = rest			n.s.		
MI: task < rest	1,8	9.24	.016		
rest: M < MI	1,8	9.32	.016		
task			n.s.		
lows					
level: task > rest	1,9	20.13	.002		
highs vs lows					
bM			n.s.		
M			n.s.		
bMI: highs > lows	1,8	8.77	.009		
MI: highs < lows		4.36	.052		

d.f., degrees of freedom; *M*, movement; *MI*, motor imagery; *n.s.*, not significant.

Table S4. Dorsolateral prefrontal cortex. Significant interactions for [OHb]

mean	**df**	**F**	**p**	**η2**	**1−ß**
group	1,18	4.27	.054	.201	.496
level x group	1,18	18.66	.0001	.523	.982
level x side x group	1,18	13.44	.002	.442	.932
cond x level x side x group	1,18	9.95	.006	.369	.844
highs					
cond x level x side	1,8	5.10	.054		
left, level	1,8	11.71	.009	task < rest	
right, level			n.s.		
right vs left					
M task, rest			n.s.		
MI rest			n.s.		
MI task	1,8	9.19	.016	left < right	
lows					
level x side	1,9	7.20	.025		
left, level	1,9	14.63	.004	task > rest	
right			n.s.		
left vs right					
task			n.s.		
rest			n.s.		
highs vs lows					
MI task left	1,18	13.80	.002	highs<lows	
MI task right			n.s.		
MI rest left	1,18	13.42	.002	highs > lows	
MI rest right			n.s.		
M task left			n.s.		
M rest left			n.s.		
M task right			n.s.		
M rest right			n.s.		
peak					
level x group	1,18	11.42	.004	.402	.889
cond x level x group	1,18	8.55	.009	.335	.787
highs			n.s.		
lows					
level	1,9	14.87	.004	task > rest	
highs vs lows					
BM			n.s.		
M			n.s.		
BMI	1,18	7.13	.016	highs > lows	
MI	1,18	15.34	.001	highs < lows	

BM, baseline after movement; *BMI*, baseline after motor imagery; *d.f.*, degrees of freedom; *M*, movement; *MI*, motor imagery; *n.s.*, not significant.

Table S5. Primary motor cortex and sensorimotor cortex. Significant interactions for [OHb]

	mean					
M1	**df**	**F**	**p**	**η^2**	**1−ß**	
cond	1,18	4.38	.052	.205	.506	M > MI
peak						
cond x level x group	1,18	5.09	.037	.231	.567	
highs			n.s			
lows						
cond x level	1,9	6.02	.037			
M, level	1,9	7.95	.02	task < rest		
MI, level			n.s.			
task	1,9	6.21	.034	M > MI		
rest			n.s.			
highs vs lows						
BM			n.s.			
BMI			n.s.			
M	1,18	4.47	.05	highs > lows		
MI	1,18	4.94	.04	highs < lows		
M1/S1	**peak**					
level x group	1,18	5.01	.039	.228	.560	
highs			n.s.			
lows			n.s.			

BM, baseline after movement; *BMI*, baseline after motor imagery; *d.f.*, degrees of freedom; *M*, movement; *MI*, motor imagery; *M1*, primary motor cortex; *n.s.*, not significant; *S1*, primary sensory cortex.

APPENDIX B

Study 2

Table S6. Region effects in the studied rhythms

	d.f.	F	p	η^2	1 - β	
mu	1,18	27.93	.0001	.608	.999	Fz < Cz
alpha	1,18	416.23	.0001	.959	.999	FC < PO
low beta	1,18	169.10	.0001	.904	.999	FC < PO
high beta	1,18	38.40	.0001	.681	.999	FC < PO

d.f., degrees of freedom; *FC*, fronto-central; *PO*, parieto-occipital.

Table S7. Questionnaires scores

		highs		mediums		lows	
questionnaire		mean	sd	mean	sd	mean	sd
TAS		24.17	3.66	24.67	4.42	19.69	6.43
Betts	V	2.84	1.28	3.72	1.89	2.35	0.68
	K	2.94	1.53	3.53	1.98	2.06	0.87
MAIA	noticing	3.77	0.55	3.66	0.84	3.35	0.65
	not distracting	1.61	0.66	1.69	0.56	1.77	0.64
	not worrying	2.28	0.95	2.57	1.43	3.13	0.78
	attention regulation	3.31	0.43	3.28	0.72	3.48	0.75
	emotional awareness	4.03	0.60	3.62	1.04	3.34	0.80
	self regulation	2.85	0.93	3.4	0.73	3.31	0.64
	body listening	2.89	0.82	3.04	1.03	2.59	0.78
	trusting	3.36	1.19	3.76	1.12	3.74	1.09

K, kinesthetic*; Sd,* standard deviation*; V,* visual.

Table S8. SDNN and RMSSD

		Mean	**S.D.**	**Mean**	**S.D.**
S1	B	86.7	31.60	83.86	27.524
	M	24.53	21.678	27.62	23.897
	V	29.08	30.898	33.65	36.284
	K	23.08	21.958	26.96	19.263
S2	B	32.53	30.417	38.66	40.299
	M	26.8	22.738	24.08	23.087
	V	26.41	29.994	38.39	46.384
	K	26.13	24.079	30.59	27.45

B, baseline; *M*, movement; *S1*, first session; *S2*, second session; *S.D.,* standard deviation; *V,* visual; *K,* kinesthetic.

Table S9. Midline fronto-central (A) and hemispheric (B) offset. Decomposition of Session x Condition x Group

	A			B		
group		**F**	**p**		**F**	**p**
highs (df = 1,11)						
	B S1 < S2	15.60	.002	B S1 < S2	18.55	.001
	M S1 = S2	1.08	.32	M S1 = S2	3.61	.084
	V S1 < S2	5.31	.042	V S1 < S2	8.11	.016
	K S1 < S2	6.67	.025	K S1 = S2	3.11	.105
	S1 B > M	12.10	.005	S1 condition	2.14	.11
	B = V	1.10	.31			
	B = K	3.72	.08			
	M < V	5.70	.036			
	M = K	.38	.55			
	V = K	3.92	.073			
	S2 B > M	17.45	.002	S2 B > M	16.83	.002
	B > V	13.51	.004	B > V	13.00	.004
	B > K	21.83	.001	B > K	16.67	.002
	M < V	8.35	.015	M < V	6.46	.027
	M < K	4.98	.047	M < K	4.60	*.055*
	V = K	1.88	.20	V = K	.15	.70
mediums (df = 1,8)	session	.14	.71	B > M	11.19	.010
	condition	2.63	.073	B = V	.86	.38
				B > K	7.66	.024
				M < V	13.45	.006
				M = K	3.77	.088
				V = K	.47	.51
lows (df = 1,12)	S1 < S2	4.89	.047	S1 < S2	5.69	.034
	B > M	8.01	.015	B > M	9.53	.009
	B = V	3.60	.082	B = V	2.73	.12
	B = K	4.15	.064	B = K	1.20	.30
	M = V	1.46	.25	M = V	2.88	.12
	M = K	2.84	.12	M < K	9.41	.010
	V = K	.62	.45	V < K	7.36	.019

B, baseline; *df,* degrees of freedom; *M*, movement; *S1*, first session; *S2*, second session; *V,* visual; *K,* kinesthetic.

Table S10. Regression of SHSS, MAIA, Betts' V and K on aperiodic components

	SHSS		MAIA not distracting		MAIA not worrying		MAIA self regulation		MAIA trusting		Betts' V		Betts' K		adj R2
	B	p	B	p	B	p	B	p	B	p	B	p	B	p	
FzCz offset															
ΔB									-.475	.005					.201
ΔM			.363	.039											.116
ΔV			.332	.055											.082
ΔK															
FCPO offset															
left															
ΔB									-.510	.002					.237
ΔM			.453	.002			.456	.003							.488
ΔV															
ΔK															
right															
ΔB									-.379	.027					.117
ΔM			.364	.031			.381	.036							.173
ΔV									-.334	.053					.084
ΔK															
FzCz exponent															
ΔB	.374	.019													.361
ΔM	.594	.0001							-.358	.019			-.808	.043	.333
ΔV	.551	.001													.282
ΔK	.503	.002													.229
FCPO exponent															
left									-.296	.053	.896	.033	-.982	.017	.337
ΔB	.341	.034													.349
ΔM	.417	.009			-.342	.029									.328
ΔV	.590	.0001													.345
ΔK	.420	.009			-.334	.033									
right													-.861	.032	.342
ΔB	.417	.004													.435
ΔM	.544	.0001													.340
ΔV	.530	.001													.321
ΔK	.407	.012			-.325	.041									

Adj R^2; adjusted R^2*; Δ*, difference between S2 and S1 in baseline conditions (B), actual movement (M), visual (V) and kinesthetic (K) imagery*; FzCz,* fronto-central midline region; *FCPO,* frontocentral-parietooccipital hemispheric regions.

Table S11. Alpha PSD. Decomposition of Session x Side x Condition

		df	F	p
left, B	S1 > S2	1,33	4.55	.040
left, M	S1 > S2	1,33	4.45	.043
left, V	S1 > S2	1,33	5.49	.025
left, K	S1 > S2	1,33	6.88	.013
right, B	S1 > S2	1,33	7.44	.010
right, M	S1 > S2	1,33	4.06	.052
right, V	S1 > S2	1,33	5.10	.031
right, K	S1 > S2	1,33	7.70	.009
S1, B	left < right	1,33	4.27	.047
S1, M	left = right	1,33	.021	.89
S1, V	left = right	1,33	.36	.55
S1, K	left = right	1,33	.62	.43
S2, B	left = right	1,33	.82	.37
S2, M	left = right	1,33	.082	.78
S2, V	left = right	1,33	3.52	.07
S2, K	left = right	1,33	.23	.63
left, S1	B > M	1,33	15.51	.0001
left, S1	B > V	1,33	4.08	.051
left, S1	B = K	1,33	2.38	.13
left, S1	M < V	1,33	12.57	.001
left, S1	M < K	1,33	14.92	.0001
left, S1	V = K	1,33	1.66	.20
right, S1	B > M	1,33	22.53	.0001
right, S1	B > V	1,33	6.10	.019
right, S1	B > K	1,33	4.27	.047
right, S1	M < V	1,33	18.48	.0001
right, S1	M < K	1,33	19.34	.0001
right, S1	V = K	1,33	1.30	.26
left, S2	B > M	1,33	38.65	.0001
left, S2	B > V	1,33	20.11	.0001
left, S2	B > K	1,33	22.87	.0001
left, S2	M < V	1,33	15.97	.0001
left, S2	M < K	1,33	13.17	.001
left, S2	V = K	1,33	.02	.89
right, S2	B > M	1,33	39.39	.0001
right, S2	B > V	1,33	11.13	.002
right, S2	B > K	1,33	16.61	.0001
right, S2	M < V	1,33	17.88	.0001
right, S2	M < K	1,33	13.10	.001
right, S2	V = K	1,33	1.00	.32

B, baseline; *d.f.*, degrees of freedom; *K*, kinesthetic; *M*, movement; *S1*, first sessions; *S2*, second session; *V,* visual.

Table S12. Low-beta PSD. Decomposition of Session x Side x Condition

		df	F	p
left, B	S1 = S2	1,33	.022	.88
left, M	S1 = S2	1,33	.13	.72
left, V	S1 = S2	1,33	.23	.63
left, K	S1 = S2	1,33	.04	.84
right, B	S1 = S2	1,33	.27	.61
right, M	S1 = S2	1,33	.14	.71
right, V	S1 = S2	1,33	.11	.74
right, K	S1 = S2	1,33	.04	.83
S1, B	left < right	1,33	10.40	.003
S1, M	left = right	1,33	.01	.92
S1, V	left < right	1,33	4.34	.045
S1, K	left = right	1,33	1.18	.28
S2, B	left = right	1,33	.44	.51
S2, M	left = right	1,33	.06	.81
S2, V	left < right	1,33	4.70	.037
S2, K	left = right	1,33	.72	.40
left, S1	B > M	1,33	33.66	.0001
left, S1	B > V	1,33	15.96	.0001
left, S1	B > K	1,33	4.03	.053
left, S1	M < V	1,33	8.77	.006
left, S1	M < K	1,33	14.53	.001
left, S1	V < K	1,33	7.61	.009
right, S1	B > M	1,33	43.65	.0001
right, S1	B > V	1,33	16.32	.0001
right, S1	B > K	1,33	7.58	.010
right, S1	M < V	1,33	24.64	.0001
right, S1	M < K	1,33	27.93	.0001
right, S1	V = K	1,33	2.10	.15
left, S2	B > M	1,33	21.88	.0001
left, S2	B > V	1,33	12.67	.001
left, S2	B > K	1,33	13.76	.001
left, S2	M < V	1,33	11.19	.002
left, S2	M < K	1,33	8.65	.006
left, S2	V = K	1,33	.001	.97
right, S2	B > M	1,33	20.56	.0001
right, S2	B > V	1,33	6.00	.020
right, S2	B > K	1,33	9.02	.005
right, S2	M < V	1,33	14.02	.001
right, S2	M < K	1,33	9.77	.004
right, S2	V = K	1,33	.87	.36

B, baseline; *d.f.*, degrees of freedom; *K*, kinesthetic; *M*, movement; *S1*, first sessions; *S2*, second session; *V,* visual.

Table S13. Regression of SHSS, MAIA, Betts' V and K on PSD

	SHSS		MAIA not distracting		MAIA not worrying		MAIA noticing		MAIA trusting		Betts' V		adj R2
mu	B	p	B	p	B	p	B	p	B	p	B	p	
ΔB	.659	.0001					-.434	.005					.401
ΔM	.512	.002											.239
ΔV	.524	.001											.252
ΔK	.617	.0001	.320	.028	.350	.031			-.336	.027			.400
alpha													
left													
ΔB	.581	.001											.389
ΔM	.454	.007											.181
ΔV	.457	.007											.184
ΔK	.438	.010											.167
right													
ΔB	.432	.005							-.299	.039	.319	.030	.392
ΔM	.441	.009											.169
ΔV	.523	.002											.262
ΔK	.553	.001											.301
low beta													
left													
ΔB	.572	.0001											.306
ΔM	.570	.0001											.397
ΔV	.597	.0001											.477
ΔK	.580	.0001											.315
right													
ΔB	.556	.0001											.371
ΔM	.563	.0001											.398
ΔV	.619	.0001											.364
ΔK	.591	.0001											.329

Adj R^2, adjusted R^2*; Δ*, difference between S2 and S1 in baseline conditions (B), actual movement (M), visual (V) and kinesthetic (K) imagery*; SHSS,* Stanford Hypnotic Susceptibility Scale.